

**ROLE OF CITICOLINE IN MODULATION OF  
ANGIOGENESIS AND APOPTOSIS IN  
VASCULAR/HUMAN BRAIN MICROVESSEL  
ENDOTHELIAL CELLS**

**Dina Alshammari**

**A Thesis submitted in partial fulfilment of the  
requirements of the Manchester Metropolitan  
University for the degree of Doctor of Philosophy**

**School of Healthcare Sciences  
Manchester Metropolitan University  
October 2014**

## Contents

Background and purposes .....	5
Methods .....	5
Results .....	5
Conclusions.....	6
Declaration .....	7
Acknowledgment.....	8
List of abbreviations .....	9
List of units .....	10
Chapter 1 Introduction.....	11
General introduction.....	12
Citicoline: .....	12
Citicoline Structure .....	12
Citicoline Metabolism.....	14
Citicoline in Trials:.....	18
Stroke .....	29
Blood Vessels .....	37
Endothelial Cells.....	40
Blood Brain Barrier.....	41
hCMEC/D3 cell line.....	44
Angiogenesis .....	49
Matrigel™ .....	52
Cell Migration.....	55
Apoptosis .....	57
Aims .....	60
Chapter 2 Materials & Methods.....	61
Materials and Methods.....	62
Materials .....	62
Equipment.....	62
Required buffers .....	65
Cell culture medium.....	66
Methods.....	66

Cell culture and sub-culture.....	66
Preparation of freezing medium.....	67
Freezing and thawing of cells.....	67
Cell counting .....	67
Angiogenesis assays.....	68
Cell proliferation assay.....	68
Cell migration (Wound Healing).....	68
Tube like-structure formation in Matrigel™. ....	69
Hypoxia studies .....	69
Protein extraction and estimation. ....	70
Western blotting .....	72
Blotting.....	73
Blocking.....	74
Imaging and data analysis.....	75
Flow Cytometry. ....	75
Immunofluorescence.....	77
RNA extraction. ....	78
Quantification of nucleic acid. ....	79
cDNA Synthesis Using the RT <sup>2</sup> First Strand Kit.....	79
PCR microarray.....	80
Kinexusphospho-protein array analysis.....	81
Statistical analysis.....	82
Chapter 3 Results.....	83
Angiogenesis.....	84
Kinexus Assay .....	84
Pro-angiogenic effects of citicoline on hCMEC/D3 proliferation, migration and tube formation.....	85
Pro-angiogenic effects of citicoline on hCMEC/D3 tube formation. ....	87
HER-2 inhibition. ....	87
Erk 1/2.....	91
Pro-angiogenic effects of citicoline on hCMEC/D3 migration. ....	96
Apoptosis. ....	99

Protective effect of citicoline against hypoxia induced DNA damage in endothelial cells.....	99
Western Blotting .....	103
PARP expression.....	103
Caspase-3 expression.....	106
H2B Ser14 expression .....	110
Immunofluorescence .....	113
Active caspase-3.....	113
H2B Ser14.....	119
Flow Cytometry .....	124
Real Time PCR .....	131
Chapter 4 Discussion .....	133
Discussion .....	134
Conclusion. ....	158
Further Work .....	161
Chapter 5 References .....	162
References.....	163
Appendices .....	181
Appendix 1 .....	181
Reagents.....	181
Appendix 2 .....	184
Preparation of the Kinexus buffer.....	184
Appendix 3 .....	185
List of figures.....	185
Appendix 4 .....	190
List of tables .....	190
Appendix 5 .....	191
PCR data .....	191
Appendix 6 .....	198
Protein Estimation .....	198

**Background and purposes:** Citicoline, also known as CDP-choline (cytidine-5-diphosphocholine), is a naturally-occurring endogenous nucleoside, which is one of the neuroprotective drugs that have been used as a therapy in stroke patients. However, the mechanisms through which it acts are not fully understood. In terms of analysis of the signalling mechanisms associated with citicoline-induced protection, it has been previously shown that citicoline may protect the ischemic neurons by suppressing caspase apoptotic pathway activation. Moreover, preliminary in vitro studies have shown that citicoline induces angiogenesis (the formation of new blood vessels from pre-existing capillaries). However, the possible beneficial effects of citicoline treatment on revascularization and angiogenesis after stroke have not been fully examined. The present study was designed to investigate the key signalling mechanisms through which citicoline modulates apoptosis and angiogenesis-associated with stroke recovery.

**Methods:** An analysis of citicoline signalling pathway was studied from phospho-protein screening array done by Kinexus. In vitro angiogenesis assays: migration, proliferation and differentiation into tube-like structures in Matrigel™™ assays, have been used in human brain microvessel endothelial cells (hCMEC/D3). Western blotting was performed on protein extraction from hCMEC/D3 stimulated with citicoline. Analysis of apoptosis by flow-cytometry in hCMEC/D3. A hypoxia induced apoptosis assay was performed by seeding hCMEC/D3 on to glass coverslips in serum poor medium. Quantification of apoptotic cells were carried out under fluorescence microscopy using a combination of propidium iodide and DAPI stain solution. Apoptotic pathways in hCMEC/D3 stimulated with citicoline were examined by indirect immunofluorescence and real time PCR. Pharmacological inhibitor of Her2 (GW2974) was used to investigate the angiogenic signalling pathway by western blotting and Matrigel™ assay in hCMEC/D3 in the presence or absence of citicoline.

**Results:** Kinexus results showed an over-expression of ASK-1, HER2, IRS-1 and Jun and inhibition of Hsp27, Integrin alpha4, MEK1 (MAP2K1) and Histone H2B Ser14 proteins. Citicoline induced EC migration and differentiation in poly-l-lysine and Matrigel™. Using microarray screening, the Histone H2B (Ser14) appeared to be the main phosphor-protein expression blocked by citicoline in hCMEC/D3, and the expression of tyrosine-protein kinase erbB-2 receptor (Her2) appeared to be induced by citicoline in hCMEC/D3. Treatment with the Her2 inhibitor (GW2974) totally blocked citicoline induced endothelial tube formation in EC, whereas treatment with GW2974 in combination with FGF-2 did not affect FGF-2 induced endothelial tube formation. In cultured hCMEC/D3 treatment with GW2974 inhibited citicoline induced phosphor-Erk expression, whereas treatment with GW2974 in combination with FGF-2 did not affect FGF-2 induced phosphor-Erk expression. However, Citicoline had no mitogenic effects on hCMEC/D3. Phospho-Caspase-3 and phosphor-H2B (Ser14) expression were inhibited by citicoline in hCMEC/D3 whereas the expression of phosphor-Her2 and

phosphor-Erk expression were increased. Moreover, citicoline treatment showed a decrease in number of apoptotic cells (positive PI staining) in hypoxia induced apoptosis compared to untreated cells. In cell migration assay, treatment with citicoline significantly increased cells migration in hCMEC/D3 compared to untreated cells on hypoxia conditions. Detection of apoptotic cells by flow cytometry showed inconclusive results in both treated and untreated hCMEC/D3. Results from indirect immunofluorescence showed a significant increase in active Caspase-3 and H2B (Ser14) expression in citicoline treated cells in comparison with untreated cells in hypoxia conditions. Results from PCR showed inhibition of pro-apoptotic genes including BNIP3, BNIP3L, caspase 4, caspase 8, caspase 9, CIDEA, DFFA, LTBR, TP53BP2, TRADD, and TRAF3 with citicoline treatment. They also show an over-expression of a number of anti-apoptotic genes including NAIP, NOD1, TNFRSF25, and TP53.

**Conclusions:** A screening of phosphor-protein expression revealed that citicoline specifically over-expressed Her2 which demonstrated that citicoline plays a key role in Her2 induced angiogenesis. Blocking of Her2 pathway inhibited the formation of tube-like structures in citicoline treated cells and therefore citicoline induces angiogenesis through Her2 pathway, and that is important in terms of understanding the molecular pathway in which citicoline acts as a pro-angiogenic molecule in tissue remodelling after stroke. Citicoline decreased active caspase-3 and H2B (Ser14) expression, and positive PI staining which demonstrates a protective effect of citicoline against endothelial cells apoptosis. Citicoline also improved cell survival by decreasing the expression of BNIP3, BNIP3L, caspase 4, caspase 8, caspase 9, CIDEA, DFFA, LTBR, TP53BP2, TRADD, and TRAF3 genes and inducing the expression of NAIP, NOD1, TNFRSF25, and TP53. Citicoline treatment significantly promotes wound healing in stroke mimicking conditions (hypoxia). Thus, the therapeutic properties of citicoline has the potential to promote vessel formation whilst reducing the risk cell death from hypoxic stress following ischemic stroke.

**Key words:** Citicoline, angiogenesis, apoptosis, stroke.

**Declaration:**

I hereby declare that this work has been composed by myself, and has not been accepted for any degree before and is not currently being submitted in candidature for any degree other than the degree of Doctor of Philosophy of the Manchester Metropolitan University.

Dina Alshammari

## **Acknowledgment:**

No project such this can be carried out by only one individual. Foremost, thanks to almighty God, the source and origin of all knowledge.

I would like to express my sincere appreciation and gratitude to my advisor Prof. Mark Slevin for the continuous support of my Ph.D study and research, for his patience, motivation, enthusiasm, constructive criticism, and immense knowledge. His kindness and guidance helped me throughout my research and writing of this thesis. One simply could not wish for a better supervisor

I would like to express my deep gratitude and respect to Mr. Glenn Ferris an excellent technical officer who helped me learn several laboratory techniques including; fluorescence microscopy, flow cytometry, transporting hypoxia cylinder, indirect immunofluorescence, and providing quotes for ordering laboratory materials. His outstanding attitude and vast knowledge helped me to carry on my laboratory work. Dr.Ria Weston have helped me with RNA work and her advices were of a great assistance to me.

In my daily work I have been blessed with a friendly and cheerful group of fellow students. Kamela Ali, who helped in cell culture, wound healing assay, and PCR work. Manal Abudawood, who provided good arguments about western blotting techniques and buffers preparations. Hana Sharif, who gave me great tips in how to write up my thesis. They also gave me the moral support that helped during me work. Stuart Fielding who helped me with PCR microarray and in preparing buffers and showed me how to use a nano drop. Daniel Watkinson, who provided me with a great assistance in flow cytometry work.

My sincere deepest gratitude to all my family; my parents, my husband, and my children for their support and encouragement through this work.

Finally I would also like to extend my greatest thanks to my sponsor (Ministry of Higher Education) Thank you for the financial and moral support throughout my course, without you this work could not have been possible.



## List of abbreviations

BSA	Bovine Serum Albumin
DMSO	Dimethyl sulfoxide
DNA	Deoxyribonucleic acid
EBM-2	Endothelial cell basal medium-2
EDTA	Ethylenediaminetetraacetic acid
ERK1/2	phospho-extracellular-signal regulated kinase 1/2
FBS	Foetal Bovine Serum
FGF-2	Fibroblast Growth Factor-2
H2B	Histone H2B
Her2	Receptor tyrosine-protein kinase erbB-2
HCMEC/D3	Human Cerebro-vascular Microvessel endothelial cell line
PBS	Phosphate Buffered Saline
PCR	Polymerase chain reaction
P.I	propidium iodide
RNA	Ribonucleic acid
Rpm	Round per minute
SDS	Sodium dodecyl sulfate
SPM	Serum Poor Medium
TBST	TBS Tween
TEMED	N,N,N",N"- tetramethylethylenediamine

## List of units

%	Percentage
µg	microgram
µL	microliter
µm	micrometer
bp	base pair
cm	centimetre
Da	Dalton
g	gram
h	hour
k	kilo
min	minute
ml	millilitre
mm	millimetre
mM	millimolar
°C	degree Celsius
RPM	revolutions per minute
Sec	second

# Chapter 1 Introduction

## **General introduction.**

### **Citicoline:**

#### **Citicoline Structure:**

Cytidine 5'-diphosphocholine, CDP-choline, or citicoline is a crucial intermediate in the biosynthesis of structural phospholipids in cell membranes, specifically phosphatidylcholine. CDP-choline ( $C_{14}H_{26}N_{11}O_4P_2$ ) is a polarised molecule with a molecular weight of 488.33 g/mol. The monosodium salt of CDP-choline (MW=510.31) is a white, crystalline, spongy, very hygroscopic powder that is soluble in water and almost insoluble in alcohol. Citicoline is the International Nonproprietary Name (INN) for cytidine diphosphate-choline (CDP-Choline) and cytidine 5'-diphosphocholine. Citicoline has been extensively studied in numerous countries in different parts of the world and has more than 70 trade names. The use of CDP-choline (citicoline) as a therapy to enhance endogenous phosphatidylcholine synthesis, is an attractive concept, because it might speed up the replacement or repair of cellular membranes which could play a critical role in the function of numerous physiological processes. It could have a potential medicinal efficacy in numerous diseases in which membrane disorder, dysfunction, or degeneration results in cellular and tissue ischemia and necrosis. Following administration by both the oral and parenteral routes, CDP-choline is hydrolysed to choline and cytidine. Orally administered CDP-choline is efficiently absorbed, and therefore, bioavailability by the oral route is almost the same as the intravenous route. After absorption, citicoline is extensively dispersed throughout the body, crosses the blood-brain barrier and reaches the central nervous system (CNS), where it is incorporated into the membrane and microsomal phospholipid fraction.

Citicoline increases brain metabolism, activates biosynthesis of structural phospholipids of neuronal membranes, and regulates the levels of different neurotransmitters. In the brain, choline is metabolized to phosphorylcholine, which then integrates with CTP to produce intracellular CDP-choline which is subsequently converted to phosphatidylcholine. In the brain, Choline is also converted to acetylcholine especially in cholinergic neurons. Choline from neuronal membrane phosphatidylcholine is used for the synthesis of acetylcholine in case of depletion in acetylcholine levels in the brain (Secades & Lorenzo, 2006, Rema et al., 2008, Weiss, 1995).

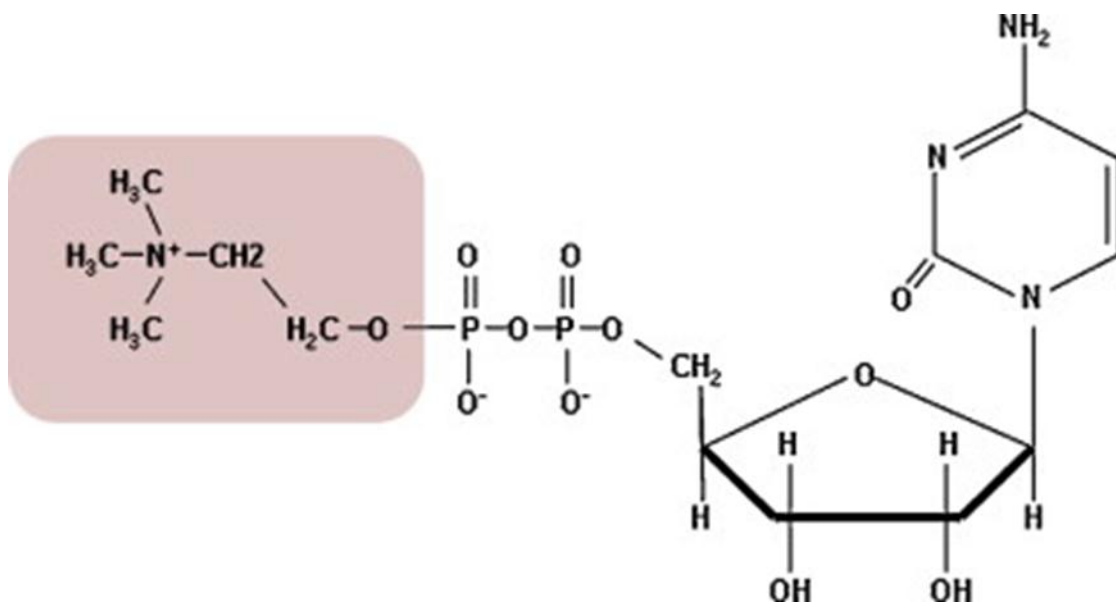


Figure 1. Citicoline Structure. It is composed of ribose, pyrophosphate, cytosine and choline. It is organized in two moieties, cytidine and choline, that are linked by a diphosphate bridge (Jamboua et al., 2009).

## **Citicoline Metabolism.**

Exogenous CDP-choline when administered orally or by injection to rats, is fully metabolized to produce two intermediates; choline and cytidine. These intermediates pass through the circulation, cross the blood brain barrier and are partially altered to acetylcholine phosphocholine, and CTP. Previous studies demonstrated that, in humans as in rats, the metabolism of exogenous CDP-choline raises plasma levels of cytidine as well as choline (Wurtman et al., 2000). Cytidine and choline have essential roles in phospholipids production involved in membrane formation and repair. They also play part in such important metabolic functions as the production of nucleic acids, proteins, and acetylcholine. When citicoline is orally administered, it is hydrolysed in the intestine, absorbed rapidly as choline and cytidine, resynthesized in liver and other tissues, and finally mobilized in CDP-choline synthetic pathways (Weiss, 1995). In animals, choline can be obtained from the diet and via de novo biosynthesis: choline is produced through the conversion of phosphatidylethanolamine (PE) to phosphatidylcholine (PC) which is catalysed by an enzyme called phosphatidylethanolamine N-methyltransferase (PEMT). Then choline can be produced from PC via the action of phospholipases (Li & Vance, 2008). The two pathways of PC synthesis and break down are important to the cellular homeostasis and therefore disruption of PC homeostasis in mammalian cells leads to apoptosis. Choline is an important compound in PC synthesis as well as other major phospholipids, and an important neurotransmitter acetylcholine, and an essential nutrient that can be found in normal diet like, beef, liver, eggs, cauliflower, whole milk, grapes, etc. Mitogenic stimulations by growth factors or oncogenic transformation activate PLD-driven PC hydrolysis to yield choline and phosphatidic acid (PA). This type

of choline along with choline from external sources enters the Kennedy pathway (Janardhan et al., 2006).

The process of choline transportation across the cell membrane is an important process that is highly regulated and associated with CDP-choline pathway and choline metabolism. Choline transporters play two roles including mainly choline uptake from the extracellular space and directing choline to mitochondria for degradation, cellular exit of choline in mammals, and betaine generation. Betaine is an osmolyte, which is used in the kidney to regulate physiological osmotic pressure. In the liver betaine is utilized in methyl group metabolism which is linked to PC synthesis via the PEMT reaction (Fagonea & Jackowski, 2013).

Choline is a neutral molecule with a positive and a negative electrical charge (zwitterion) that is positively charged at certain pH, which requires transport systems to allow this amine to cross the phospholipid bilayer of cellular membranes. In higher eukaryotes, there are three types of transporters that mediate choline movement in and out of the membrane. Kinetic studies conducted using radiolabeled choline and inhibitors discovered three systems for choline transport including low-affinity facilitated diffusion, high-affinity, Na<sup>+</sup>-dependent transport, which are linked with the synthesis of acetylcholine in neurons, and intermediate-affinity, Na<sup>+</sup>-independent transport. However, choline transporter-like proteins have been recently identified. They include polyspecific organic cation transporters (OCTs) with low affinity for choline, high-affinity choline transporters (CHT1s), and intermediate-affinity choline transporter-like (CTL1) proteins. CTL1 is Na<sup>(+)</sup>-independent and sensitive to inhibition by the drug hemicholinium-3. The expression of genes associated with cell proliferation,

differentiation, and apoptosis, are affected by choline deficiency and it has been involved in liver dysfunction and cancer. Abnormalities in choline transport and metabolism have been associated with a number of neurodegenerative disorders such as Alzheimer's and Parkinson's disease (Michel & Bakovic, 2012, Michel et al., 2006).

The Kennedy (CDP-choline) pathway and the phosphatidylethanolamine (PE) methylation pathway are the two pathways in which PC can be synthesized de novo in mammalian cells. In the CDP-choline pathway, there are three reactions: the first reaction is the ATP-dependent phosphorylation of choline, which is catalysed by an enzyme called choline kinase (CK) to form phosphocholine (P-Cho), and the byproduct ADP. The second reaction is considered to be the rate-limiting step of the Kennedy pathway, CTP:phosphocholinecytidyltransferase (CCT) phosphoethanolamine and CTP to form the high-energy donor CDP-phosphocholine with the release of pyrophosphate. In the final reaction of the pathway, cholinephosphotransferase (CPT) transfers a phosphocholine group from CDP-choline to diacylglycerol (DAG) to form PC (Aoyama et al., 2004, Henneberry et al., 2001).





## Citicoline in Trials:

There has been an increased recognition of citicoline as a neuroprotectant drug that may act both in early and late stages of ischemic damage, resulting in an escalation in experimental and clinical trials studying safety and efficacy of its use as a treatment for stroke. The neuroprotective properties that citicoline exhibits could be due to its ability to enhance PC synthesis in the injured brain. Citicoline increase membrane stability and promotes repair drives the synthesis of nucleic acids, proteins, acetylcholine, and other neurotransmitters; reduces the free radical formation; inhibits free fatty acid production and has anti-apoptotic effects (Sahota & Savitz, 2011). In a study, it was found that in normal rats treated daily with citicoline for 3 months, PC levels increased by 25%.

Treatment with citicoline prior to an ischemic event decreased the loss of PC during ischemia. It also decreased the levels of arachidonic acid release and in part restored phospholipid loss after ischemia/1-day reperfusion. It has also been demonstrated to have inhibitory effects against phospholipase A2 activation. Phospholipase A2s (PLA2s) is a family of esterases that hydrolyze the sn-2 ester bond in phospholipids, producing free fatty acids and lysophospholipids. PLA2s play an important role in the signalling pathways of numerous cellular processes including inflammation. Reports demonstrate that PLA2s control cell damage caused by drug, chemical and ischemia/reperfusion.

The role of PLA2s in apoptosis and ischemic cell death relies on the PLA2 isoform, the cell type, and the cause of injury. Citicoline may alter the levels of several lipids after ischemia and reperfusion. It has been previously reported that citicoline administered at 0 and 3 hours after transient ischemia demonstrated significant neuroprotection, however treatment with citicoline after the first 2 doses showed greater protection.

These data suggest that citicoline has an effect in events beyond the first day of reperfusion that are important for its neuroprotective effects. Glutathione is one of the main endogenous antioxidant defence systems in the brain, and it plays important roles in antioxidant defence, nutrient metabolism, and regulation of cellular events (including gene expression, DNA and protein synthesis, cell proliferation and apoptosis, signal transduction, cytokine production and immune response, and protein glutathionylation). It can be produced through a process in which choline released from citicoline is metabolised to methionine which in turn might be converted to glutathione through S-adenosyl-L-methionine. Glutathione deficiency contributes to oxidative stress, which plays a key role in aging and the pathogenesis of many diseases including kwashiorkor, seizure, Alzheimer's disease, Parkinson's disease, liver disease, cystic fibrosis, sickle cell anemia, HIV, AIDS, cancer, heart attack, stroke, and diabetes. It has been reported that significant reduction in glutathione and glutathione reductase activity after transient cerebral ischemia. Since oxidative damage contributes to neuronal death, citicoline may provide neuroprotection by increasing this defence system (Wu et al., 2004, Cummings et al., 2000, Adibhatla et al., 2001). The CDP pathway has been a major target for drug development since the appearance of citicoline in the clinical field. This caused a development in dosage, administration techniques, and defining criteria of patients to which the therapies were given. It also created variations in clinical studies, including length of observation, severity of disturbance, and methodology of evaluation of the results. Citicoline is a commonly prescribed treatment for cognitive impairment in many European countries, especially when the clinical picture is mainly one of cerebrovascular disease (Fioravanti & Yanagi, 2000).

Citicoline is also involved in the biosynthesis of sphingolipids especially in that of sphingomyelin in the following reaction; ceramide reacts with citicoline to form sphingomyelin, the reaction is being catalysed by CDP choline ceramidophosphocholinetransferase. Sphingomyelin is an important component of neuronal membranes. Citicoline crosses the blood-brain barrier as cytidine and choline, which reach the brain and resynthesize citicoline in the cytoplasm. Citicoline is integrated widely in several brain areas. It also affects the levels of various neurotransmitters including dopamine, serotonin and noradrenaline. Citicoline was shown to elevate noradrenaline levels in the cortex and hypothalamus. Furthermore, it was demonstrated to elevate overall urinary excretion of 3-methoxy-4-hydroxyphenilglycol, which reflects noradrenergic activity in rats and humans, indicating that citicoline increases noradrenaline release (Vasudevan et al., 2013, Platarasa et al., 2000).

Citicoline has the potential to improve endogenous brain plasticity and repair which may reduce acute brain damage and improve functional recovery in animal models of stroke, even when it is administered several hours after the ischemic event. Moreover, it has been demonstrated that citicoline affects different levels of the ischemic cascade, and a series of brain repair have been documented. It also have been reported that citicoline restores the activity of mitochondrial ATPase and membrane Na<sup>+</sup>/K<sup>+</sup> + ATPase, and to accelerate reabsorption of cerebral edema in numerous experimental models (Overgaard, 2014).

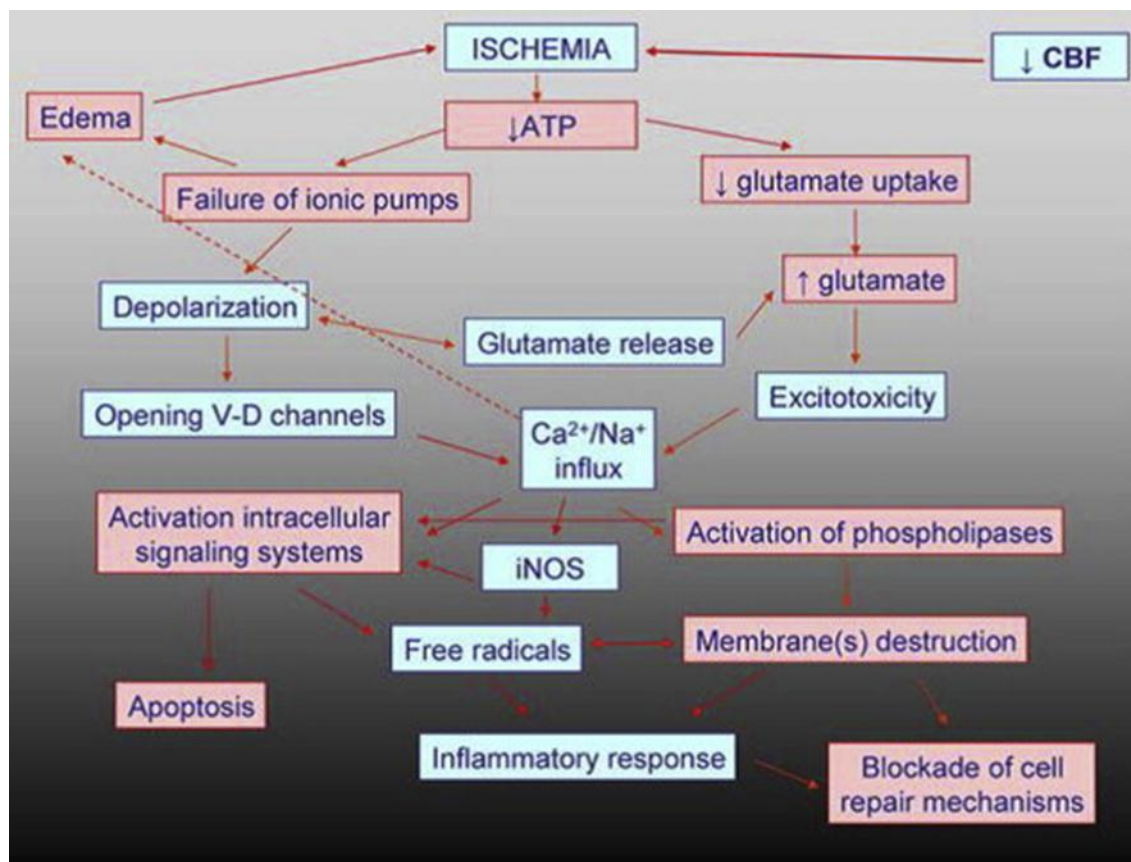


Figure 3. The points where citicoline has been reported to have a pharmacologic effect in the ischemic cascade are marked in red (Overgaard, 2014).

The initial properly designed clinical trials using citicoline in acute stroke patients demonstrated positive outcomes; however, the sample size of these studies was insufficient. In the United States, the clinical development of citicoline as a therapy of acute ischemic stroke started in the 1990s. The first US phase II to III trial was preformed to assess the effect of 3 doses (500, 1000, and 2000 mg/d) of citicoline against placebo. Treatment using citicoline at doses of 500 and 2000 mg/d showed significant improvement of neurological (National Institutes of Health Stroke Scale [NIHSS]), functional (Barthel Index [BI]), and global (modified Rankin Scale [mRS]) results in comparison with placebo 12 weeks after stroke onset. In the second study,

treatment with citicoline 500 mg displayed significant improvements in a subgroup of patients with moderate to severe strokes (baseline NIHSS  $\geq 8$ ) with regard to functional recovery (BI  $\geq 95$ ) compared with placebo (Dávalos et al., 2002). There are other numerous clinical trials conducted to examine the effect of citicoline, however the results were inconclusive. One of the main reasons behind the controversy on the effectiveness of citicoline is the variations in the drug administration in the clinics (oral versus intravenous), considering that only 0.2–2.0% of the administered citicoline reaches in the brain parenchyma, subject to the administration route. The polar nature of citicoline compromises the passing of the drug through the blood brain barrier (BBB). Thus, using alternative methods of citicoline administration to enhance its bioavailability in the brain parenchyma, would potentially improve the therapeutic effects of this drug in stroke treatment. One of these drug delivery systems is the use of liposome encapsulation. In a study using longitudinal MRI, volumes and edema in an animal model of stroke were measured. Nineteen rats were subjected to permanent occlusion of the middle cerebral artery and treated with saline, intraperitoneal citicoline (500 mg/kg), intravenous citicoline (48 mg/kg), and intravenous liposome-encapsulated citicoline (48 mg/kg). Lesion volumes were measured by MRI at days 0, 1, 3 and 7 following surgery. The results demonstrated that the therapeutic efficiency of citicoline has increased using encapsulation in liposomes. There was a 32% reduction of the infarct sizes at day 7, in comparison with controls where infarct sizes at day 7 increased by 39%, respect to values at day 0. Intravenously injected citicoline reduced infarct sizes by 9% while intraperitoneal citicoline increased the infarct sizes by 10%. Animals treated with citicoline, in all of the forms of delivery, displayed an insignificant reduction

of edema formation. There was a clear reduction in lesion volumes using liposome-encapsulated citicoline at days 1, 3 and 7 following permanent stroke compared to control, citicoline I.P and I.V (Ramos-Cabrer et al., 2011).

Moreover, citicoline can be used in combination with other treatments. In a study, the effects of citicoline were evaluated on the suppression of apoptotic processes after transient focal cerebral ischemia, either administered alone or combined with hypothermia. To conduct this study, middle cerebral artery occlusion (MCAo) was performed for 2 hours on Sprague-Dawley (SD) rats using intraluminal thread insertion. There were five groups with different treatments including, sham-operated, saline, citicoline (400 mg/kg intraperitoneal.), hypothermia ( $34 \pm 1$  °C) and citicoline + hypothermia group. For 24 hours, all rats were reperfused, and after transcatheter perfusion, immunohistochemical studies were conducted for markers of apoptosis. The saline group exhibited lower Bcl-2 immunostaining score compared to the citicoline, hypothermia and citicoline + hypothermia groups. Bcl-2 family members acting as oncogenic and anti-death molecules regulate various homeostatic, developmental and disease progressions. Anti-apoptotic protein bcl-2 binds to beclin 1 under non-stress conditions and inhibits autophagy. In the sham-operated group, the Bcl-2 immunostaining score was lower compared to compared to the citicoline, hypothermia and citicoline + hypothermia groups. There was higher expression of caspase-3 proteins in the saline group compared to citicoline + hypothermia group. Cysteiny aspartate-specific proteases (caspases) include a dozen of distinct enzymes that are involved in inflammation, activation, or execution of the apoptotic biochemical events. They play an important in role in programmed cell death, which occurs physiologically through

defined morphological and biochemical features, namely apoptosis, necroptosis, or programmed necrosis. Bax proteins were also increased in saline group compared to citicoline + hypothermia group and inhypothermia group compared to citicoline + hypothermia group. Bax is a proapoptotic member of the Bcl-2 family, which is normally found in the cytosol and is trans-located to mitochondria when cells are under apoptotic stress. Bax induces opening the mitochondrial permeability transition pore, which stimulates the release of cytochrome C followed by an apoptotic cascade. In the saline group, significant differences in caspase-9 immunostaining results were revealed compared to citicoline + hypothermia group; citicoline group compared to citicoline + hypothermia group; and hypothermia group compared to citicoline + hypothermia group. Therefore, by inhibiting apoptotic pathways using citicoline in combination with hypothermia is more effective than either used alone in ameliorating cerebral damage after transient focal ischemia (Sahina et al., 2010, Sawadaa et al., 2014, Nicholson et al., 2013, Baspinara et al., 2014).

Citicoline has also been used in combination with lithium, which is the first drug to show significant upregulation of Bcl-2 in rodent brain in vivo and cells with human neuronal phenotype. In a study, citicoline in combination with lithium (Li-) have been demonstrated to promote retinal ganglion cell (RGC) survival and axon renewal in vitro. A model of both brain axonal injury and particular aspects of the glaucomatous degeneration of RGC, which is an optic nerve crush (ONC) model, was used to measure the level of protection provided by citicoline and lithium to RGC and to determine whether their effects are regulated by increased expression of Bcl-2. The study was conducted using Adult rats (6–12 per group) that were subjected to ONC



accompanied by a contralateral sham operation. The treatments included intraperitoneal injection with either vehicle, citicoline sodium (1 g/kg daily for up to 7 days and 300 mg/kg daily afterwards), lithium chloride (30 mg/kg daily), or both drugs combined. Fluorogold was injected bilaterally into superior colliculi 1, 5 or 19 days after ONC. 2 days after tracer injection, stained cells were counted under a fluorescence microscope. The effects of treatments on expression of Bcl-2 in retinas were measured by immunohistochemistry in a separate set of experiments. The results showed a progressive reduction of RGC density after crush in vehicle-treated animals. In citicoline-treated animals, the reduction in RGC density was attenuated 1 week and 3 weeks after the crush. RGC protection was even more prominent in the lithium-treated group. The result from animals treated with both drugs was approximate to that achieved by lithium treatment. Bcl-2 immunoreactivity was seen mostly in retinal ganglion cells. In the lithium and citicoline group as well as in animals treated with the combination of both drugs, there was an increase in Bcl-2 immunoreactivity. Citicoline and lithium were demonstrated to be protective of RGC and their axons in vivo against delayed degeneration triggered by the ONC. Therefore, the increase in Bcl-2 expression triggered by both drugs could be the cause of the observed retino-protective action (Schuettauf et al., 2006, Goodwin & Jamison, 2007).

In another study, the combination of rtPA with citicoline as compared to either alone as monotherapy, and whether the neuroprotector should be administered before or after thrombolysis to achieve a greater decrease of ischemic brain damage was tested in a rat embolic stroke model. Recombinant tissue plasminogen activator (rtPA) is an approved drug, that is administered on stroke patients and it works by dissolving

thrombi obstructing cerebral blood flow. The aim of the study was to test if combining reperfusion mediated by thrombolytics with pharmacological neuroprotection aimed at inhibiting the physiopathological disorders responsible for ischemia-reperfusion damage, could offer a better treatment of ischemic stroke. The study was conducted using one hundred and nine rats four were sham-operated and the rest embolized in the right internal carotid artery with an autologous clot and divided among 5 groups including control, iv rtPA 5 mg/kg 30 min post-embolization, citicoline 250 mg/kg ip x3 doses, 10 min, 24 h and 48 h post-embolization, citicoline combined with rtPA following the same pattern, rtPA combined with citicoline, with a first dose 10 min after thrombolysis. To evaluate ischemic brain damage, numbers of factors were considered including death, neurological score, size of ischemic lesion and neuronal death (TUNEL) after 72 h and plasma levels of IL-6 and TNF- $\alpha$ . Compared with controls, the use of citicoline after thrombolysis produced the greatest reduction of mortality caused by the ischemic lesion, infarct volume, number of TUNEL positive cells in striatum and plasma levels of TNF- $\alpha$  at 3 h and 72 h. rtPA induced reperfusion displayed an insignificant decrease of infarct size and neuronal death, although it reduced mortality due to brain damage, an increase in the risk of fatal bleeding was observed. Citicoline as monotherapy only produced a significant reduction of neuronal death in striatum. The combination of citicoline before rtPA did not add any benefit to rtPA alone. The superiority of the combined treatment with rtPA followed by citicoline suggests that early reperfusion should be followed by effective neuroprotection to prevent ischemia-reperfusion injury and improve the level of protection of the tissue at risk (Alonso de Leciñana et al., 2006, Ryou et al., 2013).

Another study was conducted to analyse the effects of citicoline in staurosporine-induced cell death in human SH-SY5Y neuroblastoma cells. The results showed that citicoline decreases apoptosis induced by 100 nM staurosporine for 12 h in SH-SY5Y cells. Pre-treatment of 60 mM citicoline for 24 h after staurosporine stress, yield a higher reduction in apoptosis. Furthermore, glutathione redox ratio reduced after staurosporine stress was restored after citicoline treatment. When citicoline was added to the cell culture 24 hr before the addition of staurosporine, the expression levels of active caspase-3 and cleaved PARP induced by staurosporine were inhibited by the action of citicoline. These results show that citicoline affects the staurosporine-induced apoptosis cell-signalling pathway by interacting with the glutathione system and by inhibiting caspase-3 in SH-SY5Y human neuroblastoma cells (Barrachina et al., 2002).

In combination with levodopa, citicoline has been used as a therapeutic agent in the treatment of Parkinson's disease (PD). Levodopa is a precursor of dopamine and norepinephrine, and is one of the most effective symptomatic treatment options for Parkinsonism with a preferred safety and tolerability profile. In a study, the effects of citicoline was evaluated by using validated in vivo and in vitro models. Citicoline plays a neuro-protective role in 6-OHDA-treated SH-SY5Y neuroblastoma cells and following 6-hydroxydopamine (6-OHDA)-induced neurodegeneration. 6-Hydroxydopamine (6-OHDA) is a selective catecholaminergic neurotoxin extensively used to examine the pathogenesis and progression of PD. Citicoline also increased the levels of reduced glutathione (GSH), a major antioxidant agent, in 6-OHDA-treated SH-SY5Y neuroblastoma cells. Furthermore, citicoline (500 mg/kg i.p.) administered for 7 days improved functional behaviour by significantly decreasing the number of apomorphine-

induced contralateral rotations in 6-OHDA rats. Finally, citicoline considerably decreases substantia nigra (SN) dopaminergic cell dropout and tyrosine hydroxylase immunoreactivity in the ipsilateral striatum in rats injected intrastratially with 6-hydroxydopamine (6-OHDA) (Noack et al., 2014, Barrachina et al., 2003).

Citicoline has also been a subject of interest in the search for a combination of treatments with corresponding effects that could act at different stages in the ischemic cascade. In an experiment, the effects of nimodipine, a dihydropyridine that blocks L-type  $\text{Ca}^{2+}$  channels, in combination with citicoline have been tested in a rat model of reversible focal cerebral ischemia. The method of drug delivery involved intracarotid injection of citicoline and nimodipine to the ischemic cerebral tissue, prior to blood recirculation. When using an intravenous way, the efficiency of the treatment would be obstructed due to an inadequate perfusion in the ischemic zone. Nevertheless, the drug therapy reaches the ischemic area in a fast, concentrated and effective way when using an arterial route. The results showed that intracarotid injection of nimodipine in order to permeate the ischemic cerebral tissue just before recirculation or regular administration of citicoline by an i.p. route in order to decrease the harmful effects caused by cell membrane damage, during either ischemia or reperfusion, reduced infarct volume in an animal model of temporary focal cerebral ischemia with complete reperfusion and 7 days of survival. Moreover, the combination of both drugs caused a greater reduction in infarct volume, compared with when either drug was given independently. Similarly, this combined treatment produced a higher reduction in apoptotic cell death and increased Bcl-2 expression in the inner boundary zone of the infarction 3 days after reperfusion (Sobrado et al., 2003).

In a study, the neuroprotective effect of citicoline on experimental models of KA-induced retinal damage was evaluated. KA is a structural analogue of L-glutamate and an agonist of ionotropic KA receptors. Intravitreal injection of kainic acid (KA) triggers rapid and selective lesions in the inner retina of rats with the photoreceptor cell-sparing, it is well established that glutamate receptor-related neurotoxicity can be induced by NMDA (N-methyl-D-aspartic acid) and KA. Exposure to high concentrations of glutamate and glutamate analogues induces neuronal damage followed by cell loss in retinas stimulating the activation of NMDA receptors or KA/AMPA (kainic acid/ $\alpha$ -amino-3-hydroxy-5-methyl isoxazole-4-propionic acid) receptors. Citicoline treatment twice daily for 7 days inhibited the thinning of the inner retinal layers resulting from KA-injection and the degradation of the immune-reactivities of retinal choline acetyltransferase (ChAT), which is a key constituent of cholinergic neurons required for acetylcholine (ACh), and tyrosine hydroxylase (TH), which is the rate-limiting enzyme in the biosynthesis of the catecholamines dopamine, noradrenaline, and adrenaline (Lévesque & Avoli, 2013, Park et al., 2005, Dickson & Briggs, 2013).

**Stroke:**

Stroke is a general term that refers to a focal neurologic event that is severe in onset and may have a vascular cause, etiology, or relevance. There are numerous terms that could be used to specify stroke depending on the type or the location of stroke such as hemorrhagic stroke, ischemic stroke, lacunar stroke, embolic stroke, young stroke, thrombotic stroke, spinal cord stroke, venous stroke, brain-stem stroke, and cerebellar stroke (Wityk & Llinas, 2007). It is estimated that stroke is the cause of 9% of deaths and is the second foremost cause of mortality around the world. Currently there are an

estimated 5.7 million stroke deaths which by 2030 is expected to increase to 7.8 million. It is expected that in low-income and middle-income countries most stroke mortality (87%) will take place. In developing countries, a rise in stroke mortality is equivalent to an increase in chronic stroke disease burden of almost 50% of total disease burden in the past 10 years. These tendencies could be related to the aging population and changes in cardiovascular disease risk factor profiles which contribute to early death (Bornstein, 2009). Previous predictions indicated that there would be a 30% increase in numbers of patients suffering a first-ever stroke in the UK between 1983 and 2023, therefore increasing the demand on stroke medical facilities. Although there is a recent reduction in the rate of stroke incidence, there is an increase in the number of aging populations and the general burden of stroke which is likely to increase because of the rise in prevalence. Recent research demonstrates that survival after stroke is increasing, however patients could live with the consequences which can have significant effects on their lifestyle. It is important to improve stroke survival rate and decrease disabilities through medical interventions (Williams et al., 2010).

Risk factors for a first stroke may be categorised according to whether they are: (1) uncontrollable; (2) well recorded and controllable, and (3) less well recorded or potentially controllable. The uncontrollable risk factors include: age, gender, family history, low birth weight and race. Well-documented and modifiable risk factors include: cardiovascular disease, coronary heart disease, heart failure, peripheral arterial disease hypertension, tobacco smoking, diabetes mellitus, asymptomatic carotid stenosis, atrial fibrillation, sickle cell anaemia, dyslipidaemia, high total cholesterol, low high-density lipoprotein cholesterol, dietary factors ( sodium intake >2300 mg, potassium intake

<4,700 g), obesity, lack of physical exercise and postmenopausal hormone replacement therapy. Less-well recorded or potentially controllable risk factors include: metabolic syndrome, alcohol abuse, hyperhomocysteinemia, drug abuse, hypercoagulability, oral contraceptive use, inflammatory processes, migraine, high lipoprotein (a), high lipoprotein-associated phospholipase A2 and Sleep apnoea (Binder et al., 2012). Hypertension is one of the most important stroke risk factors. As blood pressure (BP) increases above 115/75 mm Hg the risk of stroke increase. BP values above the optimal rate of (<120/80 mm Hg) are associated with an increased stroke risk in males and females equally and for both fatal and nonfatal strokes. However, hypertension prevalence is higher in women at older age which could be due to women having a longer life expectancy than men. This could be the reason behind the overall higher stroke incidence in women than in men, because women account for 60% of all stroke events (Gorgui et al., 2014).

Another major stroke risk factor is diabetes mellitus. Diabetes mellitus is a group of metabolic disorders characterized by hyperglycemia caused by abnormalities in insulin secretion, insulin action, or both. The chronic hyperglycemia of diabetes is associated with long-term damage, dysfunction, and failure of various organs, mainly the eyes, kidneys, nerves, heart, and blood vessels. It is increasingly common and it is an independent risk factor for ischaemic stroke by approximately doubling the risk. There are currently almost 2 million diabetics in the UK with an increase of 500,000 over the last 10 years. In the past 40 years, the prevalence of type 2 diabetes has doubled from 4 to 8 per cent in the USA. In China the prevalence in adults has tripled from 1 to 3.2 per cent between 1980 and 1996, and on other parts of Asia the increase is even more

worrying with rates increasing three-to fivefold in countries such as Thailand and Indonesia in the past 3 decades. Diabetes is usually associated with hypertension and higher blood cholesterol levels, and therefore it particularly increases the risk of vascular disease. Studies adjusting for these other risk factors still found that there is a two-fold increase in the risk of stroke in the presence of diabetes. Therefore, the rapid increase in obesity, and therefore in type 2 diabetes, will increase the risk of stroke. Diabetes possibly causes 10-20 per cent of all strokes (American Diabetes Association, 2008, Lindley et al., 2008).

There are two main types of stroke: haemorrhagic stroke ischemic stroke.

Haemorrhagic stroke refers to bleeding in the skull, either into the brain or into the fluid around the brain. The second main type of stroke is called ischemic, which refers to a blockage of blood supply to the brain. Hemia is a suffix that always refers to blood.

Haemorrhage and ischemia are completely opposite to each other. Haemorrhage is characterized by excess amount of blood inside the skull. In ischemia, there is insufficient blood supply to support continued normal functioning of the affected brain tissue. Brain ischemia is much more common than haemorrhage and about four strokes out of every five are ischemic (Caplan, 2010).



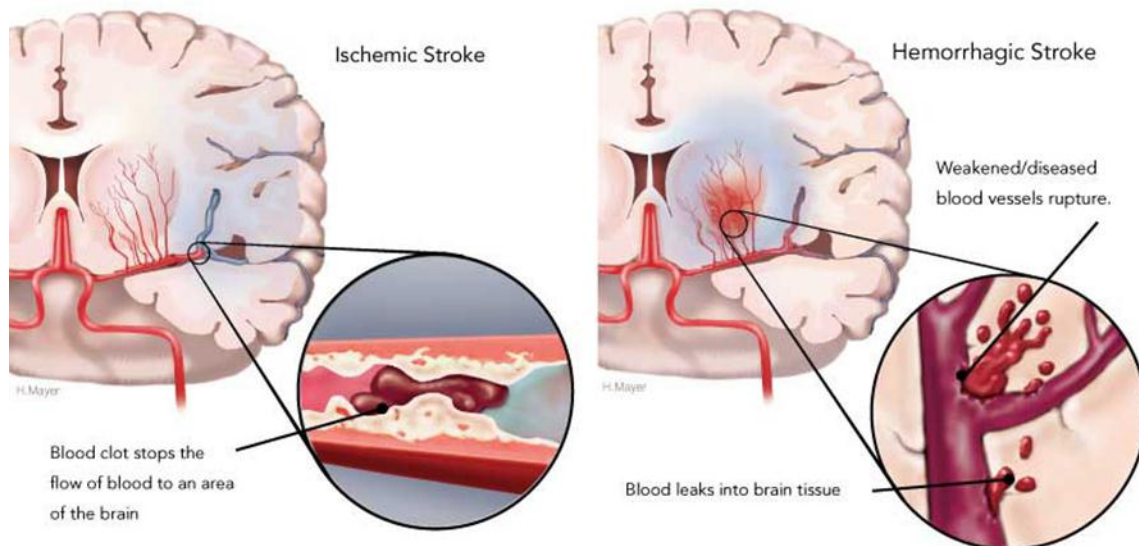


Figure 4. A representation of the two major types of stroke (Heart and Stroke Foundation, 2014).

Ischemic stroke can be subdivided into three categories: thrombosis, embolism, and decreased systemic perfusion. Thrombosis is a term that refers to an obstruction of blood supply due to a localized occlusive process within one or multiple blood vessels. The lumen of the vessel is narrowed or occluded by a change in the vessel wall or by the formation of superimposed clot. Embolism refers to the formation of material in a different location within the vascular system blocking an artery, and therefore stopping blood flow. Blockage can be transient or may continue for hours or days before moving distally. In comparison to thrombosis embolic luminal blockage is not caused by a localized process originating within the blocked artery. The material causing the blockage, arises proximally mainly from the heart; from major arteries such as the aorta, carotid, and vertebral arteries; and from systemic veins. Decreased systemic perfusion refers to restricted blood flow to brain tissue that is caused by low systemic perfusion

pressure. The most common causes are cardiac pump failure which is most often due to myocardial infarction or arrhythmia and systemic hypotension which is caused by blood loss or hypovolemia (Caplan, 2009).

The main cause of haemorrhagic stroke is primary intracerebral haemorrhage from a spontaneous rupture of small vessels, which accounts for approximately 80% of haemorrhagic strokes, and is caused mainly by unmanaged high blood pressure. Subarachnoid haemorrhage accounts for about 50% of haemorrhagic strokes, and is a result of a rupture in the intracranial aneurysm caused by a weakening in the arterial wall. Another common cause of intracerebral haemorrhage in the elderly is cerebral amyloid angiopathy, which results from a damage caused by the deposit of beta-amyloid protein in the small and medium-sized blood vessels of the brain (Smeltzer et al., 2010).

It is often difficult to differentiate between ischemic stroke and haemorrhagic stroke because they have similar symptoms. It is also difficult to distinguish between hypoglycaemia and stroke because hypoglycaemia can produce focal neurological symptoms that resemble those of stroke. However, hypoglycaemia should be ruled out in all cases of suspected stroke, especially in known diabetics. Brain tumours and other intracranial masses such as subdural hematomas can cause transient neurological deficits and other stroke like symptoms. Headache is uncommon symptom of ischemic stroke, but rather more common in haemorrhagic stroke. Early loss of consciousness, vomiting, and severely elevated blood pressure may also be symptoms of haemorrhage stroke (Popp, 2011).

The pattern of stroke symptoms occurs can be determined by the location of the stroke. One typical symptom of ischemic stroke is the absence of function such as loss of vision in a single eye or in an entire hemifield, numbness in part of the body, weakness or paralysis on one side of the body. A patient suffering from an intracerebral haemorrhage may present with the sudden occurrence of neurological dysfunction, including weakness, numbness, vision loss, diplopia, dysarthria, gait disorder, vertigo, aphasia, or disturbed level of consciousness. The rapid decline in neurological functions is typically more noticeable than with ischemic strokes. For example, if the haemorrhage is large enough, pressure effects on the whole brain and brainstem may lead to an obvious diminishing level of consciousness. In addition, a bleed that begins small (2 cm in diameter) may expand over the first few hours to become immense. This will cause a rapid deteriorating of symptoms, including a rapid reduction in the patient's level of consciousness (Always et al., 2009).

Stroke diagnosis involve several process including history taking, clinical exam, acute brain and cardiovascular imaging, and a number of basic laboratory tests are essential aids to the diagnosis of acute stroke. Acute brain imaging (CT or MM) are reliable methods of instant differentiation between ischemic stroke and intracerebral haemorrhage. After a large ischemic stroke involving the cortex or basal ganglia, early abnormalities on CT appear within 1-3 hours. Small and brainstem strokes may not be visualized for 12-24 hours on CT and may actually never be captured on CT.

Clinical report assembled by clinician and radiologist that includes information such as suspected stroke localization as well as joint visualization of images is very important in understanding subtle abnormalities on brain imaging. MRI has many advantages

including a higher resolution, faster appearance of abnormalities and improved brain-stern imaging for monitoring acute stroke patients, however it has limited access and is complicated in use. Moreover, perfusion-CT has appeared as a practical diagnosis tool for early ischemic attack and reliably differentiates reversible from irreversible ischemia. Lumbar puncture is necessary to rule out clinical suspicion of subarachnoid haemorrhage if the cranial CT or MRI is negative as in less than 10% of cases in the first 24 hours (Fisher, 2009).

Treatment for acute stroke involves management, which was largely focused on rehabilitation and avoidance of adverse outcomes in the sub-acute setting.

Administration rates of intravenous tissue plasminogen activator tPA were low despite the approval of IV tPA as an acute treatment for ischemic stroke in 1996. In the period from 1996 to 2002, only 0.6% to 8.5% of patients presenting with non-haemorrhagic stroke were being treated with IV tPA according to regional and nationwide studies in the United States and Canada. There are several possible reason for the low rate of IV tPA administration including the lack of painful symptoms, impaired communication that is often a symptom of stroke, the broad variety of possible symptoms, the frequent delays in activating emergency medical services, and the public's lack of knowledge of stroke symptoms. tPA has a limited treatment window of 3 hours and studies have demonstrated that only 17— 35% of stroke patients arrive within the time limit (Goldstein, 2011).

## Blood Vessels.

During the earliest stages of embryo development and in the absence of vascularization, nutrition is delivered through diffusion. When the embryo is developed into a highly vascular organism, it starts to depend on a functional, complex network of capillary plexuses and blood vessels. Vasculogenesis initiates vascular growth by forming primitive vessels. The second step of vascular growth is angiogenesis which causes the maturation and expansion of these vessels (Conway et al., 2001).

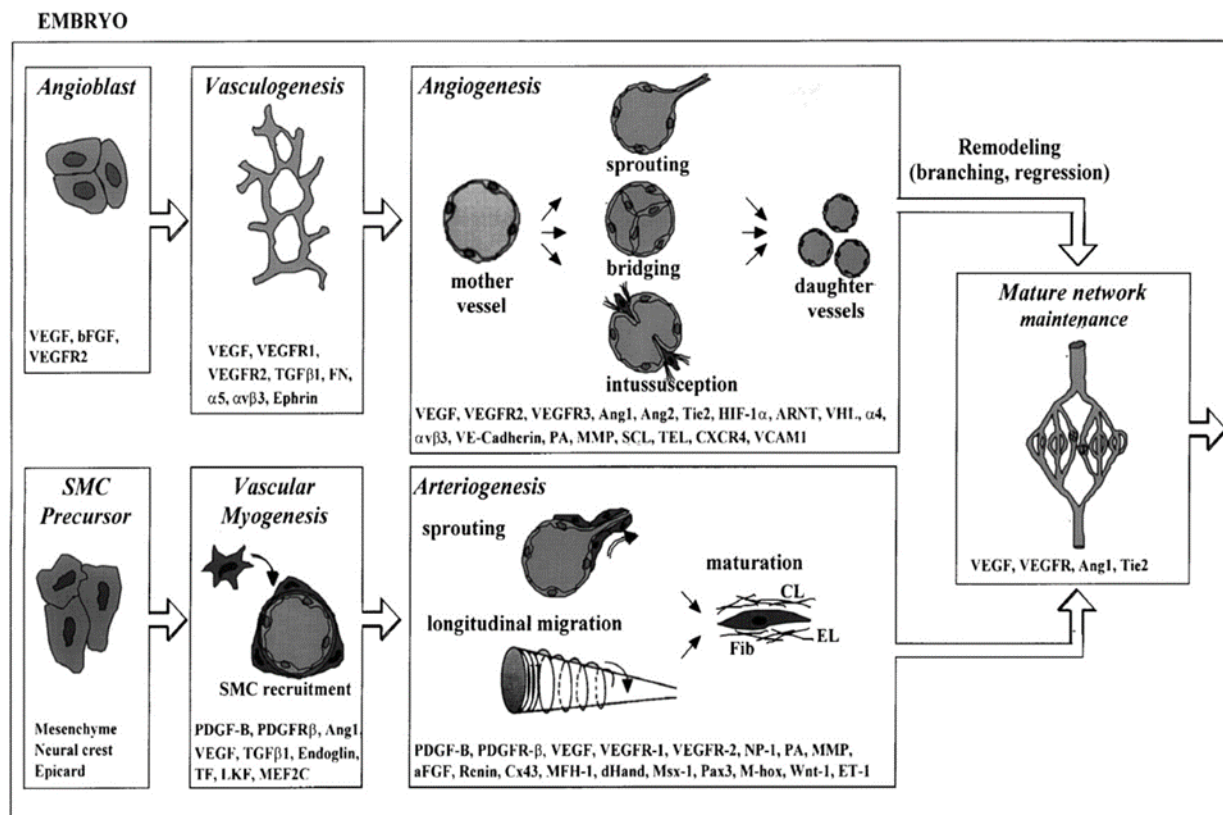


Figure 5. Angioblasts in the embryo accumulate during the process of vasculogenesis, and expands and remodels in angiogenesis. Mural cells stabilize forming vessels by inhibiting endothelial proliferation and migration, and by triggering the production of extracellular matrix during vasculomyogenesis, Smooth muscle cells (SMC) encase endothelial cells, providing

blood vessels with viscoelastic and vasomotor properties, essential to facilitate the changing requirements in tissue perfusion during arteriogenesis. CL, collagen; EL, elastin; Fib, fibrillin (Carmeliet, 2000).

The largest blood vessels are arteries and veins, which have a thick, tough wall of connective tissue and many layers of smooth muscle cells. The wall is lined by a very thin single sheet of endothelial cells, the endothelium, separated from the surrounding outer layers by a basal lamina. The amounts of connective tissue and smooth muscle in the vessel wall vary according to the vessel's diameter and function, but the endothelial lining is always present. In the finest branches of the vascular tree the capillaries and sinusoids, the walls consist of endothelial cells only and a basal lamina, together with a few dispersed but functionally important pericytes. These are cells that belong to the connective tissue family, related to vascular smooth muscle cells that surround the small vessels.

There are two cell types that compose all blood vessels; endothelial cells and mural cells. Mural cells associate with and surround the endothelial cell tube, whereas endothelial cells form the inner vessel wall. Mural cells are generally subdivided into vascular smooth muscle cells and pericytes, depending on their density, morphology, location, and expression of specific markers in mural cells. Vascular smooth muscle cells are associated with arteries and veins and they construct multiple concentric layers surrounding these vessels. The wall of arteries and veins is lined by an extremely thin single layer of endothelial cells, the endothelium, isolated from the surrounding outer layers by a basal lamina.

Depending on the vessel's diameter and function, the amounts of connective tissue and smooth muscle in the vessel wall vary, however, the endothelial lining always exists. Arterioles, capillaries, and venules belong to the smallest diameter blood vessels which are associated with pericytes and share their basal membrane with the endothelium. The walls of capillaries and sinusoids consist of endothelial cells and a basal lamina only together with few pericytes. Pericytes are either mono connected to the endothelial cell tube or form a single unconnected, cell layer encasing it. They belong to connective-tissue family, related to vascular smooth muscle cells that wrap themselves round the small vessels. The morphology and the degree by which pericyte encase endothelium significantly differ between variable tissues (Gaengel et al., 2009, Alberts et al., 2002).



Figure 6. The scanning electron micrograph displays pericytes wrapping their processes around a small blood vessel in the mammary gland of a cat (Alberts et al., 2002).

## **Endothelial Cells.**

Endothelial cells line the entire vascular system, are versatile and have variety of functions and synthetic and metabolic properties, including the regulation of thrombosis and thrombolysis, platelet adherence, modulation of vascular tone and blood circulation, and regulation of immune and inflammatory responses by controlling leukocyte, monocyte and lymphocyte connections with the vessel wall. Abnormalities in endothelial structure and function may also result in development of diseases. They play an essential role in atherosclerosis, hemostatic dysfunction, and altered inflammatory and immune response. The structure and functional stability of endothelial cell are essential in maintenance of the vessel wall and circulatory function. The endothelial cell layer is semi-permeable and controls the passage of small and large molecules (Sumpio et al., 2002). Endothelial cells play a critical role in the process of increased vascular leakage and thrombopathy during severe inflammation leading to shock. The surface of the endothelial cell alters from an anti- prothrombotic into a prothrombotic surface and the thrombosis resistance of the cardiovascular system is further reduced by the obstruction of endothelium-dependent relaxation. Endothelial cells can activate a different of cytokines and factors that change the haemostatic balance in a prothrombotic state. Endothelial cells can affect the activation, regulation and modulation of coagulation, in addition to the indirect effects of adhesion molecules, growth factor and cytokines. They regulate the activation of binding sites for anticoagulant and pro-coagulant factors on the cell surface. In normal conditions, they maintain blood flow by stimulating the activity of numerous anticoagulant pathways. The endothelium may become activated directly by pathogens or indirectly by inflammatory mediators during acute infections. There are



several pathways by which the endothelium is challenged subject to the type of pathogen. Changes in coagulation and fibrinolytic systems can be initiated by direct activation by bacteria, viruses and other pathogens or indirect activation of the endothelium. Family of gram negative bacteria can activate endothelial cells by endotoxins. There are numbers of examples where viruses can invade endothelial cells including (para-) influenza, adenoviruses, herpes simplex virus (HSV), polio virus, echovirus, measles virus, mumps virus, cytomegalovirus (CMV), human T-cell leukaemia virus type-1 (HTLV-1) and human immunodeficiency virus (HIV). Infection of endothelial cells has been established for haemorrhagic fevers (HF) caused by Dengue, Marburg, Ebola, Hantaan and Lassa HF as well. HIV infection changes the coagulation system by impairment of heparin co-factor II (Stern et al., 1991) (Keller et al., 2003).

### **Blood Brain Barrier:**

The blood–brain barrier (BBB) is a highly selective barrier that surrounds the central nervous system (CNS) including the spinal cord and protects the brain from the changing metabolite concentrations in blood. The BBB is necessary to provide an optimal chemical environment for cerebral function. It is formed by a complex cellular system of endothelial cells, astroglia, pericytes, perivascular macrophages, and a basement membrane consisting of type IV collagen; fibronectin and laminin. Astrocytes extend their end feet tightly to the cerebral endothelial cells (CEC), effecting and maintaining the barrier function of these cells. CEC are surrounded by the basal lamina along with pericytes and perivascular macrophages. Pericytes may affect the stability of the capillaries and protect the barrier function because of their tight contact with the endothelial cells. They also restrict transportation because of their ability to phagocytose

molecules that were able to cross the endothelial barrier (Vries et al., 1997, Hawkins et al., 2006).

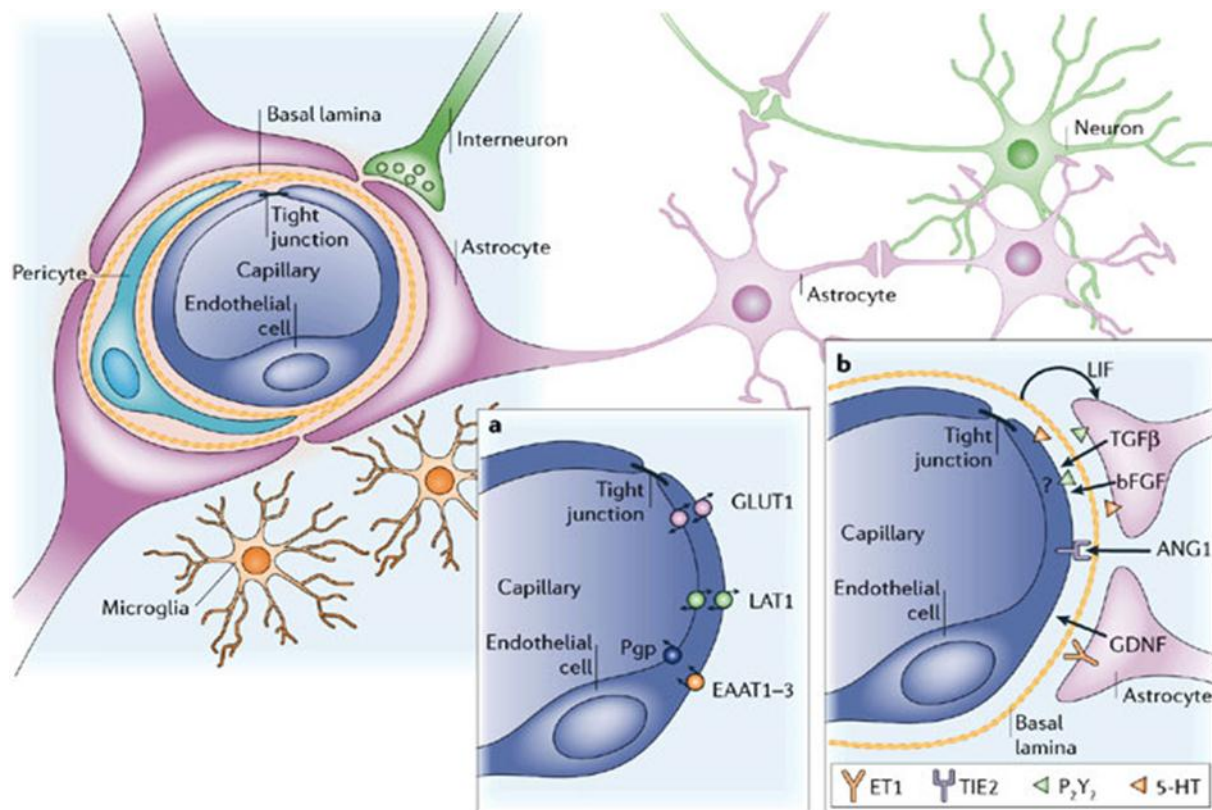


Figure 7. A representation of the BBB. It is formed by capillary endothelial cells, embedded in basal lamina and surrounded by astrocytic perivascular endfeet. The figure also shows pericytes and microglial cells. A number of transporters and receptors including EAAT1–3, excitatory amino acid transporters 1–3; GLUT1, glucose transporter 1; LAT1, L-system for large neutral amino acids; Pgp, P-glycoprotein are presented in a. Some endothelial cell receptors and transporters including 5-HT, 5-hydroxytryptamine (serotonin); ANG1, angiopoietin 1; bFGF, basic fibroblast growth factor; ET1, endothelin 1; GDNF, glial cell line-derived neurotrophic factor; LIF, leukaemia inhibitory factor; P2Y<sub>2</sub>, purinergic receptor; TGFβ, transforming growth factor-beta; TIE2, endothelium-specific receptor tyrosine kinase 2 are shown in b (Abbott et al., 2006).

BBB endothelial cells are characterized by the existence of a distinct phenotype, which is the presence of tight junctions TJs and a defined polarized transport systems. Apical intercellular junctional complex in polarized epithelium and endothelium consist of TJs. They have three major biological functions including blocking para-cellular diffusion of blood-borne polar substances, preventing the lateral diffusion of lipids and integral membrane proteins, therefore maintaining cell polarization and an intracellular signalling platform (Luissint et al., 2012). Tight junctions consist of two types of transmembrane proteins, and claudins. Occludin is a ~60-kDa tetra-span membrane protein that forms two extracellular loops separated by a short cytosolic loop, and both amino- and carboxy-terminal domains are cytosolic. Phosphorylated occludin is located at tight junctions while non-phosphorylated occludin is localized to both the basolateral membrane and in cytoplasmic vesicles. It is suggested that occludin phosphorylation states and its localization and function within the tight junction is regulated by several kinase and phosphatases. Recruiting of occludin to tight junctions and regulating the para-cellular permeability barrier between cells are controlled by the extracellular domains of occludin. The claudin family consists of a minimum of 24 members falling within the range of 20–27 kDa and consist of a tetra-span transmembrane protein with two extracellular loops. Claudins function in localization of occludin to tight junctions. Claudins directly regulate the gate function of the tight junction, which controls the para-cellular pathway for ion passage in-between cells in an epithelial layer. Most of the channels formed by claudin interactions permit the movement of cations, however the passage of anions has also been detected. Claudin ion selectivity can be influenced by changes in the type of claudin expressed, or single amino acid substitutions in claudins

(Schneeberger et al., 2004, Nelson et al., 2008). In leaky tight junctions, where a higher rate of ion flow, charge selectivity is most evident. The majority of leaky TJs demonstrate a preference for  $\text{Na}^+$  over  $\text{Cl}^-$ , Charge selectivity is most relevant in leaky tight junctions where higher amounts of ions flow. Almost all leaky TJs show a preference for  $\text{Na}^+$  over  $\text{Cl}^-$ , and between different epithelia and experimental cultured cell models, the permeability ratio within a range of 10 to 0.1. Epithelia with leaky TJs are found where movement of large amounts of isosmotic fluids is required, such as in the human gastrointestinal tract, which secretes and then reabsorbs around 10 L of fluid each day. In contrast, epithelia with tight junctions can sustain the high electrochemical gradients produced by active trans-cellular transport. This formation is used to result in either highly concentrated or diluted secretions, as in the distal nephron, which can produce urine with osmolarity several fold higher or lower than plasma (Itallie et al., 2009).

### **hCMEC/D3 cell line.**

In vivo studies have revealed a great deal of information regarding the distinctive properties of brain endothelium, however, whole animal experiments impose numbers of limitations. Therefore, new techniques to isolate and culture CNS-derived endothelial cells from various species have been developed (Weksler et al., 2005). One of these techniques includes manipulating endothelial cells with a combination of astrocyte-conditioned medium and agents that elevate intracellular cAMP to establish a cell culture model of the blood brain barrier (Rubin et al., 1991). Cyclic AMP (cAMP) is a key second messenger that transfers information to a variety of many effector proteins within the cell (Ponimaskin et al., 2007). Epithelial tight junction permeability is affected

by cyclic AMP, which is established to be involved in mediating surface membrane phenomena in a variety of cell systems (Duffey et al., 1981). However, such model exhibited high electrical resistances, low permeability to small molecular weight compounds and functional expression of the most important drug transporters (Poller et al., 2008). Different rat brain endothelial (RBE) cell lines have been developed (RBE4, GP8/3.9, GPNT, RBEC1, TR-BBBs and rBCEC4 cell lines) as in vitro models of the BBB. Primary cultures of RBE cells were transduced with an immortalizing gene (SV40 or polyoma virus large T-antigen or adenovirus E1A), either by transfection of plasmid DNA or by infection using retroviral vectors (Roux et al., 2005). Numbers of in-vitro models were developed in which EC are; either grown in astrocyte conditioned medium, or co-cultured with astrocytes or rat C6 glioma cells. The co-culture system can be either a non-contact co-culture with the glial cells seeded at the bottom of the well (Malina et al., 2009).

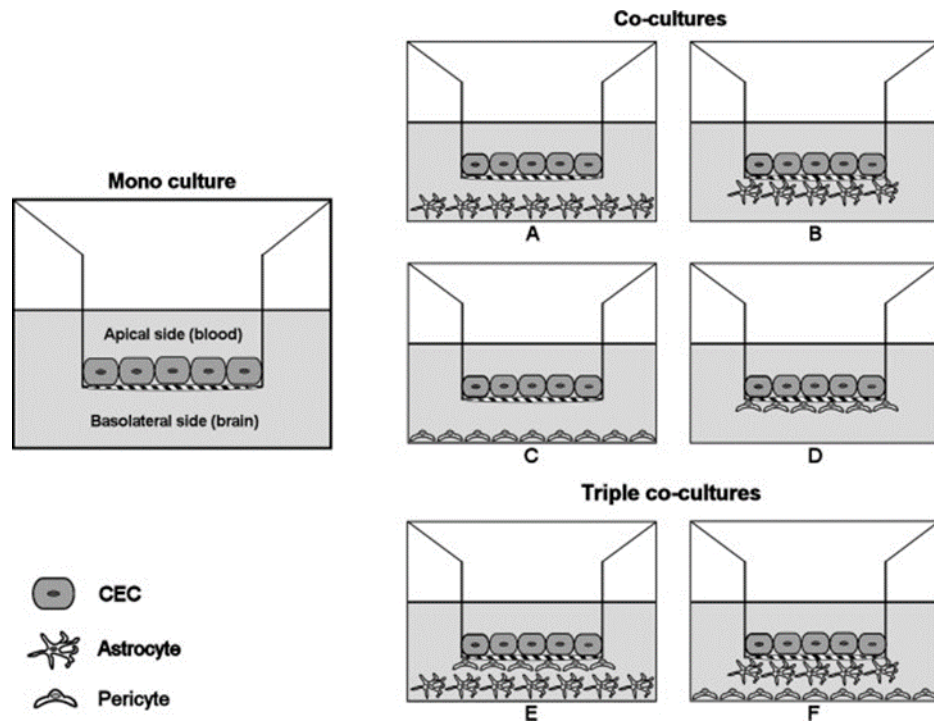


Figure 8. A representation of different in vitro cell-based blood–brain barrier (BBB) models.

Monocultures of cerebral endothelial cells (CECs) are being replaced by co-culture or triple co-culture systems. (A) CECs are seeded with astrocytes in a non-contact format. (B) CECs are seeded with astrocytes in a contact format. (C) CECs are seeded with pericytes in a non-contact format. (D) CECs are seeded with pericytes in a contact format. (E, F) Triple co-culture systems, in which more than one cell type is seeded with CECs (Bicker et al., 2014).

One of these models was established using primary cultures of three main cell types of cerebral micro-vessels in order to develop and characterise a new syngeneic BBB model. Rat brain endothelial cells, pericytes and astrocytes were co-cultured to mimic the structural condition in vivo. It resulted in the elevated levels of tight junction proteins occludin, claudin-5 and ZO-1 with a typical arrangement at the cell borders. Electron microscopy provided further morphological evidence of the existence of inter-endothelial TJs (Nakagawa et al., 2009).

Non-cell based surrogate BBB model such as parallel artificial membrane permeability assay (PAMPA) was developed. It involves a non-biological artificial membrane and therefore only concentrates on the prediction of passive trans-cellular drug absorption. The system has the ability to identify compounds as either BBB permeable (BBB+) or non-permeable (BBB-) with adequate precision due to the modifications to the lipid composition of the artificial membranes (Mensch et al., 2010).

The drawback of most of the in vitro models of the blood-brain barrier is the use of cells of non-human origin, which is not optimal for the estimation of brain permeability in humans. BB19 cells are derived from human brain endothelium and are immortalized with E6E7 genes of human papilloma virus. They in part sustain endothelial properties, which is demonstrated by tube formation in Matrigel™™ as substrate. They express Factor VIII-related antigen and von Willebrand's factor (Kusch-Poddar et al., 2005). Another human origin cell line is SV-HCEC, which is developed using human capillary and microvascular endothelial cells (HCEC) that were transfected with the plasmid pSVS-neo coding for the SV40 large T antigen and the neomycin gene (Muruganandam et al., 1997). The SV-HCEC line displays properties of the primary/ low passage brain capillary cells which include factor VIII-related antigen, uptake of acetylated low density lipoprotein, transferrin receptor mediated endocytosis, and elevated levels of the selective marker enzymes alkaline phosphatase and  $\gamma$ -glutamyl transpeptidase. However, immortalized brain endothelial cell lines including the human SV-HCEC; the mouse MBEC; the mouse TM-BBB4; the rat GPNT, the rat RBEC1; and the rat RBE4 cell line appear to generate insufficient restrictive para-cellular barrier properties that

would allow their effective use in trans-endothelial permeability screening (Gumbleton et al., 2001).

One human BBB model that closely mimics the in vivo phenotype and is reproducible and easy to grow, is brain microvascular endothelial cell line hCMEC/D3. It was derived from human temporal lobe microvessels isolated from tissue removed during surgery for control of epilepsy. The primary isolate was enriched in CECs. In the first passage, cells were consecutively immortalized by lentiviral vector transduction with the catalytic subunit of human telomerase (hTERT) and SV40 large T antigen, following which CEC were selectively isolated by limited dilution cloning, and clones were extensively characterized for brain endothelial phenotype (Weksler et al., 2013). hCMEC/D3 recapitulates many of the key characteristics of primary brain endothelial cells such as the expression of endothelial cell markers, transporters, and tight junctional proteins without the requirement of co-culturing with glial cells (Vu et al., 2009). As well as being a morphological barrier; BBB is also an active physical and metabolic barrier due to the expression of drug efflux transporters and drug-metabolizing enzymes. These transporters actively limit the entry of numerous endogenous compounds and xenobiotics into the brain. They involve ATP-binding cassette (ABC) efflux transporters, including P-glycoprotein (P-gp, ABCB1/MDR1), BCRP (ABCG2) and several MRPs (ABCCs) which are expressed at the luminal membrane of the endothelial cells forming cerebral microvessels. One of the major drug transporters at the BBB is P-gp, which is mainly expressed at the luminal membrane of brain endothelial cells in both humans and animals. All of these transporters were found to be expressed in the hCMEC/D3 cell line (Dauchy et al., 2009). hCMEC/D3 cell line provided a reliable model of the



human BBB in numbers of researches including a study designed to investigate cellular and molecular mechanisms involved in endothelial changes induced by HTLV-1-infected lymphocytes. hCMEC/D3 expresses a high restriction of permeability, and expresses chemokine receptors and up-regulated adhesion molecules in response to inflammatory cytokines which are properties of BBB. Therefore, hCMEC/D3 was used to study the mechanisms associated with retroviral-induced BBB disruption, both in terms of permeability to solutes as well as trans-endothelial migration of lymphocytes (Afonso et al., 2007).

### **Angiogenesis.**

Angiogenesis, the formation of new blood vessels, is an important process involved in both normal physiological and numerous pathological process, such as tumor growth, metastasis, inflammation and ocular disease. Angiogenesis, or neovascularization, is the process of generating new blood vessels from a pre-existent vascular system. The principal cells involved are endothelial cells, which line all blood vessels and constitute virtually the entirety of capillaries (Auerbach et al., 2003). Angiogenesis involves endothelial cell proliferation, selective breaking down of the basement membrane and the adjacent extracellular matrix, endothelial cell migration, and tube formation. The endothelial cells go through tissue-specific alterations to produce functionally distinct vessels, once new blood vessels have been formed. During embryogenesis, endothelial cell precursors (angioblasts) differentiate to form blood vessels. Angioblasts associate to form primitive vessels in a process called vasculogenesis (Hoeben et al., 2004). Vasculogenesis is required for the de novo formation of a vascular network in embryogenesis and growth. On the contrary, arteriogenesis refers to the remodelling of

pre-existing arterial vessels to form arteries. It is based on chemokine/growth factor-induced growth processes and increases in diameter of vascular wall structures at increased stress that is induced by elevated pressure rates in arteries. During their lifespan, endothelial cells maintain their plasticity to detect and respond to angiogenesis stimuli. Generally, angiogenesis is firmly regulated by well-balanced activating and inhibiting signals including cytokines, hormones, endothelial cell migration, circulating progenitor cells and destabilization of the vessel wall, the basal lamina, and the interstitial matrix (Multhoff et al., 2014). Angiogenesis is also triggered by chemical signals from cancer cells. It plays an important role in the progression of cancer since the proliferation, as well as metastatic spread, of cancer cells relies on a sufficient supply of oxygen and nutrients and the removal of waste products. In contrast, in the absence of vascular support, tumours may become necrotic or even apoptotic. There are numbers of different proteins that have been identified as angiogenic activators and inhibitors and the rate in which angiogenic factors are expressed reflects the aggressiveness of cancer cells. Thus, the use of Angiogenic inhibitors in cancer therapy could reduce both morbidity and mortality from carcinomas (Nishida et al., 2006). Anti-angiogenic therapy has the potential to overcome two major problems facing the non-surgical treatment of malignant solid tumours. First is the obstruction of drug delivery at effective concentrations to all cancer cells due to physiological barriers within tumours. Second, genetic and epigenetic mechanisms causing drug resistance reduces the effectiveness of available therapies (JAIN et al., 2001). Anti-angiogenic therapy targets vascular growth within tumours to suppress tumour growth and metastasis. Most present anti-cancer chemotherapeutic agents administered clinically indiscriminately

target all rapidly dividing cells. Therefore, they can cause acute negative effects such as immunosuppression, abdominal problems and hair loss. On the contrary, anti-angiogenic reagents have less adverse effects because, except in the uterine endometrium during the menstrual cycle, neoangiogenesis (formation of blood vessel in tumour tissue) rarely occurs in healthy adults (Kubota, 2012). In ischemic diseases, in contrast, deprivation of oxygen and nutrients causes a serious threat for tissue survival. In response to tissue ischemia, angiogenic growth factors are upregulated, and circulating cellular elements are mobilized to enable new blood vessels formation. Therefore, it is an important therapeutic option to induce vascular growth after critical ischemia. Growth factors, which mostly act on endothelial cells to stimulate endothelial cell proliferation, migration, and tube formation, are potential therapeutic genes for angiogenesis or arteriogenesis enhancement. At the same time, growth factors cause endothelial cells to become less sensitive for apoptosis induction. Fibroblast growth factor (FGF) families and Vascular endothelial growth factor (VEGF) were among the first growth factors to be identified (Losordo et al., 2004). However, VEGF-induced angiogenic vessels are haemorrhagic, aggravating inflammatory responses in the recovering area surrounding an ischemic event. The penumbra is intensely resilient and is a site of extreme remodelling and active angiogenesis (Jawahar Mehta, 2013). Angiogenesis plays an important role as a recovering mechanism in response to ischemia in numerous non-CNS tissues. For instance, drugs that enhanced angiogenesis can sometimes reduce injury in myocardial infarction and limb ischemia because these disorders can activate endogenous angiogenesis in each organ. However, the responses and regulatory mechanisms in the brain that trigger

angiogenesis might be more complex. In autopsy studies it was found that brain ischemia activates angiogenesis through Hypoxia-inducible factor (HIF) pathways. Despite the fact that increasing blood flow and reducing the size of the infarction by forming new vascular networks to improve neurological recovery through pro-angiogenic therapy, the information about such therapy remains random and indirect. In a study, it was demonstrated that the number of new blood vessels in areas surrounding stroke site associated with longer survival in stroke patients, which suggests that active angiogenesis might be beneficial for ischemic brain. It is hypothesized that in transit ischemic attacks, signals for angiogenesis should be activated, which could explain why patients with such attacks show less severe brain damage than those without such episodes (Navaratna et al., 2009).

### **Matrigel™ :**

Matrigel™ Basement Membrane Matrix, is the trade name for a cell culture medium comprised of gelatinous protein mixture secreted by Engelbreth-Holm-Swarm (EHS) mouse sarcoma cells. It has numerous uses including supporting of multicellular three-dimensional growth and altered cell morphology, proliferation, differentiation of cancer cell culture. In addition, it increases tumorigenicity for the establishment of xenograft tumour models in vivo when used as an injection medium for cancer cells (Price et al., 2012). The Matrigel™ plug assay is used to measure angiogenesis in vivo, it offers a versatile base to study the formation of new microvessels as well as the effects of pro- and anti-angiogenic factors. It forms a support for the proliferation of vascular structures by self-assembling from a liquid at 4° to a semi-solid at 37°C (Bartoli et al., 2012).

Matrigel™ provides a three-dimensional (3D) cell culture model which allows studies

into biological functions in a condition that is similar to in vivo setting and therefore provides a more physiological context. Three-dimensional model systems are presently being used in order to examine the signals that modulate normal processes of tissues and how they may be disturbed in pathological conditions such as cancer. Cell culture studies are normally conducted on synthetic substances such as glass or plastic that restrict cells to adhere to artificially flat and rigid surfaces. The benefit of using these two-dimensional (2D) in vitro cell culture systems is their ability to provide convenient and rapid methods of biochemical analysis. However, unlike 3D systems, they are inefficient in signals found in tissue microenvironments in vivo; thus, limiting the use of these studies for tissue-specific functions and structural signals (Sodunke et al., 2007).

*in Cancer Biology 15 (2005) 378–386*

Table 2

Examples of how basement membrane promotes differentiation in vitro

Cells/explant	Response
<b>Cell lines</b>	
Prostate <sup>a</sup>	Acinar formation, glands
Salivary <sup>a</sup>	Acinar formation, amylase production
Mammary epithelial <sup>a</sup>	Duct and lumina formation, increased casein
MDCK <sup>a</sup>	Polarized cyst
Pancreas <sup>a</sup>	Acinar differentiation
Schwann cells <sup>a</sup>	Differentiation
Intestinal cells <sup>a</sup>	Differentiation
Bone cells	Canaliculi formation
<b>Primary cells</b>	
Sertoli	Columnar epithelium
Hepatocytes <sup>a</sup>	Morphology maintained, albumen production
Chondrocytes	Cartilage formation
Endothelial cells <sup>a</sup>	Capillary tubes with lumen
Endometrial cells	Columnar epithelium, glands
Oviduct epithelium	Tubes with ciliated cells
<b>Tissue explants</b>	
Neural crest	Outgrowth
Dorsal root ganglia	Outgrowth with myelin production
Immature follicles	Hair growth
Aortic rings	Vessel outgrowth
Ookinetes (zygote)	Sporogonic development of malaria parasite

<sup>a</sup> Denotes activity with both primary cells and cell lines.

Table 1. Examples of how Matrigel™ promotes differentiation in different cell types. <sup>a</sup> Denotes activity with both primary cells and cell lines (Kleinman, 2005).

Matrigel™ is usually stored as a frozen solution for long term use, and thawed overnight at 4 °C before application. It solidifies at 24–37 °C in 30 min and it does not re-dissolve readily upon cooling. Cells are either seeded on top of the gelled material, or mixed with the matrix before gelling. When exposed to Matrigel™, many cell lines and primary cells, differentiate rather than proliferate (Kleinman et al., 2005). Its main constituent is laminin, followed by collagen IV, heparansulfate proteoglycans, entactin, and nidogen. It also contains growth factors such as transforming growth factor-beta, fibroblast growth factor, tissue plasminogen activator, and others. It can be adjusted to remain in a liquid form by adding different amounts of Matrigel™ to pure cell culture medium to recreate an environment as close as possible to the *in vivo* one (Lazzaroni et al., 1999).

Matrigel™ contains many essential components of the extracellular matrix such as collagen, laminin, entactin, and other important growth factors. Cultured epithelial cells respond to such appropriate matrix proteins which are similar to the components of matrix found in the tissue of origin. In a study, Matrigel™ was utilized using mammary gland to provide an ideal model for understanding connection between normal tissue function and architecture. Acinus is 3D structure formed by mammary epithelial cells that exist in 3D space. In acinus, a single continuous layer of epithelial cells secrete milk into a central lumen. *In vivo*, this 3D architecture is surrounded by a layer of myoepithelial cells and extracellular matrix proteins that provide structural support and functional information. This overall structure and function can be replicated *in vitro* by culturing mammary epithelial cells completely enmeshed by Matrigel™. Growing epithelial cells in 3D cultures provides an environment where cyst-like spheroids with a hollow lumen can be formed and cells build their own basement membrane, have a firm

control over proliferation, and form apicobasal polarity. When a single human immortalized mammary epithelial cell (MCF-10A) is seeded in or on top of a layer of Matrigel™ (approximately 1 mm thick) and surrounded by additional Matrigel™, cells undergo a morphogenetic pathway that causes the formation of acini-like structures highly similar to normal epithelial architecture (Sodunke et al., 2007).

### **Cell Migration.**

The in vitro cell migration assay is a simple and cost-effective method to study cell migration in vitro. Cell monolayers act in a response in any disruption of cell-cell contacts, due to a wound or scratch, by increasing concentration of growth factors at the wound margin and healing the wound through a combination of proliferation and migration. These procedures represent the behaviour of individual cells as well as the properties of the cell sheet as a surrogate tissue. In order to conduct a cell migration assay, a pipette tip or syringe needle is used to introduce a wound in a confluent cell monolayer grown on an individual coverslip or in a multi well plate. The process of cell migration can be then observed over a period of 3–24 hrs. Cells migrate in a typical way where cells on the edge of the newly created gap polarize to the wound, start protrusion, and migrate until new cell–cell contacts are established again. The process of cell migration can be recorded by capture of images at the beginning and regular intervals during cell migration to close the scratch, and comparison of the images to determine the rate of cell migration (Yarrow et al., 2004, Liang et al., 2007). Cell migration is involved in several normal and pathological processes, including embryonic growth, protection against infections, wound healing, and tumour cell metastasis. It is commonly known that dynamic reorganization of the actin cytoskeleton, directing

protrusion at the front of the cell and retraction at the back are the stimulants of cell migration. Moreover, cell migration efficiency relies on synchronised changes in other cellular activities including provide new membrane components through directed secretion, regulating adhesion by turnover of cell–matrix interactions, and providing autocrine/ paracrine signals by alterations in gene transcription (Hall et al., 1999). Cell migration is one of many biological processes that are regulated by growth factors, cytokines and cellular matrix molecules. Paxillin is found to be involved in a number of biological functions including cell adhesion, cell migration and neurite outgrowth. It is a 68-kDa focal adhesion-associated that contains five leucine-rich regions, termed LD motifs, near the N-terminus, and four LIM domains in the C-terminus. Spread throughout paxillin are many serine/threonine and tyrosine phosphorylation sites. Phosphorylation of paxillin on these sites in response to extracellular stimuli leads to recruitment of a number of signaling molecules, therefore regulates focal adhesion dynamics and cell migration (Huang et al., 2008).



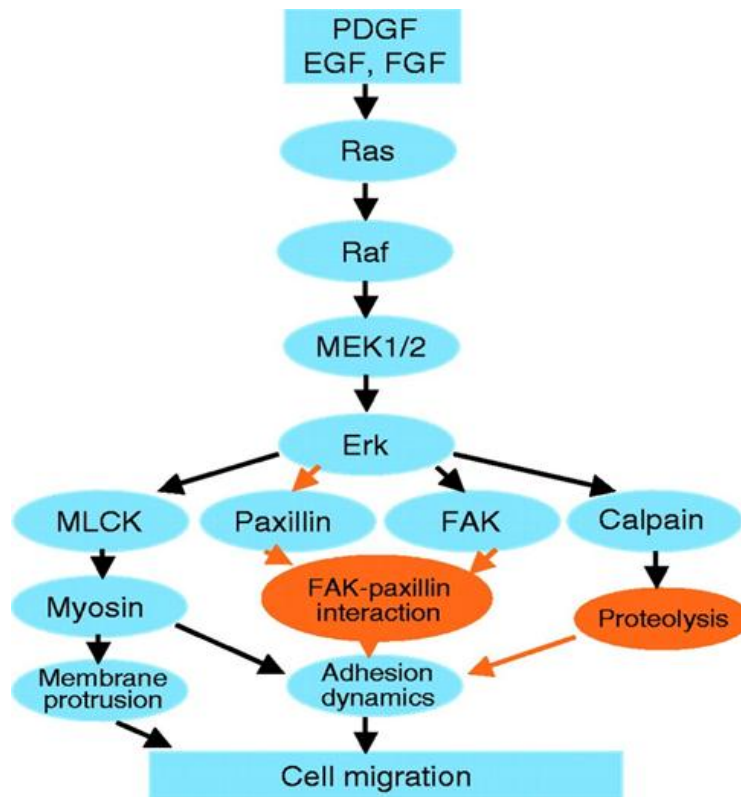


Figure 9. Signalling pathways for cell migration regulated Erk. Growth factors, such as PDGF, EGF and FGF, activate Ras-Raf-MEK1/2 which in turn activate Erk. Activated Erk mediates membrane protrusions and focal adhesion turnover via phosphorylating MLCK and stimulates focal adhesion disassembly via phosphorylating and activating calpain. Phosphorylation of FAK and paxillin by Erk may control focal adhesion dynamics, possibly by affecting the paxillin-FAK interaction. Orange lines indicate hypothetical pathways (Huang et al., 2004).

## Apoptosis:

Apoptosis or programmed cell death is the most common form of physiologic cell death in multicellular forms. It is highly cell-specific and could be induced in damaged cells, where damage is beyond repair (Rastogi et al., 2009). It has a number of characters including energy-dependent biochemical mechanisms and distinct morphological properties. Apoptosis is a key part in several biological processes such as normal cell

turnover, proper development and functioning of the defence system, hormone-dependent atrophy, embryonic development and cell death caused by chemicals. Any abnormalities in apoptosis could affect many human conditions including neurodegenerative diseases, ischemic damage, autoimmune disorders and various types of cancer (Elmore, 2007). There are two major pathways in which apoptosis is initiated. The extrinsic pathway is mediated by a sub-group of Tumor Necrosis Factor receptors (TNFR) superfamily that includes TNFR, Fas and TRAIL (Portt et al., 2011). Activation of these death receptors activate death-inducing signaling complex (DISC) formation and caspase 8 activation, which in turn activates caspase 3. The second major pathway is the intrinsic pathway which can be activated by proteolysis of BID to t-BID by caspase 8 and interaction of t-BID with BAX in the mitochondria (Chiong et al., 2011). This pathway is consequently controlled by members of the Bcl-2 family. Regardless of different modes of initiation between the extrinsic and intrinsic pathways, they both result in the same outcome; which is the activation of a cascade of proteolytic enzymes, members of the caspase family (Sprick et al., 2004).

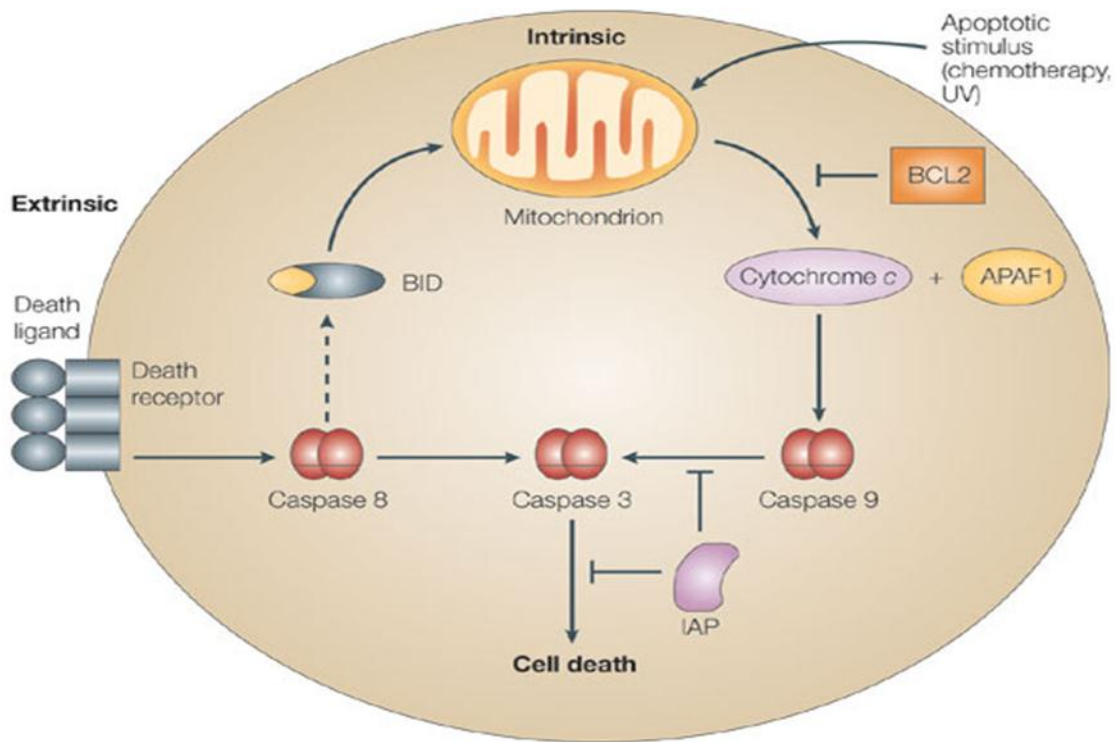


Figure 10. A representation of the two major apoptotic pathways; the extrinsic and the intrinsic pathway. The death-receptor activate the extrinsic pathway that acts through caspase 8 or mitochondrial intrinsic pathway. The intrinsic pathway activates caspase-activating complex (that includes cytochrome c and apoptosis-activating factor 1 APAF1) that acts on caspase 9 which in turn activate caspase 3. Both pathways are regulated by BCL2 and inhibitor of apoptosis IAP protein families. BCL2 proteins are believed to regulate the mitochondrial permeability promoting BID and cytochrome c release (Andersen et al., 2005).

## **Aims.**

The aims of this study were:

- To study the protective effects of citicoline on endothelial cell apoptosis.
- To investigate the key signalling mechanism through which citicoline modulates apoptosis.
- To determine the angiogenic effect of citicoline using in vitro angiogenesis assays.
- To investigate the key signalling mechanism through which citicoline modulates angiogenesis.

# **Chapter 2 Materials & Methods**

## **Materials and Methods.**

### **Materials**

- Chromatography paper (Whatman Schleicher & Schuell international Ltd, England).
- Coverslips (Scientific laboratory supplier Ltd, UK).
- Cryovials (Nunc Corporation, Roskilde, Denmark).
- Eppendorf tube 1.5 ml and 500 µl (Nunc)
- Nitrocellulose membrane (Schleicher & Schuell).
- Pipettes 0.5-10, 5-50, 50-200, 100- 1000 µL (Scientific laboratory supplies Ltd (SLS)).
- Sterile bijoux (SLS)
- Sterile plates 6-well, 24-well and 48-well (Nunc, Denmark)
- Sterile universal containers (SLS)
- Superfrost slides (76x26) mm (Thermo Scientific, Germany)
- Tips
- Tissue culture flasks (T-25) (Scientific Laboratory Supplier, UK)

### **Equipment.**

- Autoclave (Lab Impex Research, UK)
- Autovortex mixer SA1 (Stuart Scientific Co, UK)

- Axiovert fluorescence microscope (Zeiss, Oberkochen, Germany)
- Balancer (Sartorius analytic).
- BD FACSCalibur™ Flow Cytometer (BD Biosciences, UK).
- Centrifuge (Mik20).
- CO2 incubator (Lab Impex Research, UK)
- Electrophoresis unit mini-Protean® 3 (Bio Rad, USA).
- Freezer -80°C (Juan Quality System, UK).
- G-box (Syngene,UK).
- Ice maker (Borolab Ltd, UK).
- Image J software analyzer (Free on line software).
- Laboratory fridge (Scientific laboratory Supplies, UK).
- Laboratory pH/ temperature meter (Model AGB-75, UK).
- Laminar flow hood tissue culture grade (Walker safety cabinet Ltd, UK).
- Liquid nitrogen (BOC CryospeedThermolyne)
- Magent stirrer hot plate (Stuart Scientific CO., UK)
- Microscope (Nikon TMS)
- Modular incubator chamber (Billups-rothenberginc., USA).

- NanoDrop (Thermo Scientific, USA).
- Nikon camera (Nikon coolpix 4500)
- Power supply PS-251-2 (Sigma-Aldrich)
- Rotating shaker (Grant-bio PS0-300)
- Spectrophotometer (Pharmacia Biotech).
- TC10™ Automated Cell Counter (Bio-Rad, USA)
- Trans-blot SD semi-dry transfer (Bio-Rad, USA)
- Ultra low -80 freezer (Nuaire, USA)
- Water-bath (Grant instrument Ltd., UK)



## Required buffers

- Blocking buffer: 1% BSA in TBS –Tween. TBS-Tween must be stored in the refrigerator at PH7.4 or 3 % of non-fat dry milk in PBS-Tween.
- Electrode buffer: 12.02 g Tris-base, 4g SDS, 57.68g glycine made up with 2 L of dH<sub>2</sub>O.
- Milk (required for the secondary antibodies): 5% milk in TBS-Tween with PH adjusted to 7.4. Must be stored in the refrigerator for 7 days.
- Sample buffer (PH 6.8): 1.51 g of Tris-base, 20 ml glycerol mixed with 20 ml of d H<sub>2</sub>O. Then add 4g of SDS, 3.6 ml of mercaptoethanol and 0.004 g bromophenol blue made up to 100 ml with d H<sub>2</sub>O.
- Separating buffer (PH 8.8): 36.3 g Tris-base, 0.8 g of SDS dissolved in 250 ml of d H<sub>2</sub>O.
- Stacking buffer (PH 6.8): 15 g Tris-base, 1g SDS dissolved in 250 dH<sub>2</sub>O.
- Towbin buffer: 1.51 g Tris-base, 7.2 g glycine, 0.167 g SDS, 75 ml methanol. This combination was made up to 500 ml with dH<sub>2</sub>O.
- Tris buffered saline and tween-20 (TBS-Tween PH 7.4): 2.422 g Tris-base, 16.36 g NaCl and 2 ml of tween 20 mixed up to 2 L with dH<sub>2</sub>O.

**Cell culture medium.**

Endothelial cell basal medium-2 (EBM-2) supplemented with 2% FBS, Hydrocortisone, recombinant human Fibroblast Growth Factor B (rhFGF-B), recombinant human Vascular Endothelial Growth Factor (rhVEGF), Recombinant long Receptor Insulin-like Growth Factor-1(R3 IGF-1), Ascorbic Acid, recombinant human Epidermal Growth Factor (rhEGF), Gentamicin sulphate Amphotericin-B (GA-100).

**Methods.****Cell culture and sub-culture.**

Human Cerebrovascular Microvessel endothelial cell line hCMEC/D3 was grown in EBM-2 medium supplemented with growth factors and hydrocortisone. Cells were seeded into T25 flasks pre-coated Poly-L-lysine solution 0.1 % and maintained in a humidified 5% CO<sub>2</sub> atmosphere at 37 °C. Every three days reaching the confluence, the cells were detached under the enzymatic activity of the trypsin. Briefly, medium was discarded and the cells were washed with approximately 5-10 ml of PBS without Ca<sup>++</sup>, Mg<sup>++</sup>. Then, 1 ml of trypsin (2X) was added and incubated for 3 min in order to detach confluent cells from the flasks. Following that, the action of the trypsin was blocked by adding an equal amount of fresh medium. Then, the cells in the suspension were collected in a universal tube and centrifuged at 1300 rpm for 5 minutes. The supernatant was then discarded and the cell pellet was re-suspended with fresh complete medium. The cells were seeded into new pre-coated flasks. Throughout the study, the cells used in all assay were between passages 28 and 38.

**Preparation of freezing medium.**

Freezing medium was prepared containing 10% DMSO in FBS. Briefly 1 ml of DMSO in 9 ml of cold FBS was mixed and kept at -20°C until used. Fresh freezing medium was prepared or defrosted shortly before use.

**Freezing and thawing of cells.**

Cells taken from the flask were centrifuged 1300 rpm for 5 minutes, the supernatant was removed and the cells re-suspended in 250 µl of complete medium with the addition of 750 µl of 10% (v/v) Dimethyl Sulphoxide (DMSO). One ml of the medium containing approximately  $3.5 \times 10^5$  of cells was kept in 1.5 cryovials labelled with cell passage, number and date. Cryovials containing cells were kept at -20 °C (30 min). The cryovials were transferred into a -80°C freezer overnight. After at least 24 hours, cryovials were transferred to liquid nitrogen and the location was recorded. When required, cryovials containing the cells were taken from liquid nitrogen, and wiped with alcohol. The pressure inside the vial was released inside a Laminar flow hood and the frozen cells were defrosted at 37°C water path. Once defrosted, the cells were transferred immediately to pre-warmed complete medium. The cells suspension was centrifuged at 1300 rpm for 5 min, the supernatant discarded and the cell pellet suspended in 5 ml fresh medium. Cells were washed three times to removes traces of DMSO and seeded into a T25 or T75 cell culture flask at the required density.

**Cell counting:**

Cell counting was made using TC10™ automated cell counter. From sub-culturing of hCMEC/D3, 10 µl of cell suspension was added into an eppendorf tube containing 10 µl of trypan blue dye. The sample was then loaded onto a dual-chamber slide. The slide

was inserted into the TC10 cell counter and the counting automatically began. Finally, total cell count was obtained from the screen.

### **Angiogenesis assays.**

#### **Cell proliferation assay.**

hCMEC/D3 cells were seeded at a concentration of  $8 \times 10^4$  cells/ml in 1 ml of complete basal medium in each well of 6-well plates. After 24 h incubation, the medium was replaced with SPM containing 1% FBS with different concentrations of citicoline (1  $\mu$ M, 5  $\mu$ M and 10  $\mu$ M ). After 72 hours incubation, cells were washed with PBS and detached with trypsin. Then, the cells were counted in a TC10™ automated cell counter at least three times for each well. In this experiment, cells were treated in triplicate for each experimental condition.

#### **Cell migration (Wound Healing).**

Cells were seeded at a concentration of  $2 \times 10^5$  cells/ml in a 500  $\mu$ l of complete basal medium in each well of a poly l lysine pre-coated 24-well plates. After 24 hours incubation at 37 °C in 5% CO<sub>2</sub>, the medium was replaced with SPM containing 1% FBS. Each well of 24-well plates was washed with PBS 3 times and wound was made using a sterile pipette tip. The wells then were washed carefully with PBS to remove any floating cells and medium with SPM containing 1% FBS was added. Different concentrations of citicoline (1  $\mu$ M, 5  $\mu$ M and 10  $\mu$ M) were added and the cells were incubated in hypoxia (1% O<sub>2</sub>) for 24 hours. 50  $\mu$ l of 4% paraformaldehyde was added into each well to fix the cells for 5 min. The medium was then removed and the wells were washed with PBS. 100  $\mu$ l of 100% ethanol was added to the cells and left for 5

min. Then the ethanol was removed and the wells were left to dry before staining the cells with methylene blue for 5 min. The stain was removed and the wells were washed with distilled water. Finally the cells were examined under the microscope and pictures of the results were taken. In this experiment, cells were treated in triplicate for each experimental condition and pictures of five areas of each well were taken. The picture analysis was performed using image-J.

### **Tube like-structure formation in Matrigel™.**

hCMEC/D3 cells ( $1.5 \times 10^6$  cells/ml) were mixed with equal volume of growth factor-reduced Matrigel™ containing citicoline (10  $\mu$ M) with or without ErbB-2 inhibitor, FGF-2 (25 ng/ml). Any material in the contact with the gel was cold to avoid the gel polymerization. In a 48-well plate, a total amount of 35  $\mu$ l of this mixture was placed in a tear-like drop in the middle of the well and left to polymerize for 1 h incubation. Then, 500  $\mu$ l of complete medium was added into each well. After 24 h incubation, 4% of PFA was added to fix the endothelial tube-like structures in the gel. Under optical microscope, closed areas surrounded by endothelial tube like-structures were counted in 5 areas from each well.

### **Hypoxia studies.**

Here to study the protective effect of citicoline on endothelial cells in hypoxia. Glass coverslips were bathed in 100% ethanol for 10-20 min and left to air dry in a sterile environment. The coverslips were put in a 24-well plate and pre-coated with 500  $\mu$ l of 0.1 % poly-L-lysine solution. After 10 min incubation, the coverslips were washed with PBS and the cells were grown in complete medium at a cell concentration of  $5 \times 10^4$  cells/ml. After 24 hours incubation, the medium was removed and replaced with SPM

and incubated for 24 hours in normoxia. Different concentrations of citicoline was added to each well (1 $\mu$ M, 5 $\mu$ M, 10 $\mu$ M) in addition to untreated cells, then the cells were incubated in hypoxia (1% O<sub>2</sub>) for 24 h. One hour before the termination of the experiment, propidium iodide (PI; 10  $\mu$ g/ ml) was added in each well as an indicator of DNA damage without removing the medium. After 1 h incubation, the cells were washed with PBS. After 30 min, the cells were washed three times with PBS and one drop of Vectashield mounting medium with DAPI reagent was added on frosted glass slides. An average of three fields at x40 of magnification was photographed per coverslip by using Axiovert fluorescence microscope. A 24-well plate was run with similar experimental condition in normoxia. In this experiment, triplicate wells were carried out for each experimental condition with the control, the untreated cells.

### **Protein extraction and estimation.**

hCMEC/D3 cells ( $3.8 \times 10^5$  cells/ml; 2 ml) were seeded in complete medium in 6- well plate. After 48 h incubation, the medium was replaced with SPM containing 1% FBS. Different concentrations of citicoline was added to each well (1 $\mu$ M, 5 $\mu$ M, 10 $\mu$ M) in addition to untreated cells, then the cells were incubated in hypoxia (1% O<sub>2</sub>) for 24 hours. Then the cells were washed with 1 ml of PBS and gently lysed on ice in 50  $\mu$ l of ice-cold homogenized lysis buffer (pH 7.2). The cells were scraped, the cell lysate proteins collected and transferred into 0.5 ml micro-centrifuge tube. The protein concentration was determined using the BioRad protein assay. Briefly, BSA was used at 1mg/ml (1  $\mu$ g/  $\mu$ l) as a standard protein, 10  $\mu$ l of protein lysate was added and completed with 90  $\mu$ l of dH<sub>2</sub>O in a bijoux. After that, 2 ml of BioRad protein assay was added in each bijoux. The O.D of each sample was measured with spectrophotometer at

590 nm. The data outlining the reading of each protein samples and the standard curve required for protein estimation are shown below.

BSA Standard ( µg)	BSA volume added (1µg/ µl)	Volume of dH2O (µl)	Volume of diluted Biorad (ml)
0	0	100	2
10	10	90	2
20	20	80	2
40	40	60	2

Table 2. The volume of BSA, dH2O and Bio-Rad required to establish the standard curve.

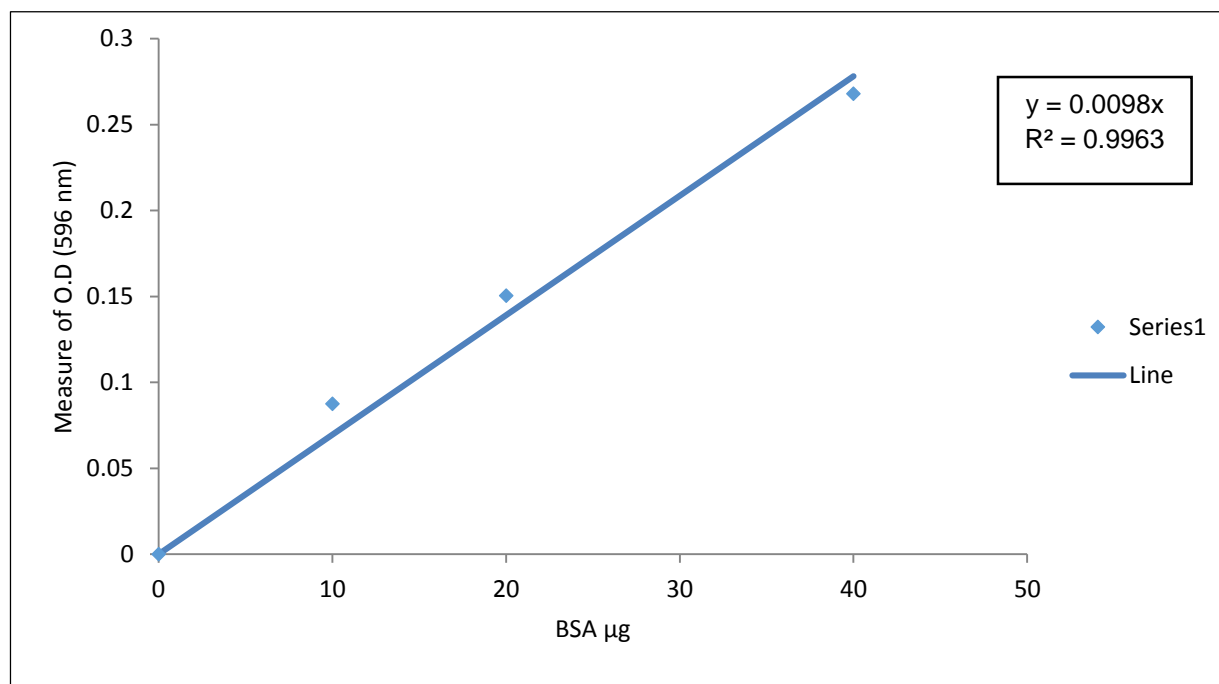


Figure 11. Standard curve for protein amount estimation in µg.

## **Western blotting.**

The acrylamide gel was prepared by mixing 3.3 ml of 40% bis-acrylamide with 4.2 ml distilled water and 2.5 ml separating buffer in a universal tube. 100 µl of 10% ammonium persulphate (APS) solution was added followed by 10 µl TEMED solutions. Few drops of isopropanol were added on top of the gel and the gel left to polymerise for 20 minutes. Isopropanol was removed after 15 minutes and rinsed with plenty of dH<sub>2</sub>O, for one minute. As much as possible, dH<sub>2</sub>O was removed by filter paper and then the stacking solution was prepared in a second universal tube, by combining 1.45 ml of 40% bis-acrylamide with 6.1 ml dH<sub>2</sub>O, and 2.5 ml stacking buffer. As before, 100 µl APS was added followed by 10 µl TEMED solution and the gel left to polymerise for a minimum of 20 minutes. Slowly the combs, clamps, and gaskets were then removed taking care not to damage the wells and the gel plates inserted into the electrophoresis chamber. The chamber was subsequently filled with electrode buffer (25 mM Tris, 192 mM glycine, 0.1% SDS, pH 8.3). A total of 500 ml electrode buffer was used to fill the tank, in the space between the two sets of glass plates. Take samples, sample buffers and molecular weight marker out of freezer and warm in room temperature. The protein concentration of each sample was determined by Bio-Rad protein assay to insure equal protein loading/well. Equal measures of protein sample and sample buffer were mixed in eppendorf tube, the tubes were placed in boiling water for 15 minutes. Molecular weight marker 5 µl and the protein samples were gently loaded. Samples containing 15 µg protein (up to 20 µl solution), along with pre-stained molecular weight markers, were separated by SDS- PAGE (12%) for ~45 minutes at 60 V (when samples were in



stacking gel) and switched to 200 V for separation until the dye, bromophenol blue, reached the bottom of the separation gel.

<b>Material</b>	<b>Volume</b>
<b>ddH<sub>2</sub>O</b>	4.2 ml
<b>40% Acrylamide</b>	3.3 ml
<b>Separating Solution*</b>	2.5 ml
<b>10% APS</b>	100 µl
<b>TEMED</b>	10 µl
	Total volume 10.11ml

\* Preparation method in page 66.

Table 3. Preparation of separating gel

<b>Material</b>	<b>Volume</b>
<b>ddH<sub>2</sub>O</b>	6.1 ml
<b>40% Acrylamide</b>	1.4 ml
<b>Stacking Solution*</b>	2.5 ml
<b>10% APS</b>	100 µl
<b>TEMED</b>	10 µl
	Total volume 10.11ml

\* Preparation method in page 66.

Table 4. Preparation of stacking gel.

### **Blotting.**

Two nitrocellulose membranes (NCM) and 12 pieces of chromatography paper were soaking for 2 minutes in towbin buffer. Stacking gels were removed from the separation

gels and discarded. The gels were sandwiched separately. The sandwich was assembled in an electro-blotter for each gel as follows: Three pieces of blotting paper /NCM/gel/3 pieces of blotting paper. Any bubbles within the sandwiches were removed by rolling a clean 5 ml tip over the sandwich. Proteins were transferred to the membrane at 45 mA per gel for one hour.

### **Blocking.**

Membranes were blocked with 1% BSA incubation for 1 hour at room temperature on rotating shaker. BSA was discarded and membranes were incubated separately in 10 ml of primary antibody solution (1:1000) dilution (rabbit polyclonal anti- ERK 1/2, mouse monoclonal antibodies to pERK1/2, rabbit polyclonal anti-Caspase 3 antibody, rabbit polyclonal anti-Caspase 3 active antibody, anti-Cleaved PARP antibody rabbit polyclonal, anti-PARP antibody rabbit polyclonal, anti-ErbB 2 (phospho Y1221) rabbit polyclonal antibody, anti-phospho-Histone H2B (Ser14) rabbit polyclonal antibody, anti-Histone H2B rabbit polyclonal antibody ) at 4°C. After overnight incubation on a rotating shaker, primary antibody solutions were transferred into labelled universal tubes and sodium azide was added to a final concentration of 0.02% (w/v) to prevent microbial contamination, the primary antibodies then should be kept at 4°C and can be used for up to a week. The membranes were washed five times in tris buffered saline and tween-20 (TBS-tween) for 10 minutes each at room temperature on rotating shaker.

Membranes were incubated for 1 hour at room temperature in 10 ml of mouse anti-rabbit or rabbit anti-mouse horseradish peroxidase-conjugated secondary antibody diluted in TBS-tween containing 5% (w/v) skim milk (1:1000). After incubation,

secondary antibody solutions were discarded and membranes were washed five times in TBS-tween for 10 minutes each at room temperature on a rotating shaker.

### **Imaging and data analysis.**

In a dark room, membranes were immersed in enhanced chemiluminescence (ECL) solution. Chemiluminescent is a chemical reaction that generates energy in the form of light and fades over time. To prepare the ECL solution, 1 ml of solution-A was added to 1 ml of solution-B and kept in the dark room for five minutes. Once the ECL solution was prepared it was then poured on to the membranes for one minute and left in the dark room excess reagent was drained off and membranes were quickly wrapped in cellophane films and kept in a box. After the dark room, the membranes in box were taken to the G-Box and were measured as a chemiluminescent samples. The intensities of bands on the membranes were quantified by image analysis software. Day to day variations in luminescence could arise due to protein degradation or experimental errors. Therefore, loading controls are essential for proper interpretation of western blots and can be used to normalize the levels of protein detected by confirming that protein loading is the same across the gel. The expression levels of the loading control should not vary between the different sample lanes. The results were semi- quantitative and compared to the control.

### **Flow Cytometry.**

The Annexin V-FITC Apoptosis Detection kit was used to detect apoptotic cells by flow cytometry. The annexins are a group of homologous proteins which bind phospholipids in the presence of calcium. Annexin V-FITC is a fluorescent probe which binds to

phosphatidylserine in the presence of calcium. The procedure consists of the binding of annexinV-FITC to phosphatidylserine in the membrane of cells, which are starting the apoptotic process, and the binding of propidium iodide to the cellular DNA in cells where the cell membrane has been completely compromised. hCMEC/D3 cells ( $3.8 \times 10^5$  cells/ml) were seeded in complete medium in 3×6- well plates. After 48 h incubation, the medium was replaced with SPM containing 1% FBS. Different concentrations of citicoline was added to each well (1µM, 5µM, 10µM) in addition to untreated cells, 6-well plate was incubated in hypoxia (1% O<sub>2</sub>) for 24 hours while the others were incubated in a 5% CO<sub>2</sub> incubator. The Annexin V-FITC Apoptosis Detection kit components were allowed to reach room temperature before use. Binding buffer was prepared by diluting 1 ml of the 10 × binding buffer with 9 ml of deionized water. Apoptosis was induced in one well with the addition of 1 mg/ml staurosporine at the same time a control of non-induced hCMEC/D3 cells was established and both (treated and untreated cells) were incubated for 1 hour in a 37 °C, 5% CO<sub>2</sub> incubator. All hCMEC/D3 cells in the experiment were re-suspended in 1× Binding Buffer. 500 µl of the all cell suspensions were added to labelled plastic 12 × 75 mm test tubes. 5 µl of Annexin V FITC Conjugate was added and 10 µl of Propidium Iodide Solution to each cell suspension. The tubes were then incubated in the dark at room temperature for 10 min. The fluorescence of the cells was measured immediately with a flow cytometer. Cells, which are early in the apoptotic process, will stain with the Annexin V FITC Conjugate alone. Live cells will show no staining by either the Propidium Iodide Solution or Annexin V FITC Conjugate. Necrotic cells will be stained by both the Propidium Iodide Solution and

Annexin V FITC Conjugate. In this experiment, triplicate wells were carried out for each experimental condition.

### **Immunofluorescence.**

Glass coverslips were bathed in 100% ethanol for 10-20 min and left to air dry in a sterile environment. The coverslips were put in a 2×24-well plate and pre-coated with 500 µl of 0.1 % poly-L-lysine solution. After 10 min incubation, the coverslips were washed with PBS and the cells were grown in complete medium at a cell concentration of  $5 \times 10^4$  cells/ml. After 24 hours incubation, the medium was removed and replaced with SPM and incubated for 24 hours in normoxia. Different concentrations of citicoline was added to each well (1µM, 5µM, 10µM) in addition to untreated cells, one 24-well plate was then incubated in hypoxia (1% O<sub>2</sub>) for 24 h while the other was incubated in normoxia for the same period of time. The medium was removed carefully and the cells were washed with PBS. Cells were fixed in 4% Paraformaldehyde (PFA) for 20 minutes at room temperature, then rinsed 3x with PBS. The samples were blocked in 10% goat serum for 30 minutes at room temperature. The samples then were incubated with primary antibody 1:100 diluted in 10% goat serum (rabbit polyclonal anti-Caspase 3 active antibody and anti-phospho-Histone H2B (Ser14) rabbit polyclonal antibody) for 1 hour at room temperature. After the 1 hour incubation the coverslips were washed in PBS 5 times for 5 minutes each wash. Then Alexa Fluor® goat anti-rabbit was added at 1:1000 concentration and the coverslips were incubated for 1 hours at room temperature in the dark. The secondary anti-body was removed and the coverslips were washed 5 times for 5 minutes each with PBS in the dark. To mount coverslips, the edge was blotted on tissue paper to dry off excess liquid and cell side was placed down on

drop of mounting media (VECTASHIELD Mounting Medium with DAPI) on glass slide. The coverslip were stabilized on slide using nail polish and left to dry overnight before viewing. The images were captured using Axiovert fluorescence microscope. In this experiment, cells were treated in triplicate for each experimental condition and pictures of five areas of each well were taken.

### **RNA extraction.**

hCMEC/D3 cells were seeded at a concentration of  $2 \times 10^5$  cells/ml in 2xT75 flasks and incubated in complete medium for 24 hours. After 24 hours incubation, the medium was removed and replaced with SPM and incubated for 24 hours in normoxia. One flask was treated with 10  $\mu$ M concentration of citicoline and the other was not treated, then both flasks were incubated in 1% O<sub>2</sub> hypoxia for 24 hours. The cells were then trypsinized and the cell pellet was kept in ladled Eppendorf tubes at -80 °C to be used later in RNA extraction. The RNA extraction was done using RNeasy® Mini Kit. DNase I stock solution was prepared by injecting 550  $\mu$ l RNase-free water into the DNase I vial using an RNase-free needle and syringe, and mixed gently by inverting the vial. 350  $\mu$ l of RLT buffer was added to each cell pellet, and centrifuged for 15 s at  $\geq 8000 \times g$  ( $\geq 10,000$  rpm). 10  $\mu$ l DNase I stock solution was added to 70  $\mu$ l Buffer RDD and mixed gently by inverting the tube, then centrifuged briefly. DNase I incubation mix was added (80  $\mu$ l) directly to RNeasy column membrane, and place on bench-top (20–30°C) for 15 min. 700  $\mu$ l of the RW1 buffer was added to the RNeasy spin column. The lid was closed, and centrifuged for 15 s at  $\geq 8000 \times g$ . The flow-through was discarded. 500  $\mu$ l of the RPE buffer was added to the RNeasy spin column, and centrifuged for 15 s at  $\geq 8000 \times g$ .

The flow-through was discarded. 500 µl of the RPE buffer was added to the RNeasy spin column, and centrifuged for 15 s at  $\geq 8000 \times g$ . The flow-through was discarded. The RNeasy spin column was placed in a new 1.5 ml collection tube. 30 µl RNase-free water was added directly to the spin column membrane and centrifuged for 1 min at  $\geq 8000 \times g$  to elute the RNA.

### **Quantification of nucleic acid.**

The upper and lower optical surfaces of the NanoDrop were cleaned using Kimwipe before loading the samples. 1 µl of each sample was loaded onto the lower optical surface. Once the instrument lever arm was lowered, the upper optical surface started to engage with the sample forming a liquid column with the path length defined by the gap between the two optical surfaces. During each measurement, the sample was evaluated at both 1-mm and 0.2-mm path, providing a large dynamic range of nucleic acid detection. The measurements were evaluated using NanoDrop software.

### **cDNA Synthesis Using the RT<sup>2</sup> First Strand Kit.**

The reagents of the RT<sup>2</sup> First Strand Kit were thawed, and briefly centrifuged (10–15 s) to bring the contents to the bottom of the tubes. The genomic DNA elimination mix for each RNA sample was prepared by adding 5 µg of RNA to 2 µl of GE buffer and RNA-free water. Mixed gently by pipetting up and down and then centrifuged briefly. The genomic DNA elimination mix was incubated for 5 min at 42°C, then placed immediately on ice for at least 1 min. The reverse-transcription mix was prepared by mixing 8 µl 5x BC3 buffer, 2 µl P2 control, 4 µl RE3 reverse transcriptase mix, and 6 µl RNase-free water. 10 µl reverse-transcription mix was added to each tube containing 10 µl genomic

DNA elimination mix. Mixed gently by pipetting up and down. Incubated at 42°C for exactly 15 min. Then immediately the reaction was stopped by incubating at 95°C for 5 min. 91 µl RNase-free water was added to each reaction and mixed by pipetting up and down several times. The reactions were placed on ice.

### **PCR microarray.**

The Human Apoptosis RT<sup>2</sup> Profiler PCR Array profiles the expression of 84 key genes involved in programmed cell death. This array includes TNF ligands and their receptors, members of the bcl-2, caspase, IAP, TRAF, CARD, death domain, death effector domain, and CIDE families, as well as genes involved in the p53 and DNA damage pathways. The experiment was carried out by first centrifuging the RT<sup>2</sup> SYBR Green Mastermix briefly (10–15 s) to bring the contents to the bottom of the tube. The PCR components mix was prepared in a 5 ml tube by mixing 1350 µl 2x RT<sup>2</sup> SYBR Green Mastermix, 102 µl cDNA synthesis reaction, and 1248 µl RNase-free water. The RT<sup>2</sup> Profiler PCR Array was carefully removed from its sealed bag. 25 µl PCR components mix was added to each well of the RT<sup>2</sup> Profiler PCR Array. The RT<sup>2</sup> Profiler PCR Array was tightly sealed with optical adhesive film. Centrifuged for 1 min at 1000 g at room temperature (15–25°C) to remove bubbles. The plate was visually inspected from underneath to ensure no bubbles are present in the wells. The real-time cycler was programmed according to table below.



Cycles	Duration	Temperature
1	10 min	95°C
40	15 s	95°C
	1 min	60°C

Table 5. The real-time cycler settings.

The RT2Profiler PCR Array was placed in the real-time cycler and the run was started. Threshold cycle (CT) was calculated for each well using the real-time cycler software.

### **Kinexusphospho-protein array analysis.**

Cells were seeded in 6-well plate at a concentration of  $3 \times 10^5$  cells / ml in complete medium. After 48 h incubation, the medium was replaced with SPM for further 24 h incubation then 10  $\mu$ M of citicoline was added to the cells for 10 min stimulation at 37°C and one well was used for control (untreated cells). Proteins were extracted according to Kinetworks instructions. Briefly, cells were washed twice with cold PBS. Protein was extracted using a buffer (pH 7.2) containing 20 mM 3-(N-morpholino) propanesulfonic acid (MOPS), 2mM EGTA, 5 mM EDTA, 30 mM sodium fluoride, 60 mM  $\beta$ -glycerophosphate, 20 mM sodium pyrophosphate, 1 mM sodium orthovanadate, 1 mMphenylmethylsulfonylfluoride, 3mM benzamidine, 5  $\mu$ M pepstatin A, 10  $\mu$ M leupeptin, 1% Triton X-100 and 1 mM dithiothreitol on ice for cell lysis. Cell extracts were then collected and protein concentrations were measured by the Bradford protein

assay according to the manufacturer's instructions (Bio-rad, Munchen, Germany). For each sample, protein (100 µg in 50 µl) was transferred to a fresh 1.5 ml Eppendorf screw cap then sent to Kinexus (Bioinformatics Corporation, Vancouver, Canada) to investigate the proteins involved in citicoline signalling pathways.

### **Statistical analysis.**

Statistical analysis was made through using Microsoft Excel 2007 program. The results of each experiment determined as the mean  $\pm$  Standard Deviation. Data shown were analysed for significance using one way ANNOVA and Student t-test. Differences with p values  $\leq 0.05$  were considered statistically significant. Each experiment was repeated at least three times.

# Chapter 3 Results

**Angiogenesis.**

**Kinexus Assay.**

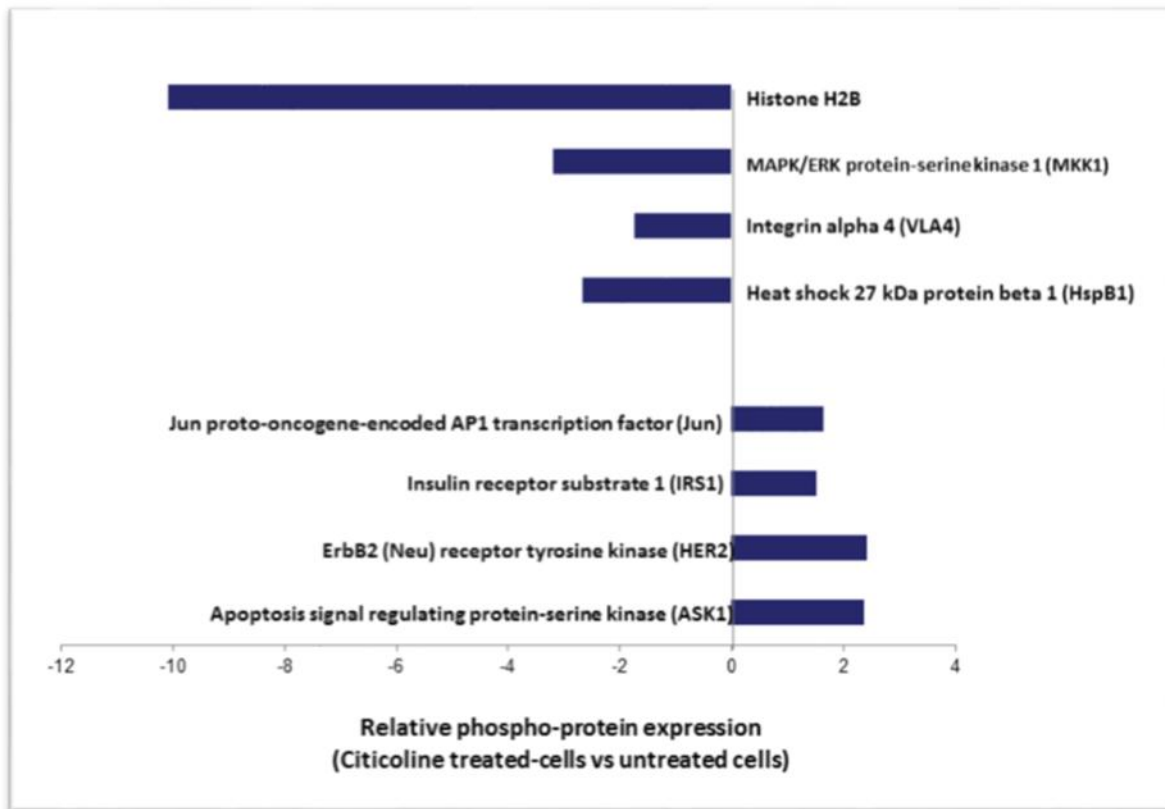


Figure 12. The Kinexus antibody microarray screen performed by Kinexus on BAEC. It showed a notable increase (> 100 %) of the phosphorylation of ASK-1, HER-2, IRS-1 and Jun and an inhibition (< 50%) for Hsp-70, Integrin alpha4, MEK-1 and Histone H2B proteins.

### **Pro-angiogenic effects of citicoline on hCMEC/D3 proliferation, migration and tube formation.**

Generally, there are three classes of additives that are required in the growth medium of cells to obtain continuous proliferation in vitro. The first class include nutrients such as glucose, amino acids, vitamins, iron, cobalt, manganese and selenium. The second class include cell adhesives which enable cells to attach to solid surfaces such as fibronectin, collagen and vitronectin. The third class of additives is serum which acts as a source of growth factors (Heath, 2008). Growth factors, cytokines, mitogens, hormones, and oxidative or heat stress are extracellular stimuli that can activate ERK1 and ERK2. Extracellular signal-regulated protein kinases 1 and 2 (ERK1/2) are members of the mitogen-activated protein kinase super family that can mediate cell proliferation and apoptosis (Cobb et al., 1995, Tesfaigzi et al., 2009). Treatment with citicoline stimulates the phosphorylation of ERK, therefore it could play a role as a mitogen. However, in this study, citicoline had no mitogenic effect on hCMEC/D3 cells when the cell proliferation assay was performed.

Condition	Cell Number ×10 <sup>4</sup>	SD ×10 <sup>3</sup>	Percentage increase	P Value
<b>Control</b>	13.6	14.1		
<b>1 μM Citicoline</b>	15.4	15.3	13%	0.34
<b>5 μM Citicoline</b>	17.6	7.2	29%	0.18
<b>10 μM Citicoline</b>	24.4	23.2	78%	0.16

Table 6. The effects of citicoline on hCMEC/D3 cells proliferation were determined and show statistically a non-significant increase in number of cells compared to control.

## **Pro-angiogenic effects of citicoline on hCMEC/D3 tube formation. HER-2 inhibition.**

Human epidermal growth factor receptor HER-2 plays an important role in cellular process including proliferation, metastasis, and angiogenesis. It is also found to be overexpressed in tumourigenesis and implicated in different types of cancers including gastric, prostate and breast cancer. HER-2 is mainly activated through heterodimerization with other members of the epidermal growth factor receptor (EGFR) family which causes downstream signalling through the Ras and phosphoinositide-3-kinase pathways. HER-2 inhibition has been a major interest as therapeutic strategy in cancer treatment (Boone et al., 2009, Slamon et al., 2001, Gomez-Martín et al., 2014). Overexpression of HER-2 in cancer is associated with aggressive histology, poor prognosis, and unresponsiveness to the standard endocrine therapies and shorter survival (Bauer, 2007). In view of the importance of the HER-2 pathway in the pathogenesis of breast cancer, there has been major interest on the inhibition of this pathway as a therapeutic strategy (Moasser et al., 2001). GW2974 is a quinazoline derivative, which acts as an inhibitor of HER-2. In animal model of biliary tract cancer (BCT), GW2974 treatment as a supplement in the diet showed a potent chemo-preventive and therapeutic effect (Kiguchi et al., 2005).

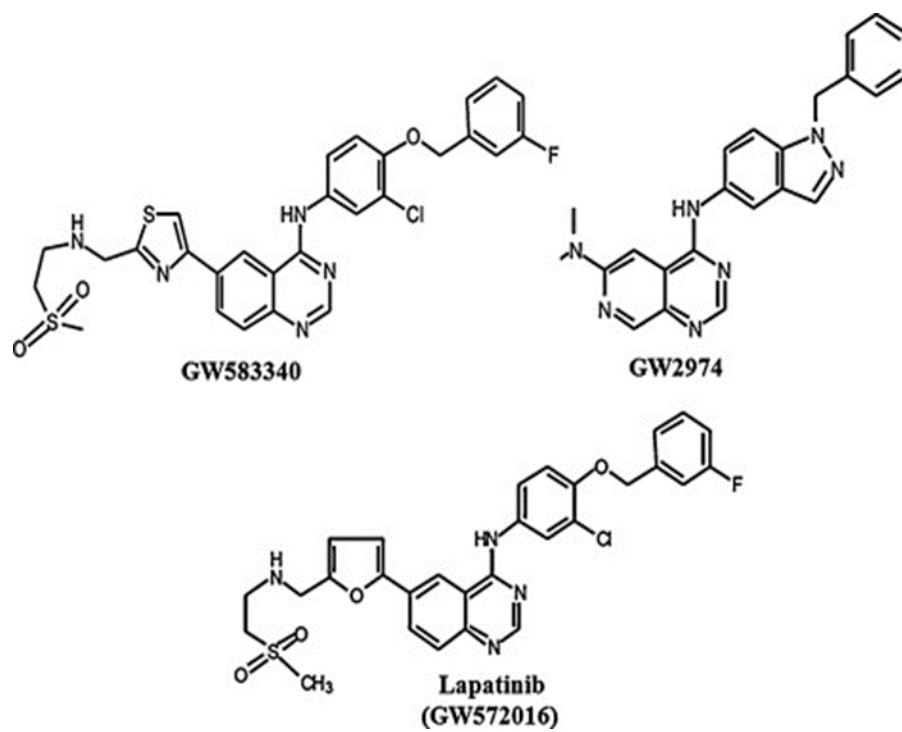


Figure 13. Chemical structure of GW2974 (Sodani et al., 2012).



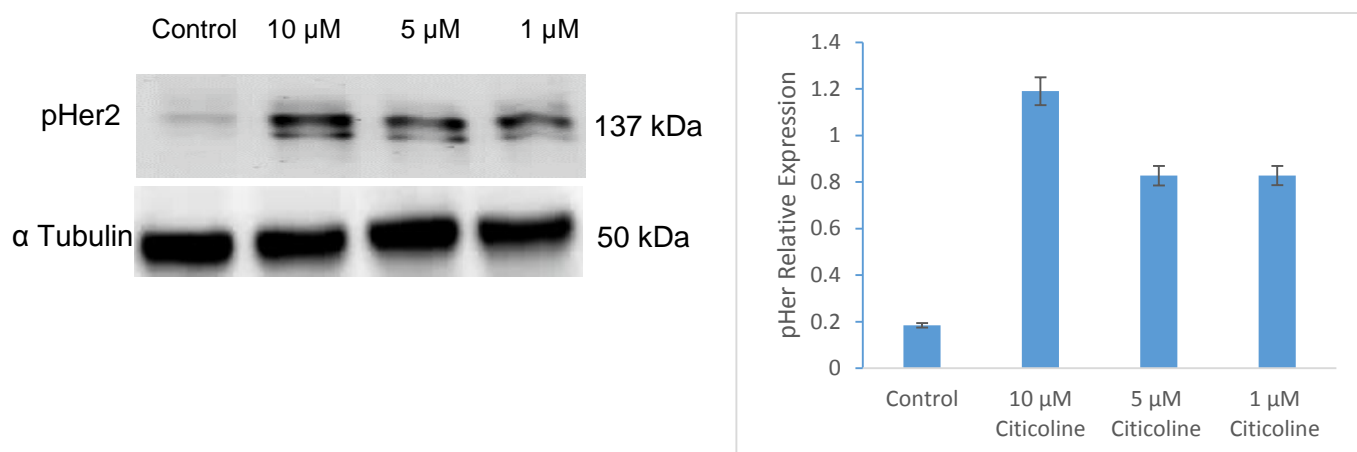


Figure 14. Representative western blot showing HER2 expression in cells untreated and treated with different concentrations of citicoline (1  $\mu$ M, 5  $\mu$ M and 10  $\mu$ M). Treatment with 10  $\mu$ M citicoline increased the expression of HER2 by 545.2% compared to control. Cells treated with 5  $\mu$ M citicoline showed a 348.3% increase in HER2 expression compared to untreated cells. In cells treated with 1  $\mu$ M citicoline, there was a 348.4% increase in HER2 expression compared to control.

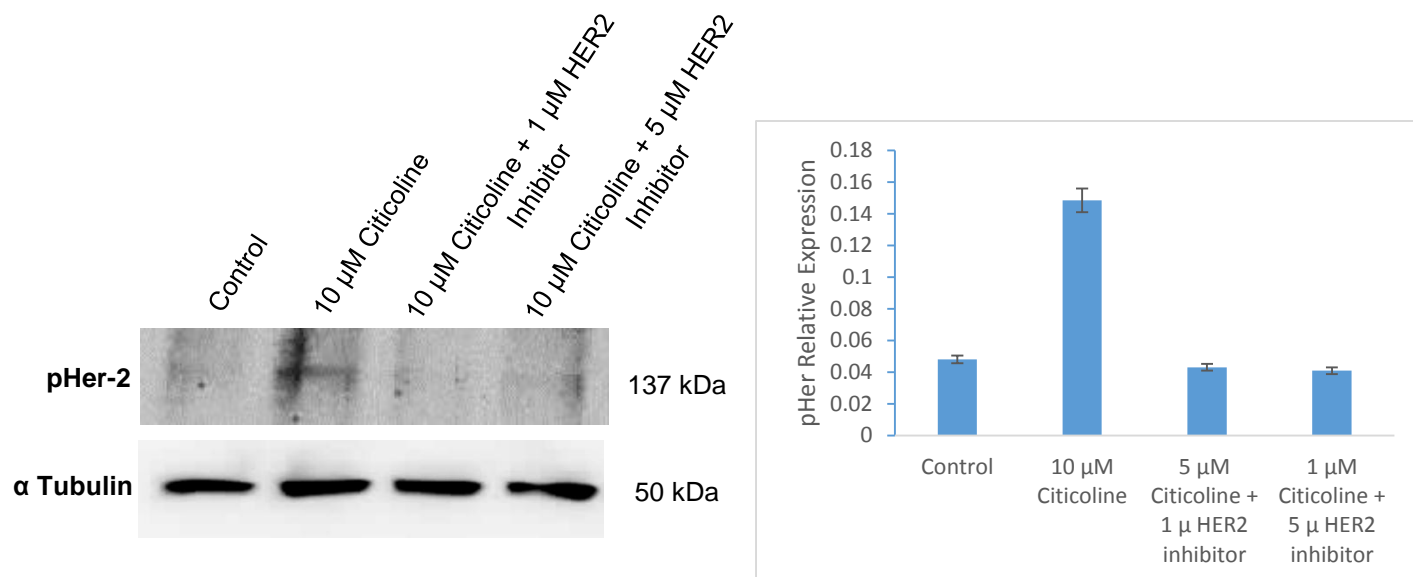


Figure 15. Representative western blot showing pilot experiment to determine optimal HER2 inhibitor concentration. HER2 expression was induced with 10  $\mu$ M citicoline which increased the expression of HER2 by 208.5% compared to control. Cells treated with 10  $\mu$ M citicoline in combination with 5  $\mu$ M HER2 inhibitor showed a 70.9% decrease in HER2 expression compared to cells treated with 10  $\mu$ M citicoline. In cells treated with 10  $\mu$ M citicoline in combination with 1  $\mu$ M HER2 inhibitor, there was a 72.4% reduction in HER2 expression compared to cells treated with 10  $\mu$ M citicoline.

## **Erk 1/2.**

The extracellular signal-regulated kinase (ERK) family belongs to the mammalian MAP kinases, and the activated MAP kinases catalyze the phosphorylation of numerous substrate proteins. ERK1 and ERK2 are related protein-serine/threonine kinases which are 84% identical in sequence and share many if not all functions, and therefore, they are referred to as ERK1/2. They are involved in the Ras-Raf-MEK-ERK signal transduction cascade which regulate of a wide range of processes including cell adhesion, cell cycle progression, cell migration, cell death, differentiation, metabolism, cell proliferation and growth, and transcription (Jr. et al., 2012, Schramek, 2002). They are 44- and 42-kDa proteins that phosphorylated a multitude of protein substrates and are expressed in almost all tissues (Tesfaigzi et al., 2009). In endothelial cells, hypoxia induces the activation of several components of signal transduction pathways. Members of the mitogen activated protein kinase MAPK superfamily, consisting of extracellular-related kinase ERK1/2 have been shown to be activated by hypoxia (Kroon et al., 2000). FGFs belong to a family of heparin-binding polypeptide growth factors that have over 20 members, including FGF-2. FGF-2, which has been shown to promote endothelial cell modifications associated with angiogenesis (Kim et al., 2014). The binding of FGF2 to its tyrosine-kinase receptors triggers downstream signalling which involves the activation of mitogen-activated protein kinase (MEK) with consequent phosphorylation of extracellular signal-regulated kinases (ERKs) (Giuliani et al., 1999).

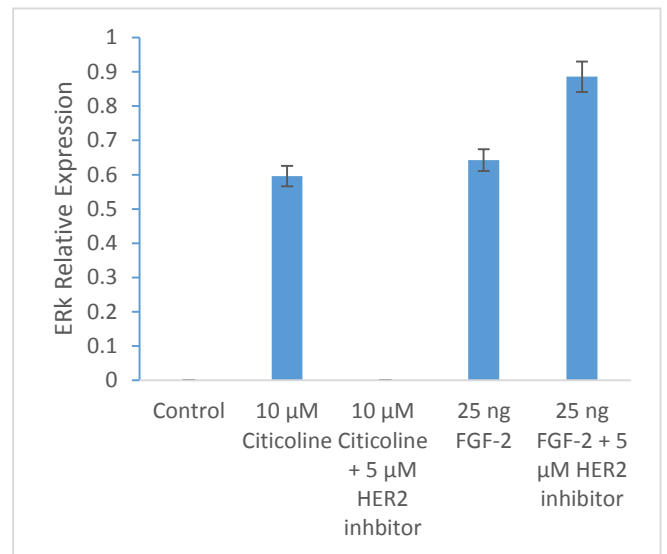
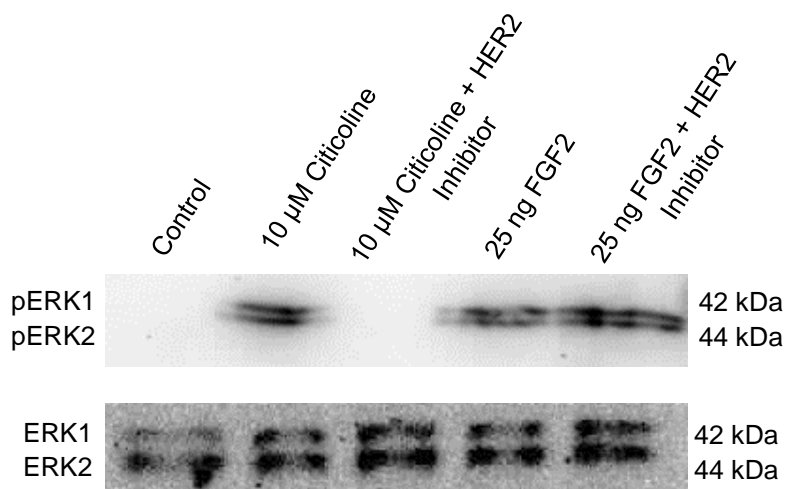
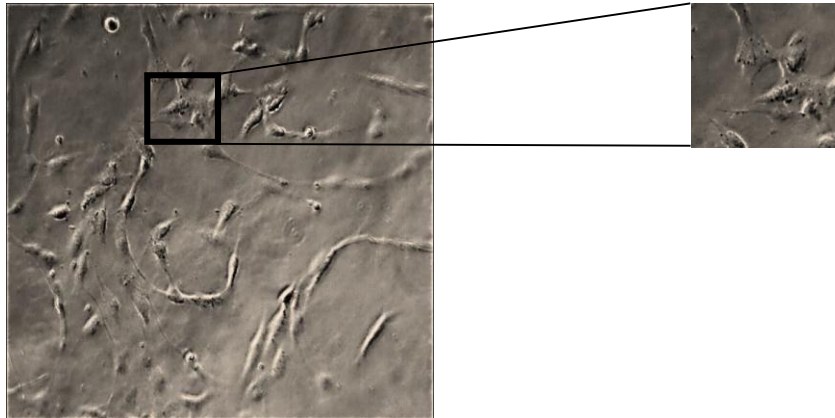


Figure 16. Representative western blot showing 25 ng FGF-2 and 10  $\mu$ M citicoline effect on pErk expression with and without 5  $\mu$ M HER2 inhibitor. P-Erk was expressed within similar range in cells treated with 25 ng FGF-2 and 25 ng FGF-2 in combination with Her2 inhibitor. P-Erk was also expressed in cells treated with 10  $\mu$ M citicoline but in cells treated with 10  $\mu$ M citicoline in combination with Her2 inhibitor p-Erk was not expressed.

**Optimisation of cell differentiation assay (Matrigel™ 3D-tube formation).  
Determine cell concentration for tube formation assay**

A) Control Cells.



B) 25 ng FGF-2.



C) 10  $\mu$ M Citicoline.

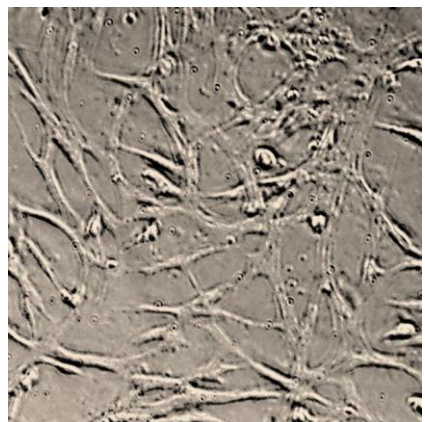


Figure 17. Citicoline (10  $\mu$ M) significantly increased the formation of tube-like structures of HCMEC/D3 with a stronger effect than fibroblast growth factor-2 (FGF-2). A) Control cells. B) Cells treated with FGF-2 (25 ng/ml). C) Cells treated with Citicoline. The tubes structures are clearly shown in the box exerted.

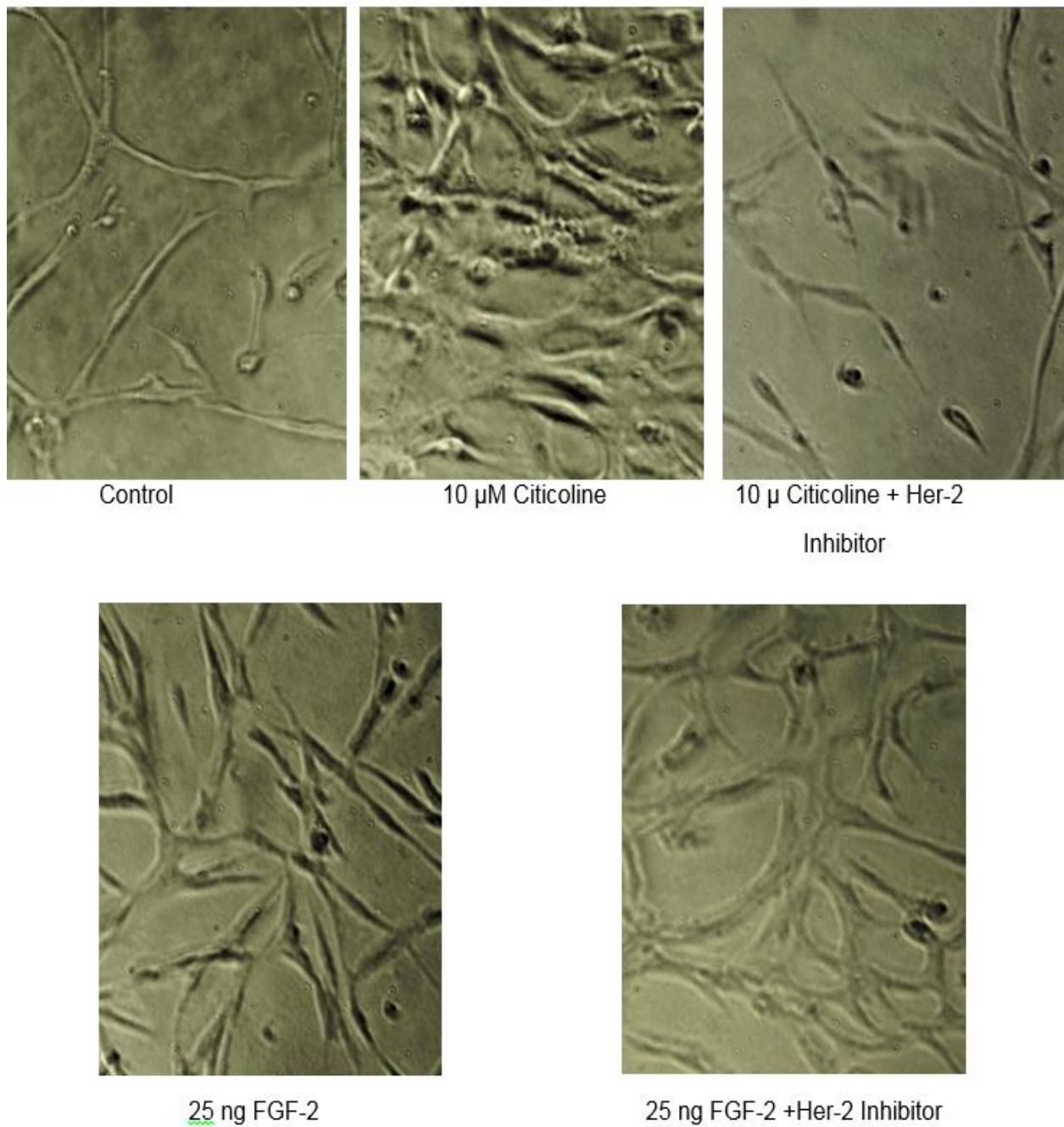


Figure 18. Representative examples of the effect of citicoline on tube formation with or without Her-2 inhibitor in comparison to FGF-2, FGF-2 + Her-2 inhibitor, and control cells.

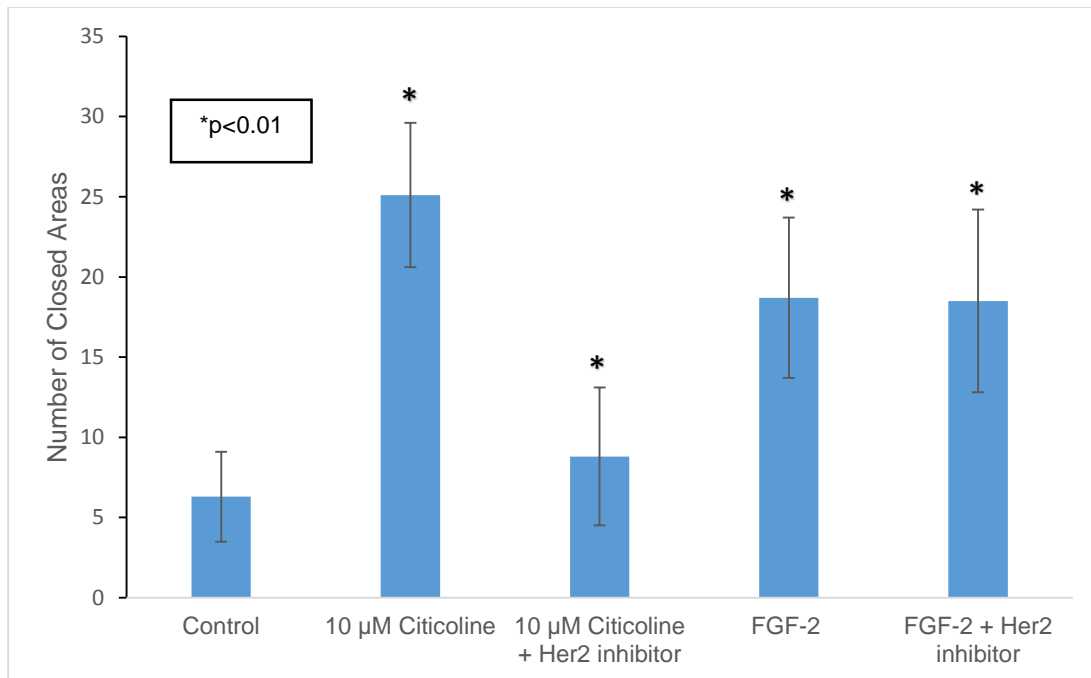


Figure 19. Pro-angiogenic effects of citicoline and FGF-2 on hCMEC/D3 tube formation. The bar graph shows the stimulatory effects of citicoline 10 μM, and FGF-2 (25 ng /ml). It also shows the inhibitory effect of Her-2 inhibitor (GW2974) on tube formation by blocking the stimulatory effect of citicoline. In combination with FGF-2, Her-2 inhibitor did not show inhibitory effect on FGF-2 activity. The bars represent the standard deviations. Experiments were performed in triplicate wells and repeated at least three times.

### **Pro-angiogenic effects of citicoline on hCMEC/D3 migration.**

hCMEC/D3 Cells were treated with different concentrations of citicoline (1  $\mu$ M, 5  $\mu$ M, 10  $\mu$ M) prior to a 24 hours incubation in stroke mimicking conditions (hypoxia). Pictures were taken at time 0 and then after 24 hours to capture the differences in number of cells migrated. In comparison to control, treatment with 1  $\mu$ M citicoline increased the number of cells migrated towards the wound site by 130% ( $P < 0.001$ ). Treatment with 5  $\mu$ M citicoline increased the number of cells migrated by 450% ( $p < 0.001$ ) in comparison to control. Treatment with 10  $\mu$ M citicoline showed the most cell movement and increase in number of cells migrated (810%) compared to control cells ( $P < 0.001$ ). The increase in number of migrated cells has been demonstrated to increase as citicoline concentration increased.



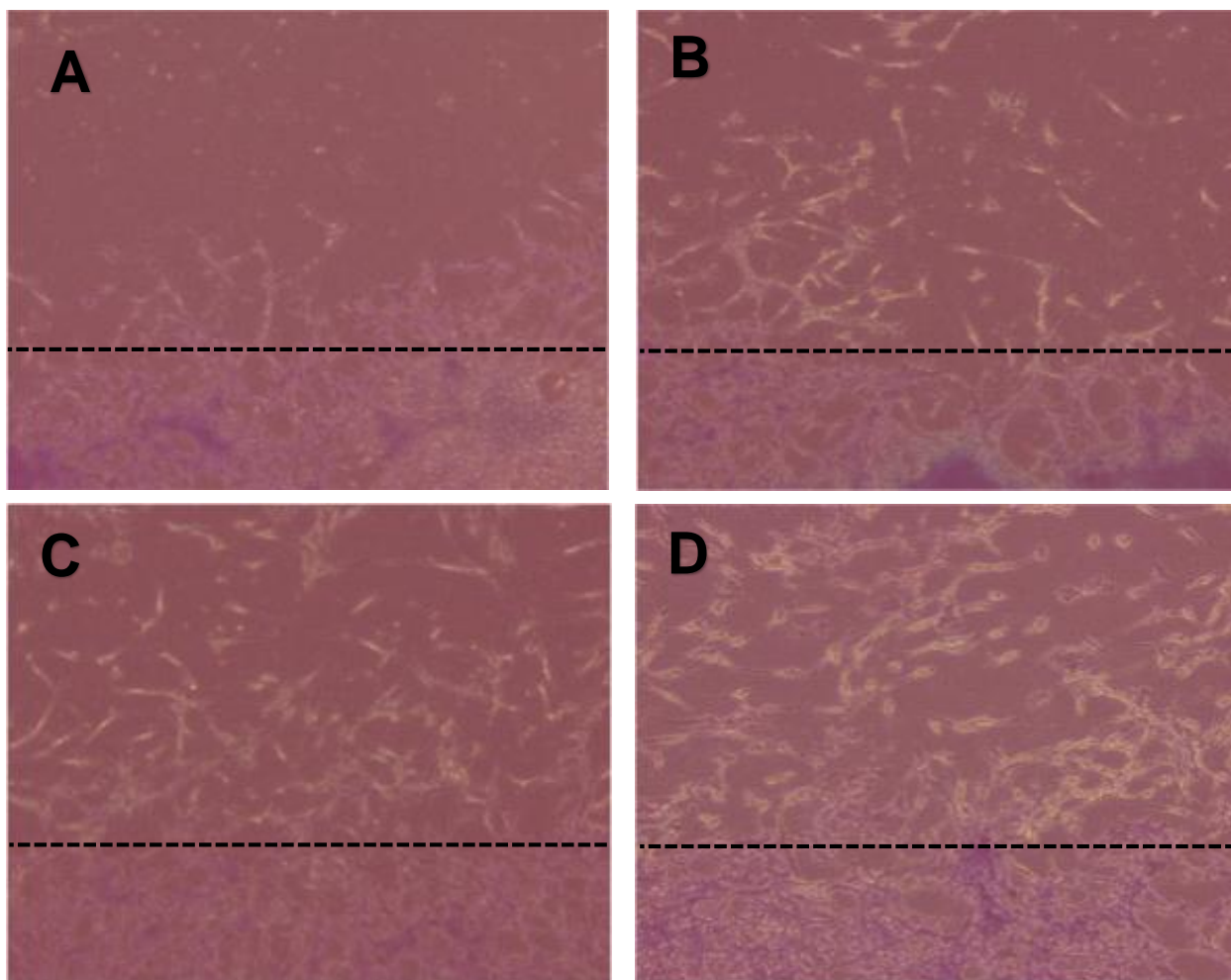


Figure 20. A) Control (untreated) cells in hypoxia. B) 1  $\mu$ M citicoline treated cells in hypoxia. C) 5  $\mu$ M citicoline treated cells in hypoxia. D) 10  $\mu$ M citicoline treated cells in hypoxia.

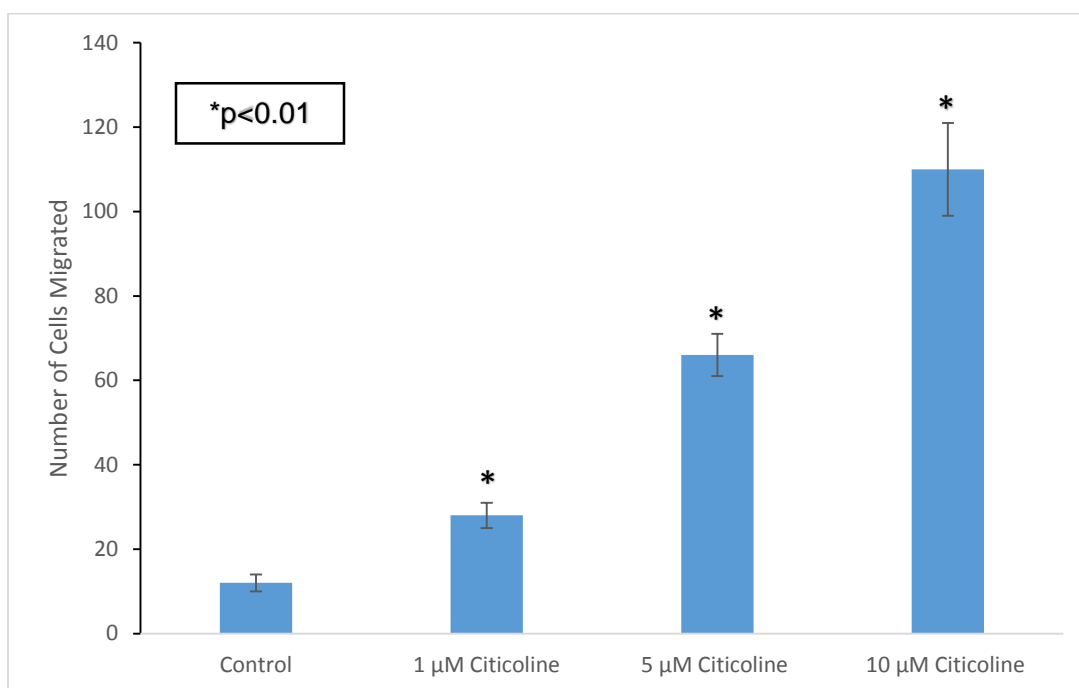


Figure 21. Pro-angiogenic effects of citicoline on hCMEC/D3 cell migration. After 24 hours incubation in hypoxia, citicoline in different concentrations (1  $\mu$ M, 5  $\mu$ M, 10  $\mu$ M) showed a significant increase in number of cells migrated. The bars represent the standard deviations. Experiments were performed in triplicate wells and repeated at least three times.

## **Apoptosis.**

### **Protective effect of citicoline against hypoxia induced DNA damage in endothelial cells.**

hCMEC/D3 cells were treated with different concentration of citicoline (1  $\mu$ M, 5  $\mu$ M, 10  $\mu$ M) prior to 24 hours incubation in hypoxia along with control (untreated) cells. PI staining was used to detect the apoptotic cells. PI is usually excluded from surviving cells and used to identify dead cells in a population. Cells were observed using fluorescence microscopy with two filter; DAPI fluorescent filter, and rhodamine filter with x40 magnification. Cells were considered apoptotic when they displayed signs of apoptosis such as condensation of nuclear materials, incorporation of PI stain (red colour) into the nucleus, disruption of cell cytoplasm and shrinkage of the cells. The normal cells appeared swollen with round clear blue nuclei.

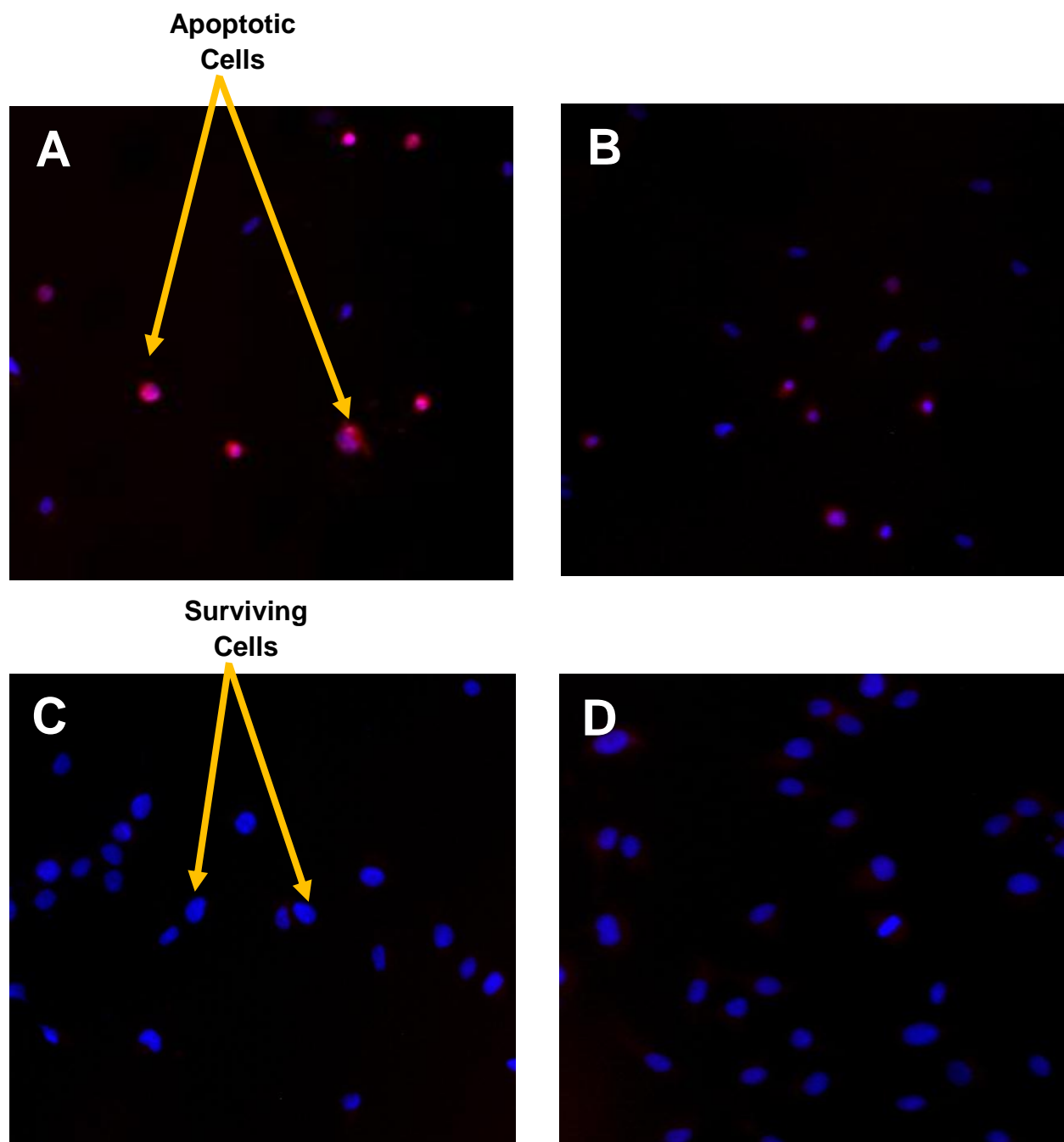


Figure 22. A) Control untreated cells in hypoxia. B) 1µM citicoline treated cells in hypoxia. C) 5µM citicoline treated cells in hypoxia. D) 10 µM citicoline treated cells in hypoxia.

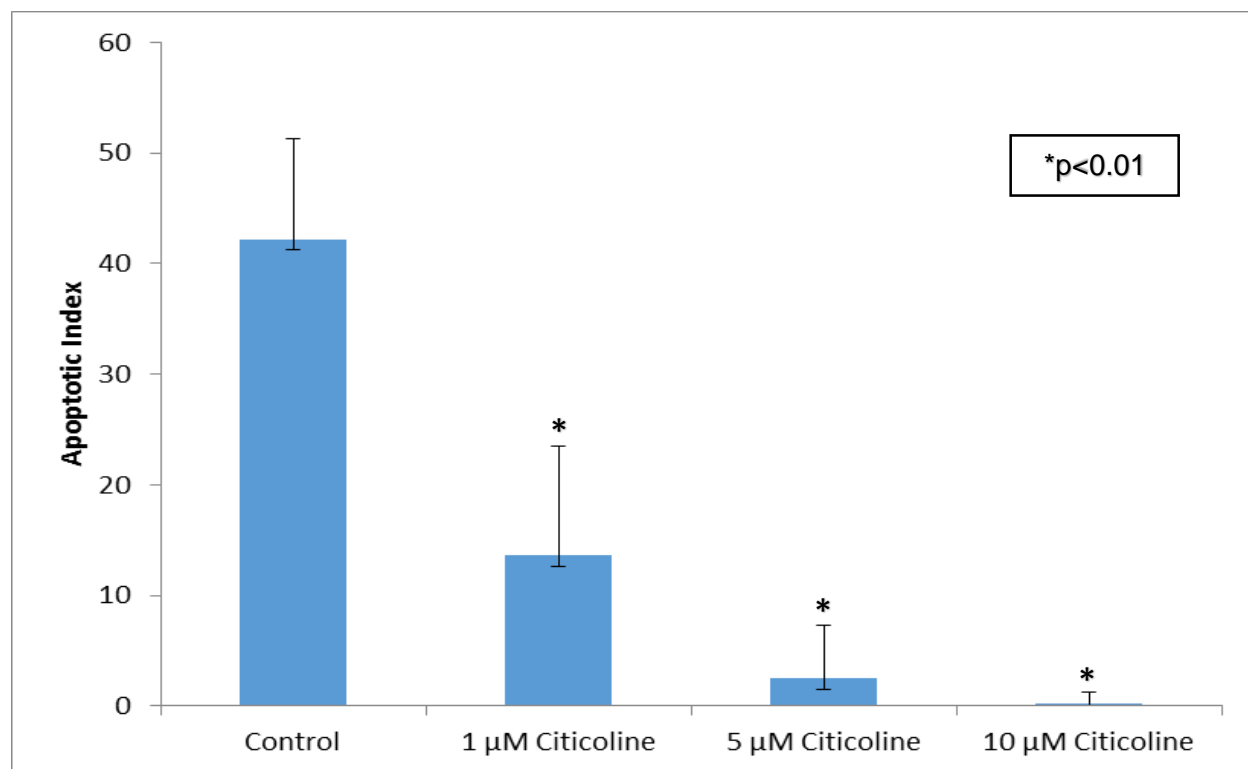


Figure 23. Quantitative analysis of the apoptotic cells in percentage. Cells treated with different concentrations of citicoline (1  $\mu$ M, 5  $\mu$ M, 10  $\mu$ M) in hypoxia conditions. Compared to control, treatment with 10  $\mu$ M citicoline showed the highest reduction (99.4%) in number of P.I positive cells. Treatment with 5  $\mu$ M citicoline showed a 95% reduction in number of P.I positive cells compared to untreated cells. 1  $\mu$ M citicoline treatment showed a reduction of 68% in comparison to control. The bars represent the standard deviations. Experiments were performed in triplicate wells and repeated at least three times.

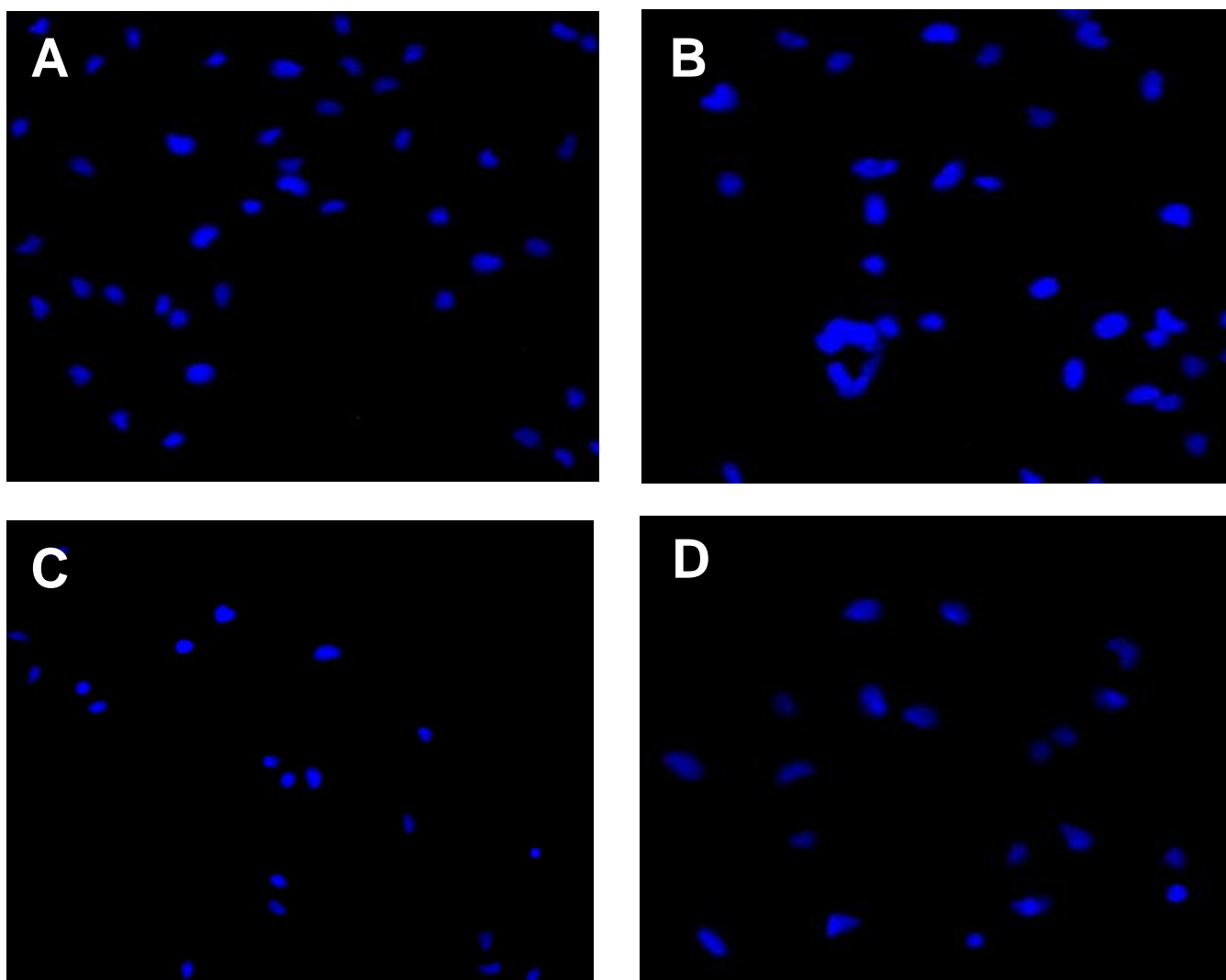


Figure 24. A) Control untreated cells in normoxia. B) 1  $\mu$ M citicoline treated cells in normoxia. C) 5  $\mu$ M citicoline treated cells in normoxia. D) 10  $\mu$ M citicoline treated cells in normoxia.

## **Western Blotting.**

$\alpha$ -tubulin, is an intracellular subunit of tubulin protein that is common in eukaryotes and makes up microtubules which are a component of the cytoskeleton and is involved in determining cell structure and providing platforms for intracellular transport, including some forms of cell locomotion, the intracellular transport of organelles, and the separation of chromosomes of during mitosis and meiosis (Ndhlovu et al., 2011, Cooper et al., 2000). In Western blotting, it is essential to correct for protein loading and factors, such as transfer efficiency using normalization against (housekeeping proteins) (Ferguson et al., 2005). Therefore, in this study, alpha tubulin was used as a loading control for Western blotting.

## **PARP expression.**

Poly (ADP-ribose) polymerase 1 (PARP-1), also known as ARTD1 (diphtheria toxin-like-ADP-ribosyltransferase), is a nuclear enzyme that is involved in both neuronal death and survival triggered by stress. PARP-1 is the most abundant of numerous PARP family members, accounting for more than 85% of nuclear PARP activity, and is present in all nucleated cells of multi-cellular animals (Castri et al., 2014, Kauppinen et al., 2007).

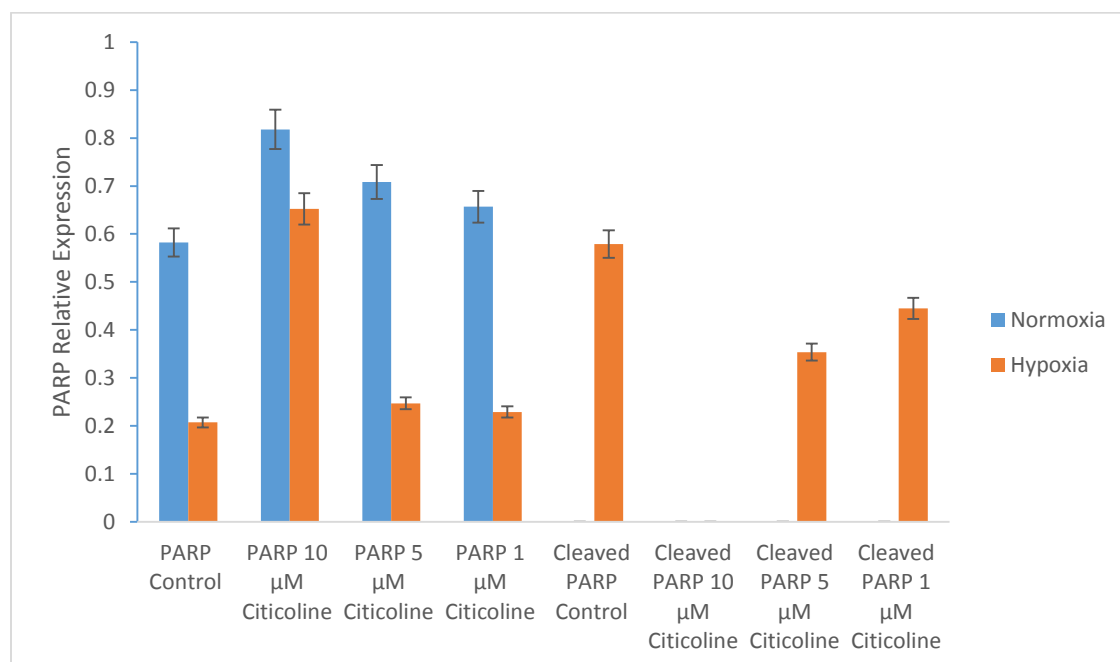
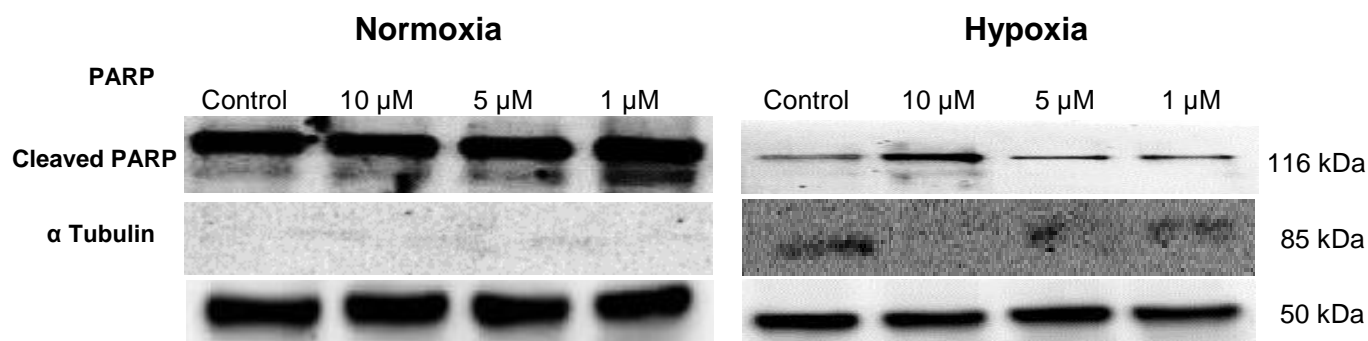


Figure 25. Representative Western blot showing the effect of citicoline on PARP expression in normoxia and hypoxia. In normoxia the expression of uncleaved PARP showed equal ranges across all conditions including control (untreated) cells, 1 μM citicoline, 5 μM citicoline, and 10 μM citicoline. Active PARP in normoxia is showing a very low expression. In hypoxia condition, the level of un-cleaved PARP expression varied among all conditions with 10 μM citicoline treated cells showing the highest (214.5%) increase of uncleaved PARP expression compared to control cells. In cells treated with 5 μM citicoline, the level of PARP expression showed a 19.0% increase compared to control condition. In cells treated with 1 μM citicoline, the level of



PARP expression showed a 10% increase compared to control condition. In hypoxia condition, the level of cleaved PARP expression varied among all conditions with 10  $\mu$ M citicoline treated cells showing the highest 100% reduction of cleaved PARP expression compared to control cells. In cells treated with 5  $\mu$ M citicoline, the level of cleave PARP expression showed a 38.9% reduction compared to control condition. In cells treated with 1 $\mu$ M citicoline, the level of cleaved PARP expression showed a 23.1% decrease compared to control condition.

### **Caspase-3 expression.**

Caspases, also known as interleukin 1 $\beta$ -converting enzyme (ICE)-like proteases play key biological roles in inflammation and mammalian apoptosis (Porter et al., 1997, Alnemri et al., 1996). The most intensively studied apoptotic caspase is caspase-3, which normally exists in the cytosolic fraction of cells as an inactive precursor that is activated by proteolysis during apoptotic cell death (Liu et al., 1997). Caspase-3 can be activated by multiple apoptotic signals including the activation of the cell receptor Fas (Apo-1/CD95). The protein Bcl-2 regulates Fas signalling which in turn activates the initiator caspases such as caspase-8 and caspase-10, and at the end activates executor caspase-3 (Hua et al., 2005). Caspase-3 can also be activated by cytotoxic T lymphocytes (CTL). CTLs are critical effector cells of the immune system and they kill their target cells mainly by induce cell death through FAS-mediated pathway (Jerome et al, 2003, Bleackley et al., 2002). Variety of pharmacological agents can also activate caspase-3 including oleanane triterpenoid 2-cyano-3,12-dioxoolean-1,9-dien-28-oic acid (CDDO) and 1-beta-D-arabinofuranosylcytosine. They both inhibit growth and differentiation of human myeloid leukemia cells and induce apoptosis through caspase-3 pathway (Ito, 2000). Caspase-3 expression and enzymatic activity can be inhibited by M826 (3-((2S)-2-[5-tert-butyl-3-[(4-methyl-1,2,5-oxadiazol-3-yl)methyl]amino]-2-oxopyrazin-1(2H)-yl]butanoyl)amino)-5-[hexyl(methyl)amino]-4-oxopentanoic acid). M826 potently inhibited both caspase-3 enzymatic activity and apoptosis in cultured cells in vitro and it provided a significant reduction (66%) in the number of neurons expressing active caspase-3 in rat model. In a rat model of neonatal hypoxic-ischemic

(H-I), M826 blocked caspase-3 activation, cleavage of its substrates and significantly reduced DNA fragmentation and brain tissue loss (Toulmond et al., 2004, Han et al., 2002).

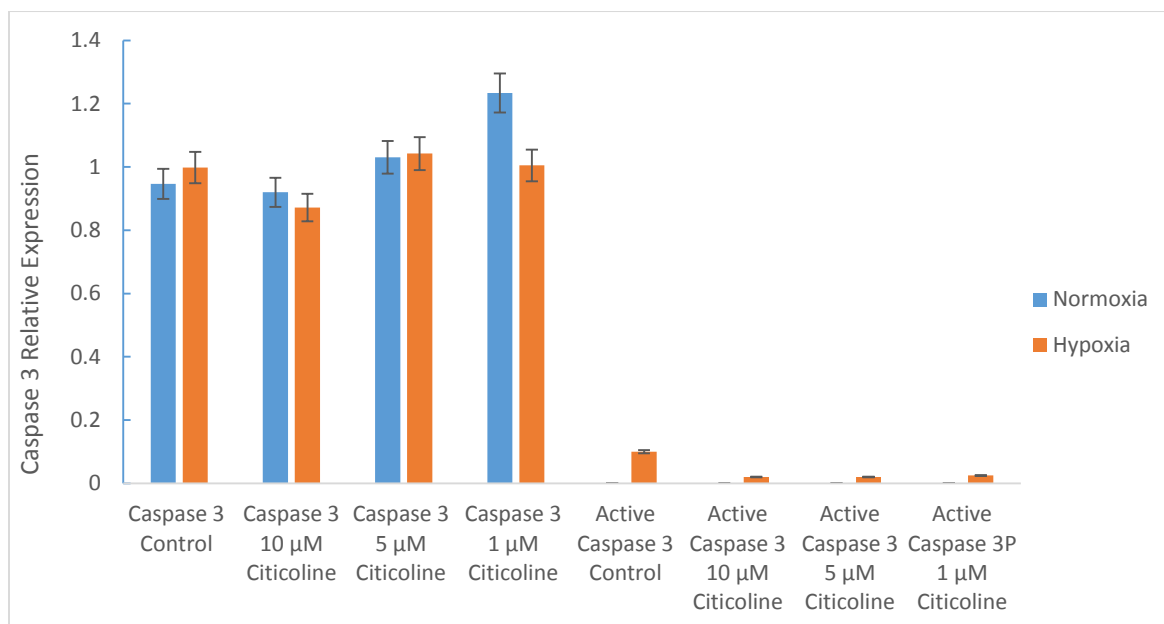
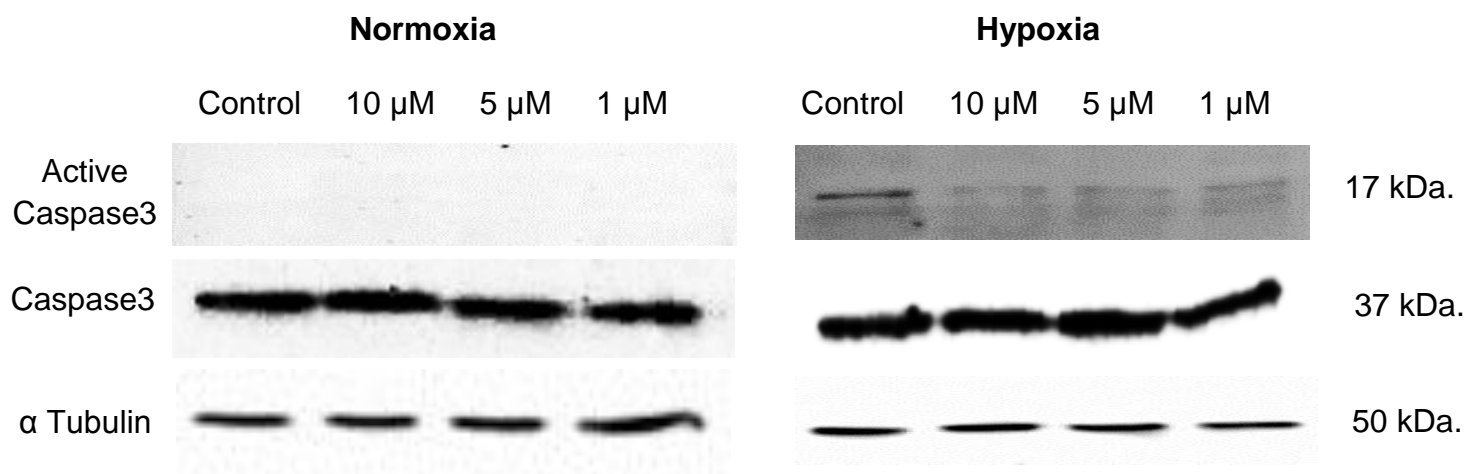


Figure 26. Representative Western blot showing showing the effect of citicoline on caspase 3 expression in normoxia and hypoxia. In normoxia, there was no expression of active caspase 3. In hypoxia condition, the level of caspase-3 varied among all conditions with 10  $\mu$ M citicoline treated cells showing the highest (79.6%) reduction of active caspase-3 expression compared to control cells. In cells treated with 5  $\mu$ M citicoline, the level of active caspas-3 expression showed a 79.5% decrease compared to control condition. In cells treated with 1 $\mu$ M citicoline, the level of

active caspase-3 expression showed a 75.2% reduction compared to control condition. The expression of total caspase-3 showed values within similar ranges across all conditions including control (untreated) cells, 1  $\mu$ M citicoline, 5  $\mu$ M citicoline, and 10  $\mu$ M citicoline.

## H2B Ser14 expression.

Histone proteins are major components of DNA in eukaryotic cells, and therefore, chromatin condensation which is one of the hallmark characters of apoptosis could be regulated by posttranslational histone modifications. Phosphorylation of histone H2B at serine 14 (S14) has been reported to be associated with cells undergoing programmed cell death in vertebrates (Cheung et al., 2003). In mammalian cells, the serine 14 residue in the NH<sub>2</sub>-terminal tail of histone H2B is rapidly phosphorylated at sites of DNA double-strand breaks (DSBs). This phosphorylation is mediated by sterile 20 kinase (Mst1) and is well known for its role during apoptosis. In a study, it has been reported that H2B-Ser14P and H2AX work in cooperation to form a heterochromatin-like state within which both damaged DNA and trigger DNA damage response (Fernandez-Capetillo et al., 2004, Altaf et al., 2007).

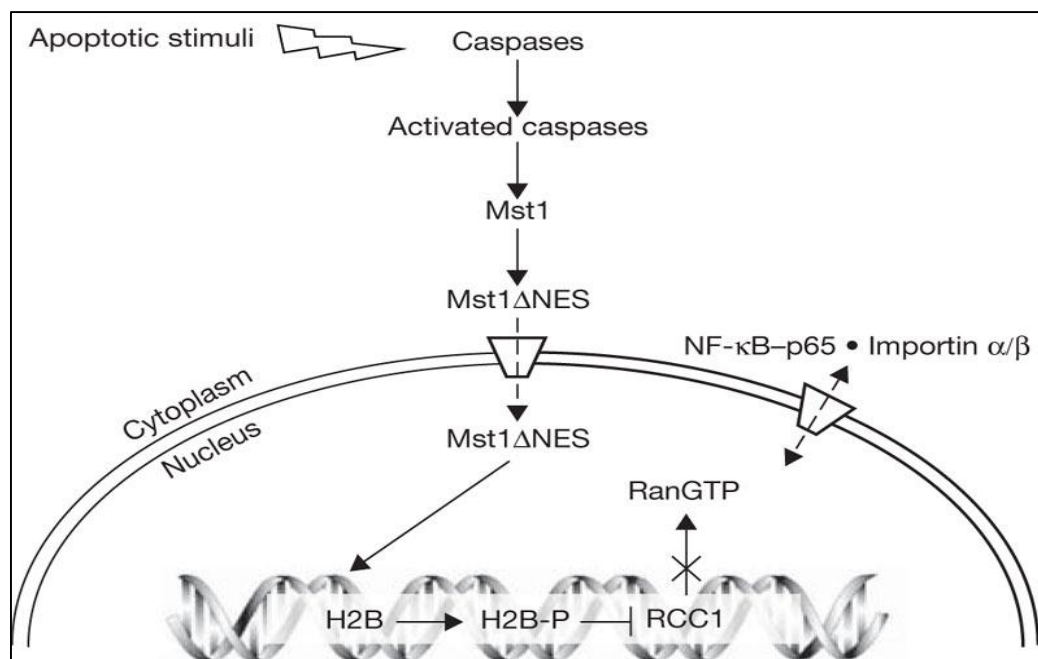


Figure 27. Apoptotic stimulation activates caspases which in turn activates Mst1. Mst1 is activated by caspases upon exposure to apoptotic stimuli. The activated Mst1 translocates to

the nucleus and phosphorylates histone H2B at Ser 14, which causes the obstruction of regulator of chromosome condensation (RCC1) mobility.

RCC1 impairment confines it in a binary complex with RAs-related nuclear protein (Ran), which affects the production of free RCC1 to catalyse another round of nucleotide transport.

Consequently, RanGTP production is affected. The diminished level of nuclear RanGTP causes inactivation of the nuclear transport machinery. As a consequence, NLS containing proteins, including NF-kappaB-p65, remain bound to importins alpha and beta in the cytoplasm (Wong et al., 2009).

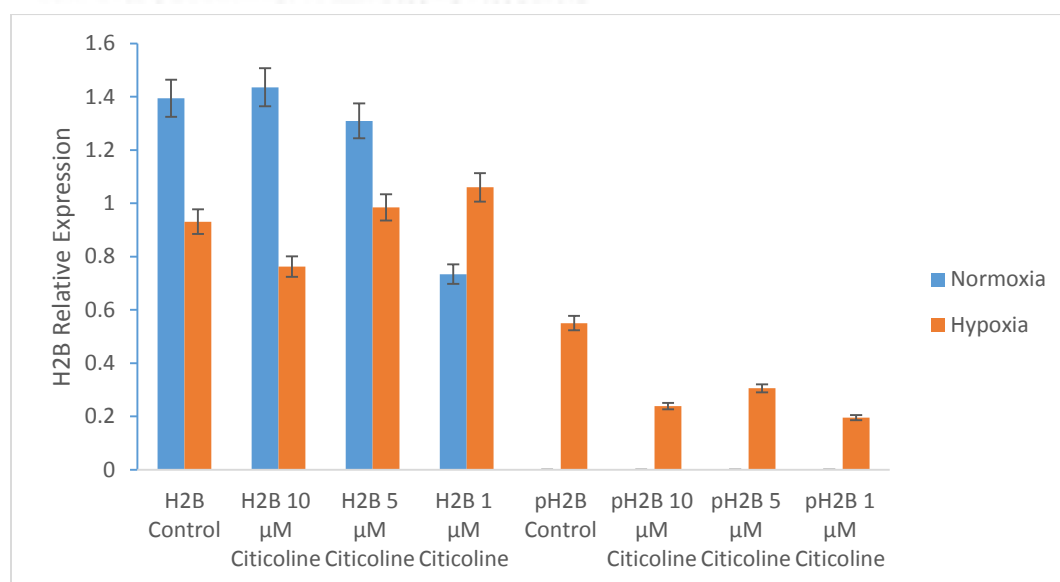
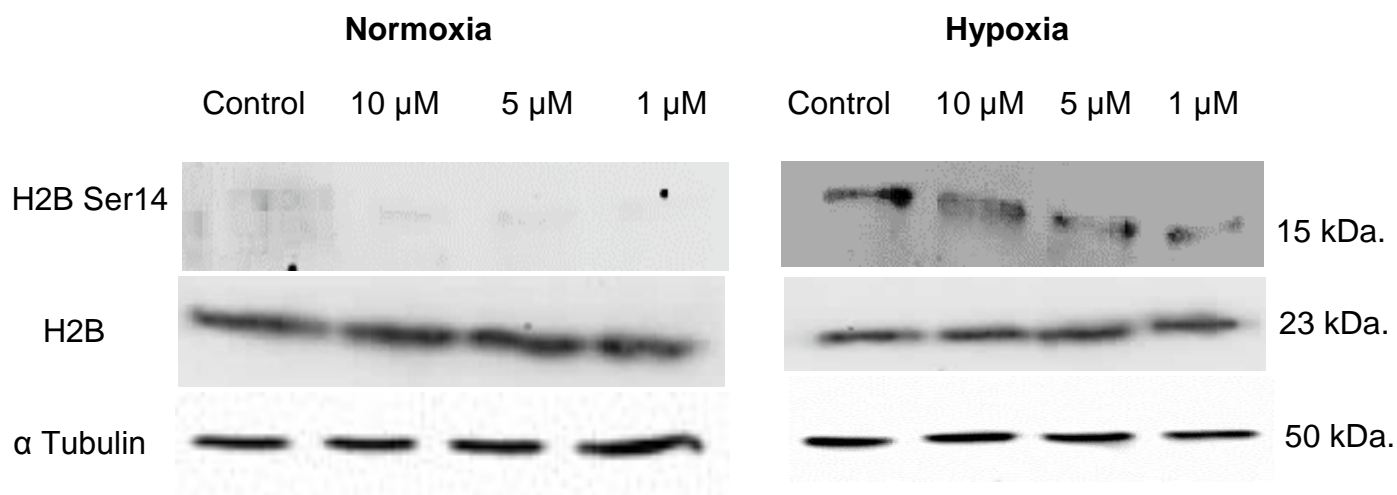


Figure 28. Representative Western blot showing the effect of citicoline on H2B expression in normoxia and hypoxia. There was an equal level of H2B and no H2B Ser14 expression in normoxia. In hypoxia condition, the level of H2B Ser14 expression varied among all conditions with 10 μM citicoline treated cells showing 56.7% reduction of H2B Ser14 expression compared to control cells. In cells treated with 5 μM citicoline, the level of H2B Ser14 expression showed a 44.5% decrease compared to control condition. In cells treated with 1 μM citicoline, there was a 64.4% reduction compared to control.



## Immunofluorescence.

### Active caspase-3.

Active caspase-3 expression was measured in hCMEC/D3 cells treated with different concentrations of citicoline (1  $\mu$ M, 5  $\mu$ M, 10  $\mu$ M) in hypoxia and normoxia conditions. After 24 hours, cells were stained with active caspase-3 antibody and photographed using fluorescence microscope. Cells in hypoxia conditions showed different levels of active caspase-3 expression, whereas in normoxia conditions, there was no visible expression of active caspase-3.

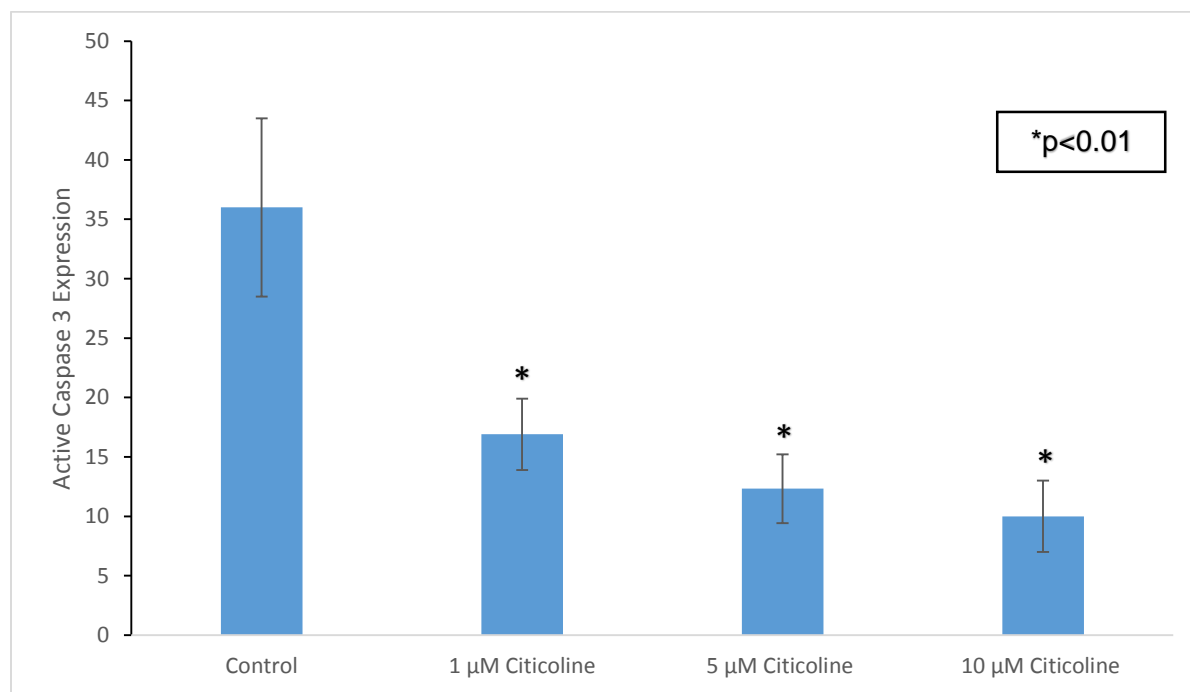


Figure 29. Active caspase-3 expression in cells treated with different concentrations of citicoline (1  $\mu$ M, 5  $\mu$ M, 10  $\mu$ M) in hypoxia conditions. The intensity of fluorescence, which was measured using fluorescence microscope, is equivalent to the level of protein expression. Compared to control, treatment with 10  $\mu$ M citicoline showed the highest reduction (72.2%) in caspase-3 expression. Treatment with 5  $\mu$ M citicoline showed a 65.8% reduction in caspase-3 expression

compared to untreated cells. 1  $\mu$ M citicoline treatment showed a reduction of 53.1% in comparison to control. The bars represent the standard deviations. Experiments were performed in triplicate wells and repeated at least three times.

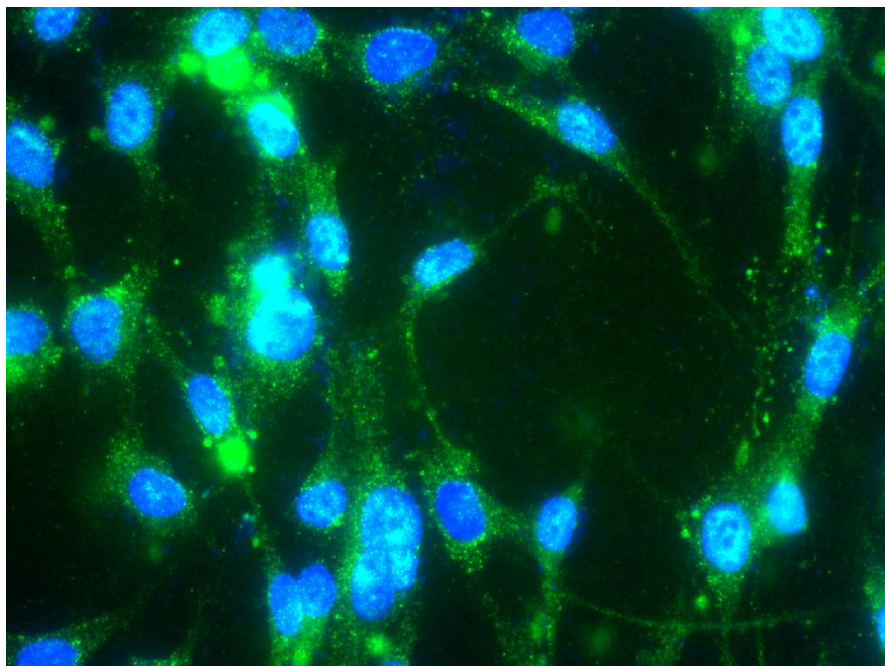


Figure 30. Control (untreated) cells in hypoxia.

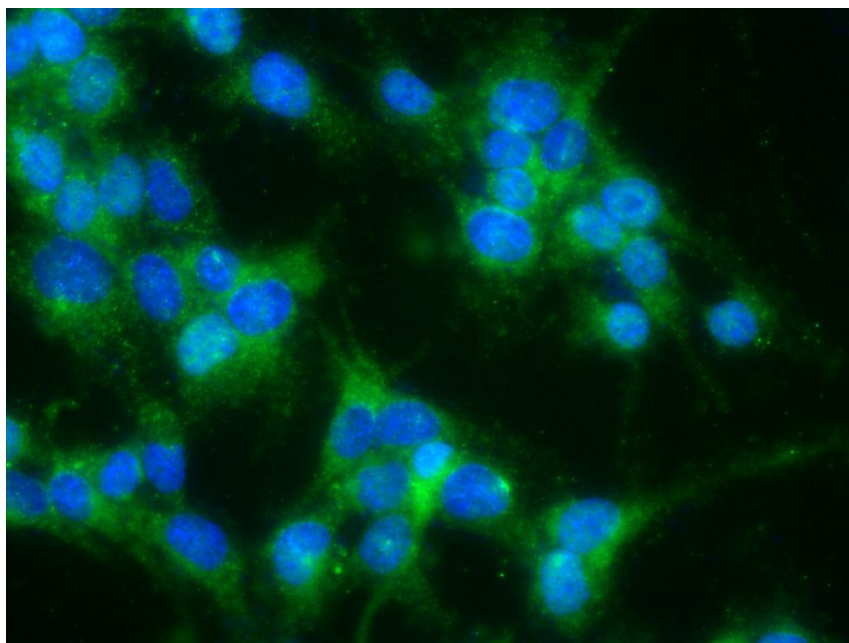


Figure 31. 1.1  $\mu$ M citicoline treated cells in hypoxia conditions.

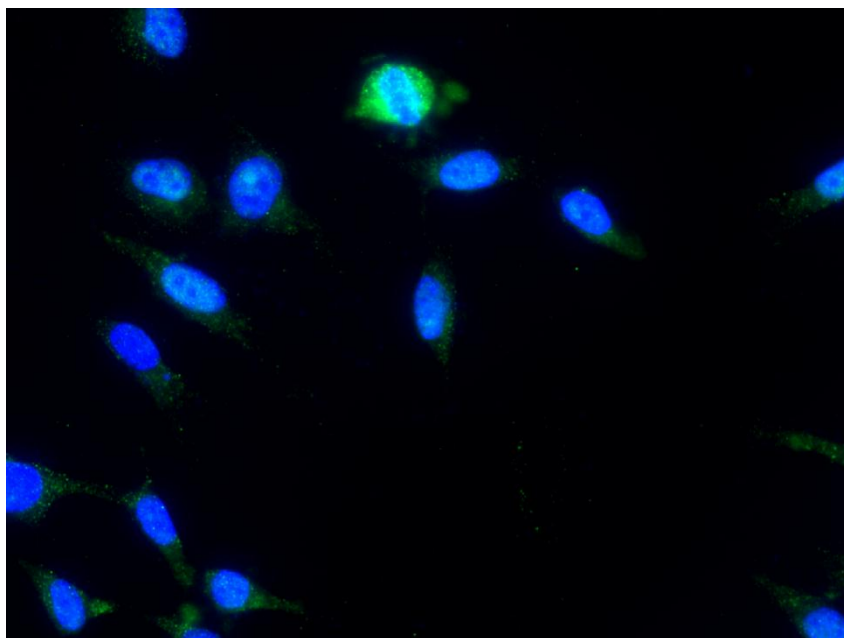


Figure 32. 5  $\mu$ M citicoline treated cells in hypoxia conditions.

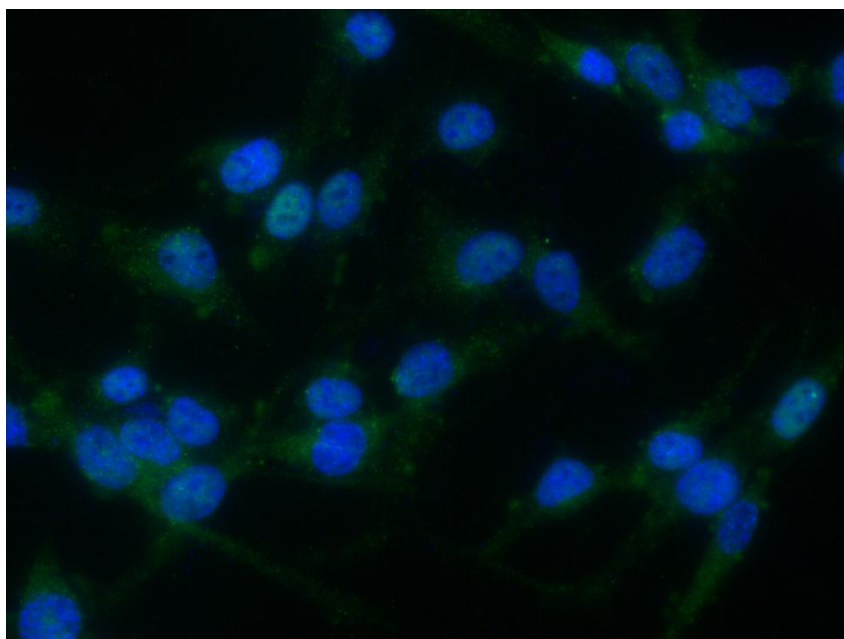


Figure 33. 10  $\mu$ M citicoline treated cells in hypoxia conditions.

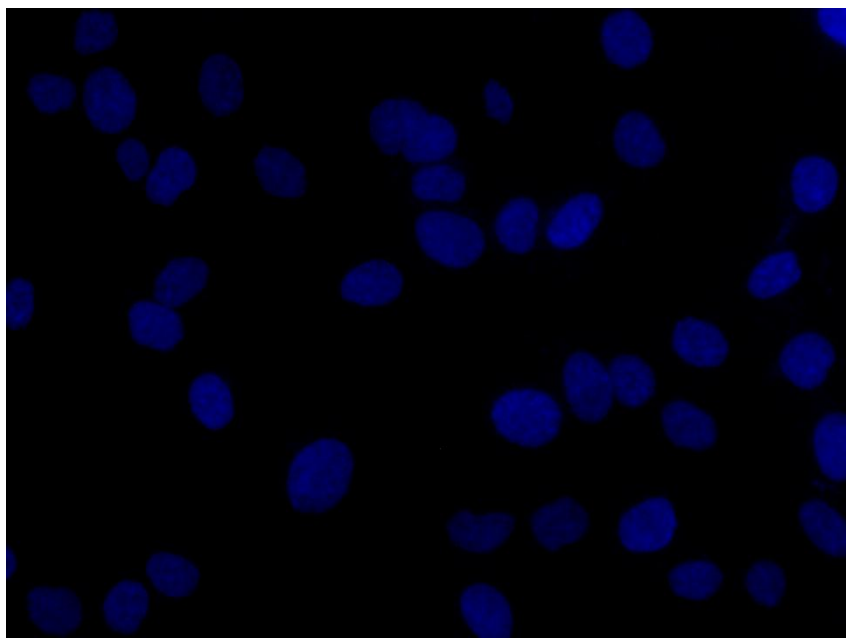


Figure 34. Control cells in normoxia conditions.

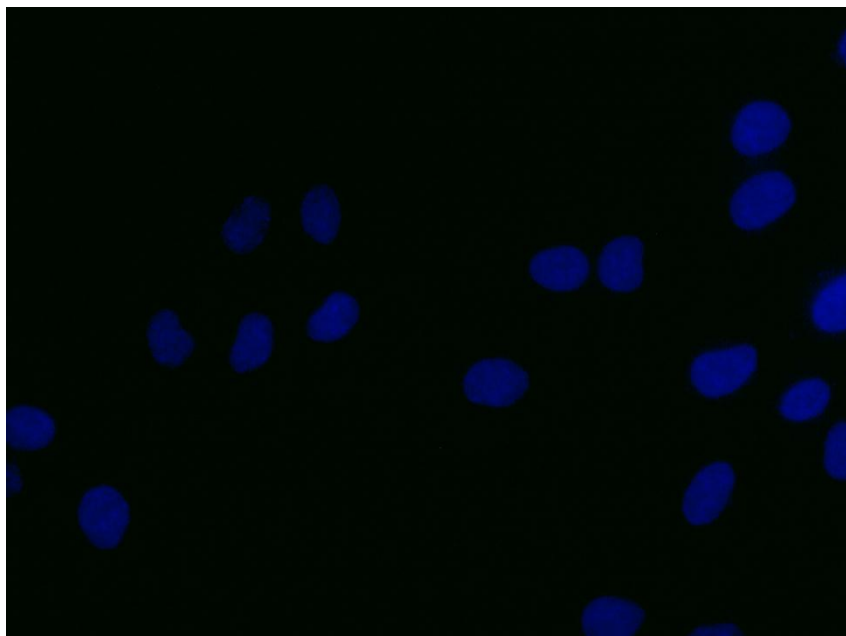


Figure 35. 1  $\mu$ M citicoline treated cells in normoxia conditions.

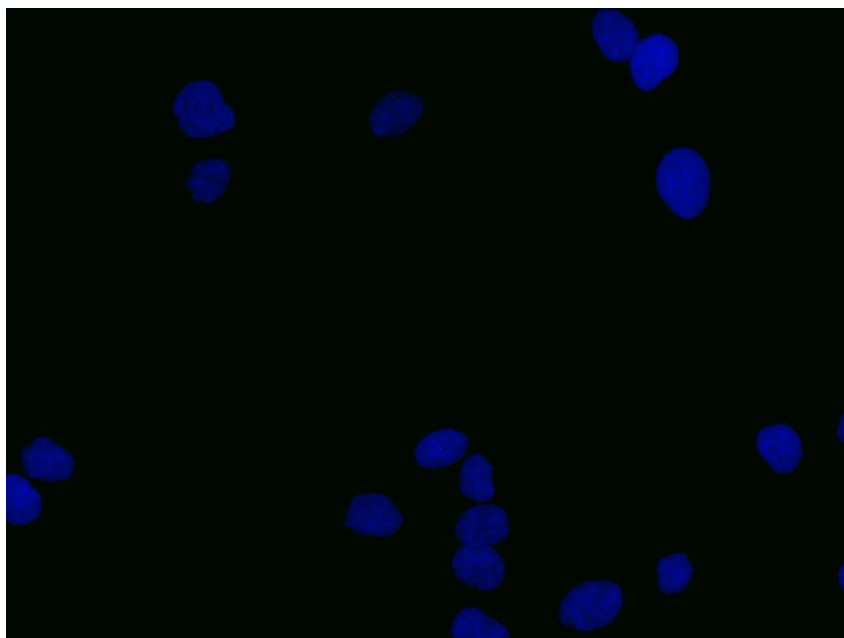


Figure 36. 5  $\mu$ M citicoline treated cells in normoxia conditions.

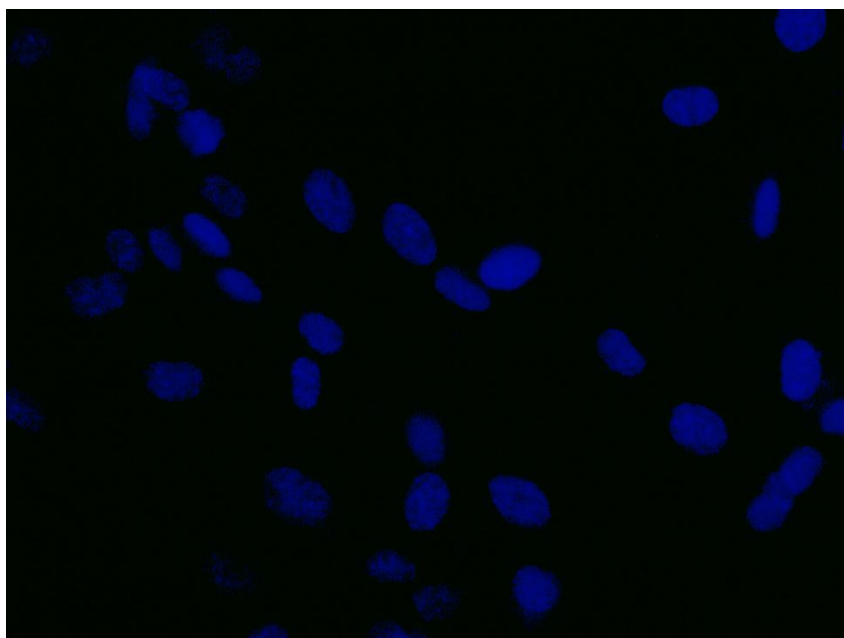


Figure 37. 10  $\mu$ M citicoline treated cells in normoxia conditions.

## H2B Ser14.

H2B Ser14 expression was measured in hCMEC/D3 cells treated with different concentrations of citicoline (1  $\mu$ M, 5  $\mu$ M, 10  $\mu$ M) in hypoxia and normoxia conditions. After 24 hours, cells were stained with H2B Ser14 antibody and photographed using fluorescence microscope. Cells in hypoxia conditions showed different levels of H2B Ser14 expression, whereas in normoxia conditions, there was no visible expression of H2B Ser14.

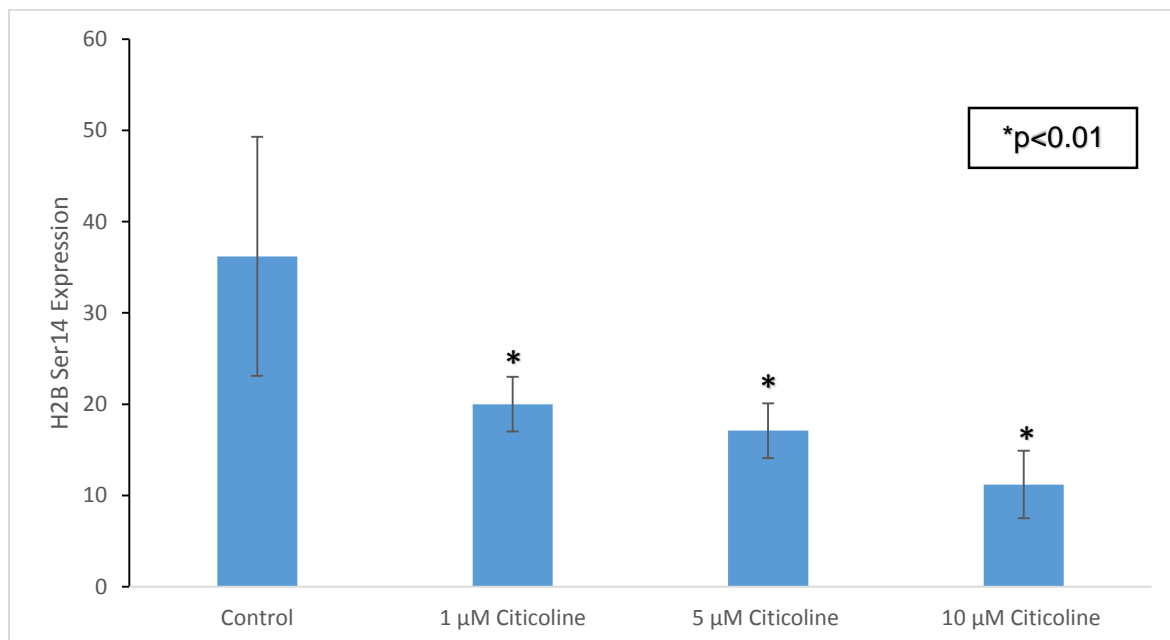


Figure 38. H2B Ser14 expression in cells treated with different concentrations of citicoline (1  $\mu$ M, 5  $\mu$ M, 10  $\mu$ M) in hypoxia conditions. Compared to control, treatment with 10  $\mu$ M citicoline showed the highest reduction (70%) in H2B Ser14 expression. Treatment with 5  $\mu$ M citicoline showed a 53% reduction in H2B Ser14 expression compared to untreated cells. 1  $\mu$ M citicoline treatment showed a reduction of 45% in comparison to control. The bars represent the standard deviations. Experiments were performed in triplicate wells and repeated at least three times.

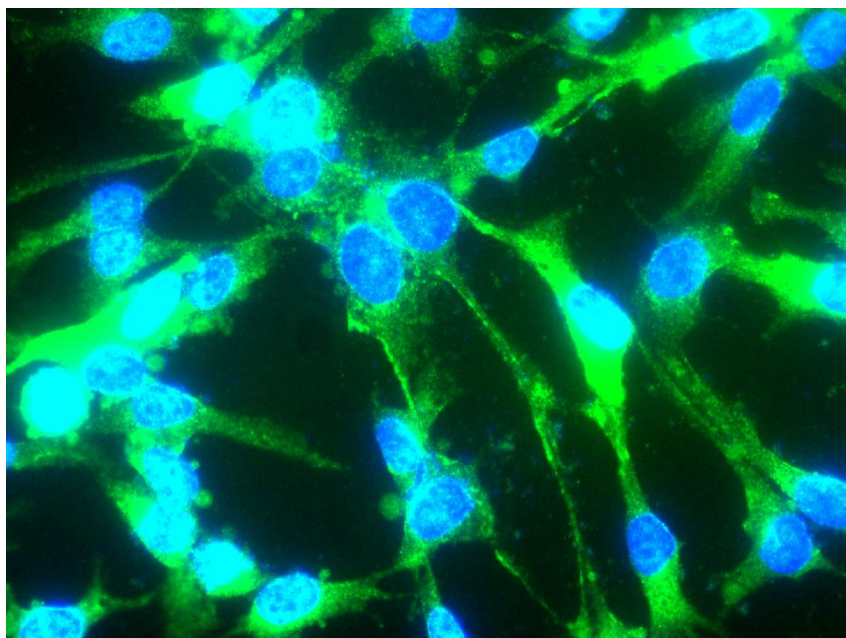


Figure 39. Control cells in hypoxia conditions.

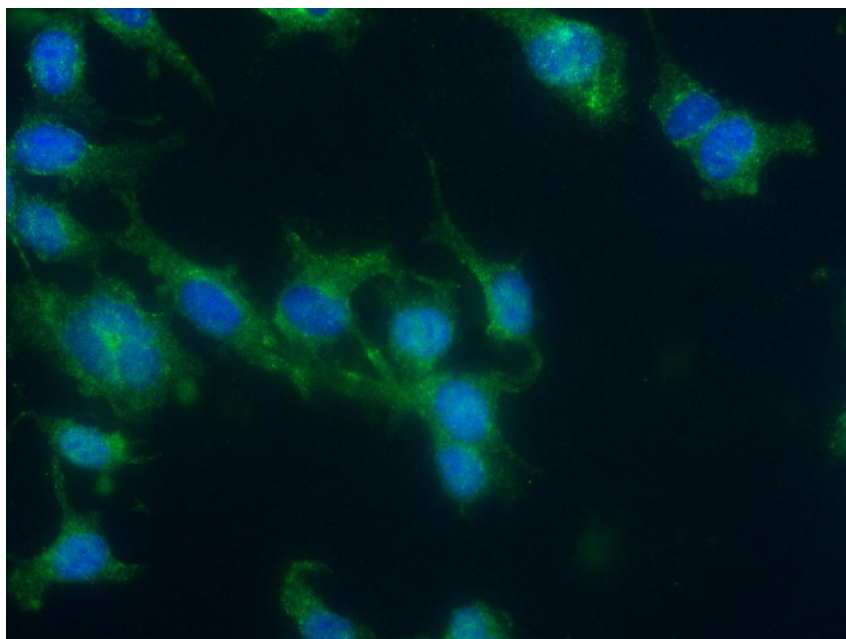


Figure 40. 1  $\mu$ M citicoline treated cells in hypoxia conditions.



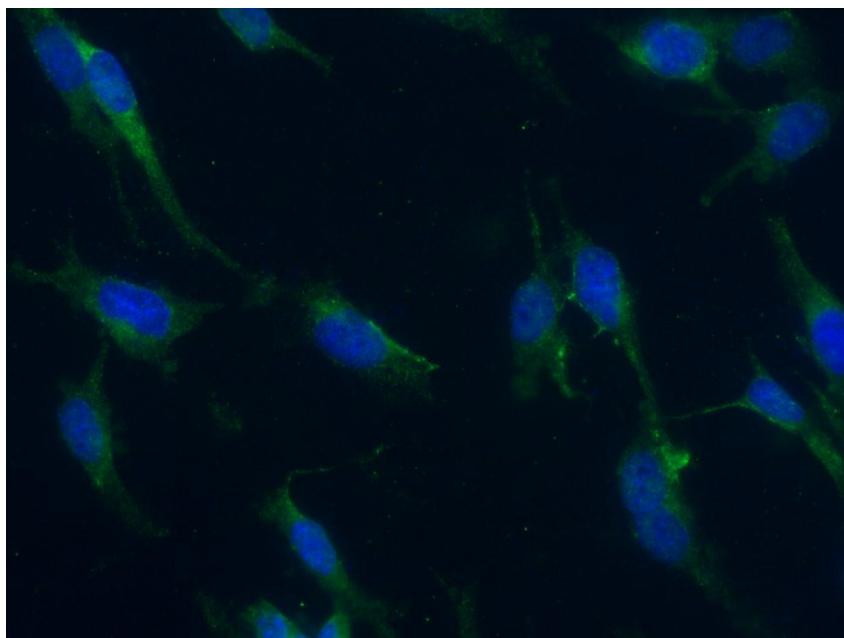


Figure 41. 5  $\mu$ M citicoline treated cells in hypoxia conditions.

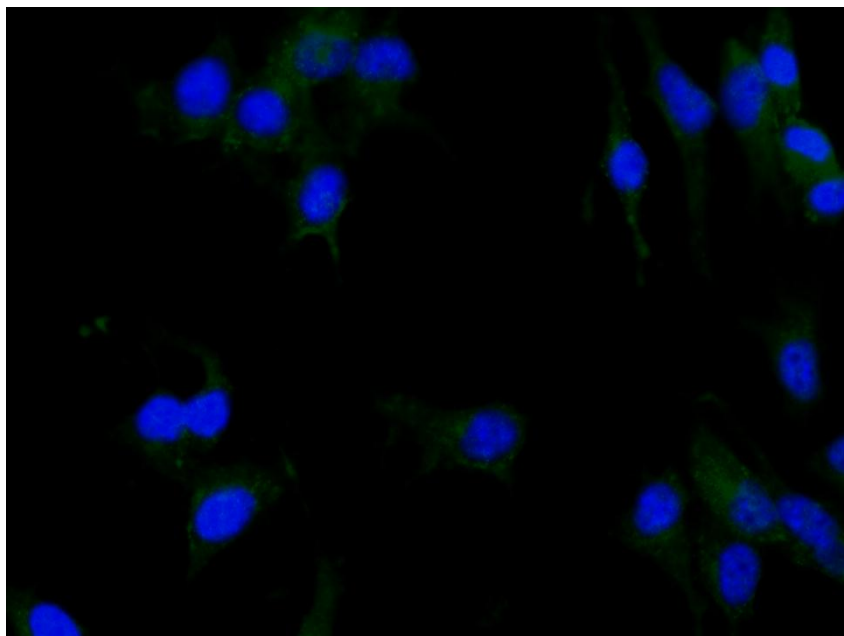


Figure 42. 10  $\mu$ M citicoline treated cells in hypoxia conditions.

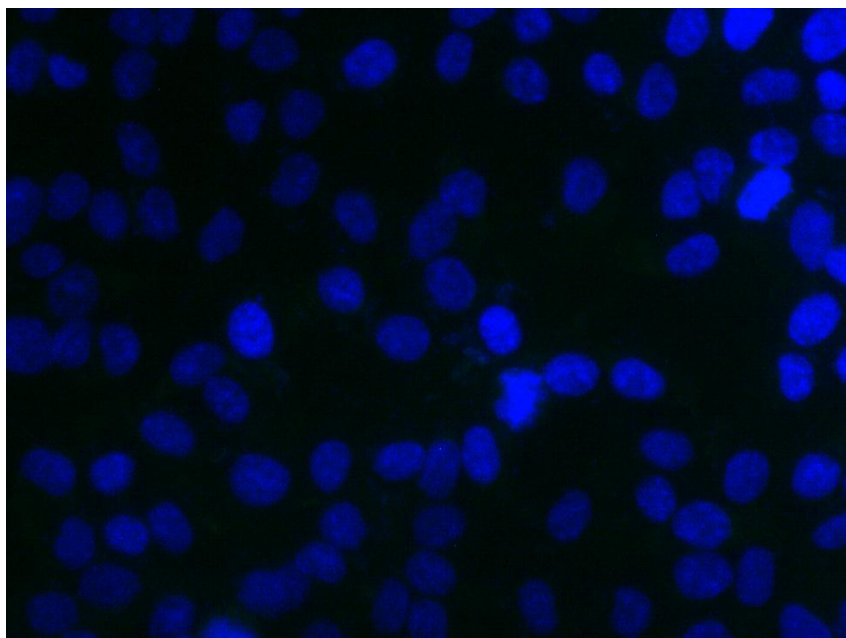


Figure 43. Control cells in normoxia.

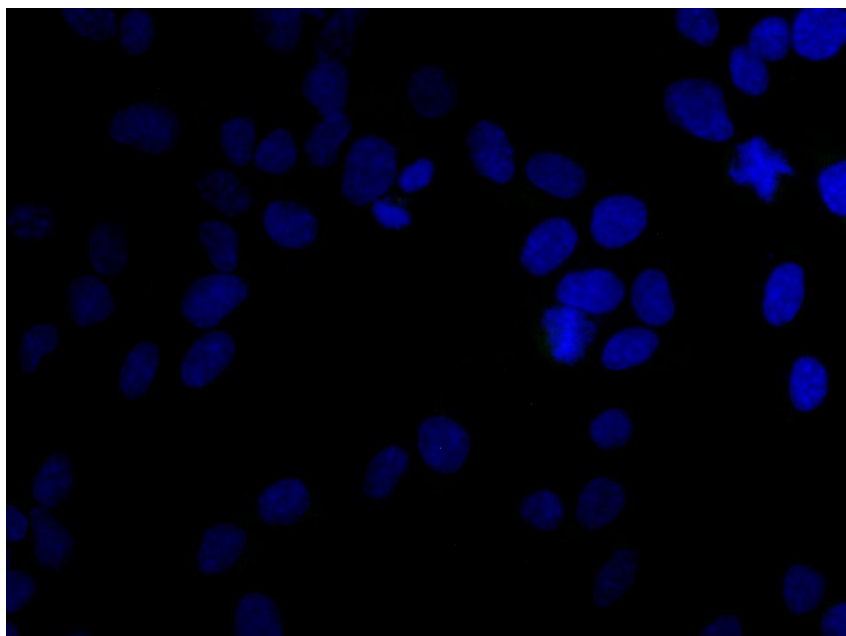


Figure 44. 1  $\mu$ M citicoline treated cells in normoxia conditions.

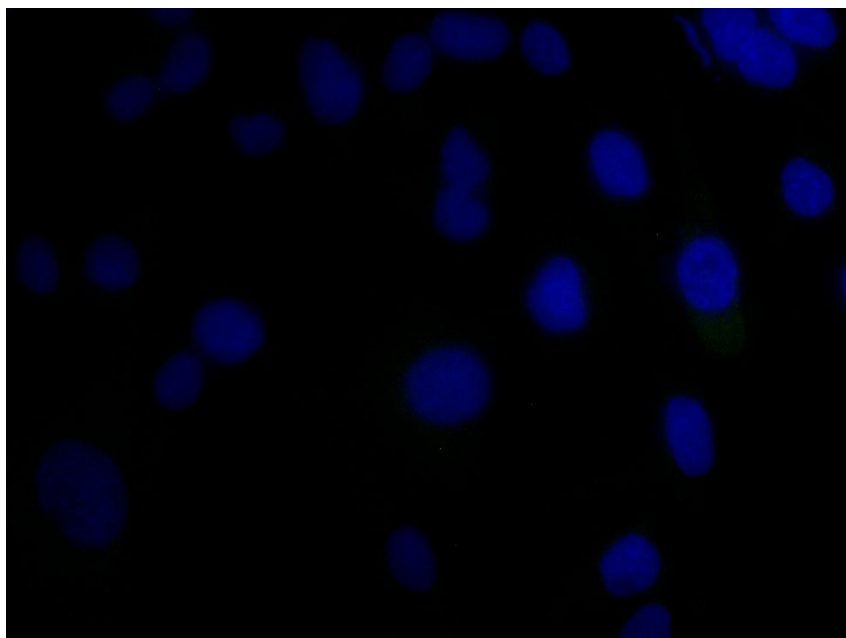


Figure 45. 5  $\mu$ M citicoline treated cells in normoxia conditions.

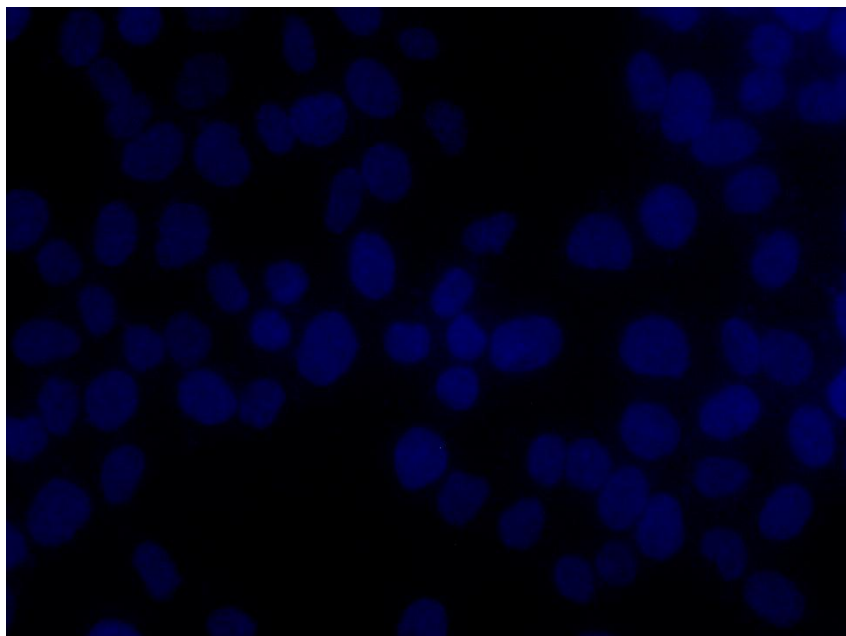


Figure 46. 10  $\mu$ M citicoline treated cells in normoxia conditions.

## Flow Cytometry.

Using Flow Cytometry, the cell population treated with different concentrations of citicoline (1 $\mu$ M, 5  $\mu$ M and 10  $\mu$ M) in hypoxia conditions for 24 hours, were tested to measure the percentage of cells undergoing apoptosis or have already died. Once fixed the population is stained using Propidium Iodide (PI) which stains dead cells and a FITC labeled antibody (Annexin V) to phosphatidylserine (PS). PS is a phospholipid normally found inside the cell membrane, but which is transferred to the outer leaflet of the cell membrane and is used as an indicator of apoptosis.

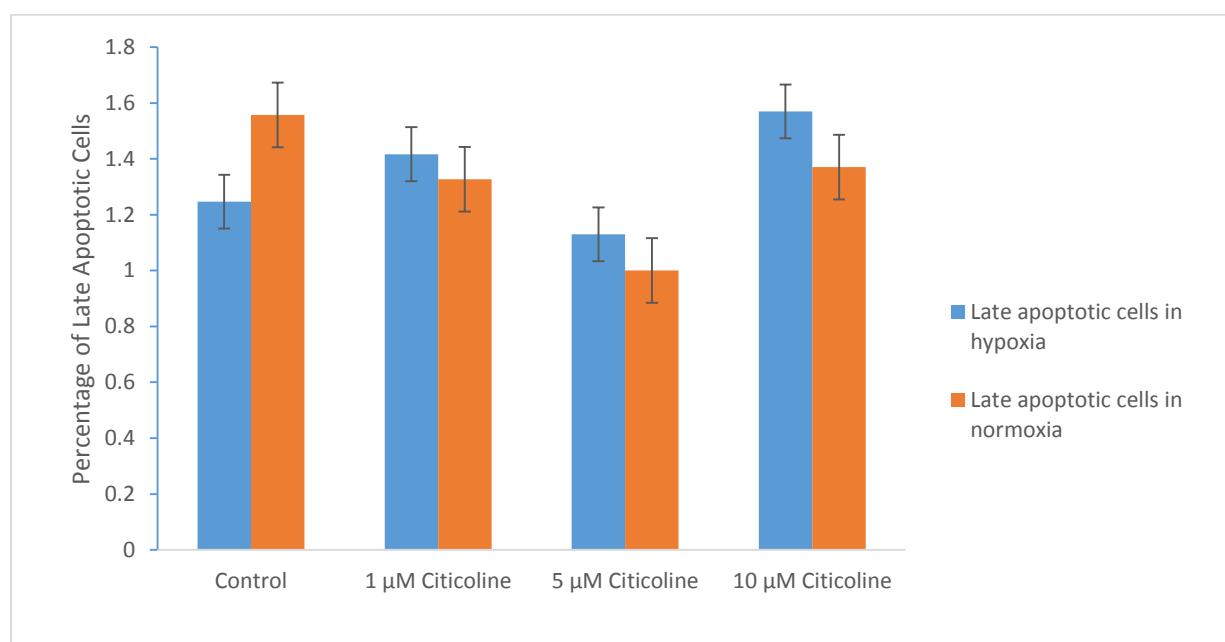


Figure 47. Percentage of late apoptotic cells treated with different concentrations of citicoline (1 $\mu$ M, 5  $\mu$ M and 10  $\mu$ M) in hypoxia and normoxia conditions. There was a 16% increase in the percentage of early apoptotic cells in 1  $\mu$ M citicoline treated cells ( $p > 0.05$ ) compared to untreated cells. In 5  $\mu$ M citicoline treated cells, the percentage of early apoptotic cells decreased by 6% ( $p > 0.05$ ), but increased by 25% ( $p > 0.05$ ) in 10  $\mu$ M citicoline treated cells compared to control cells. In normoxia, there was a 14% decrease in the percentage of early apoptotic cells in 1  $\mu$ M citicoline treated cells ( $p < 0.05$ ) compared to untreated cells. In 5  $\mu$ M citicoline treated

cells, the percentage of early apoptotic cells decreased by 34% ( $p < 0.05$ ), and decreased by 14% ( $p > 0.05$ ) in 10  $\mu\text{M}$  citicoline treated cells compared to control cells. The bars represent the standard deviations. Experiments were performed in triplicate wells and repeated at least three times.

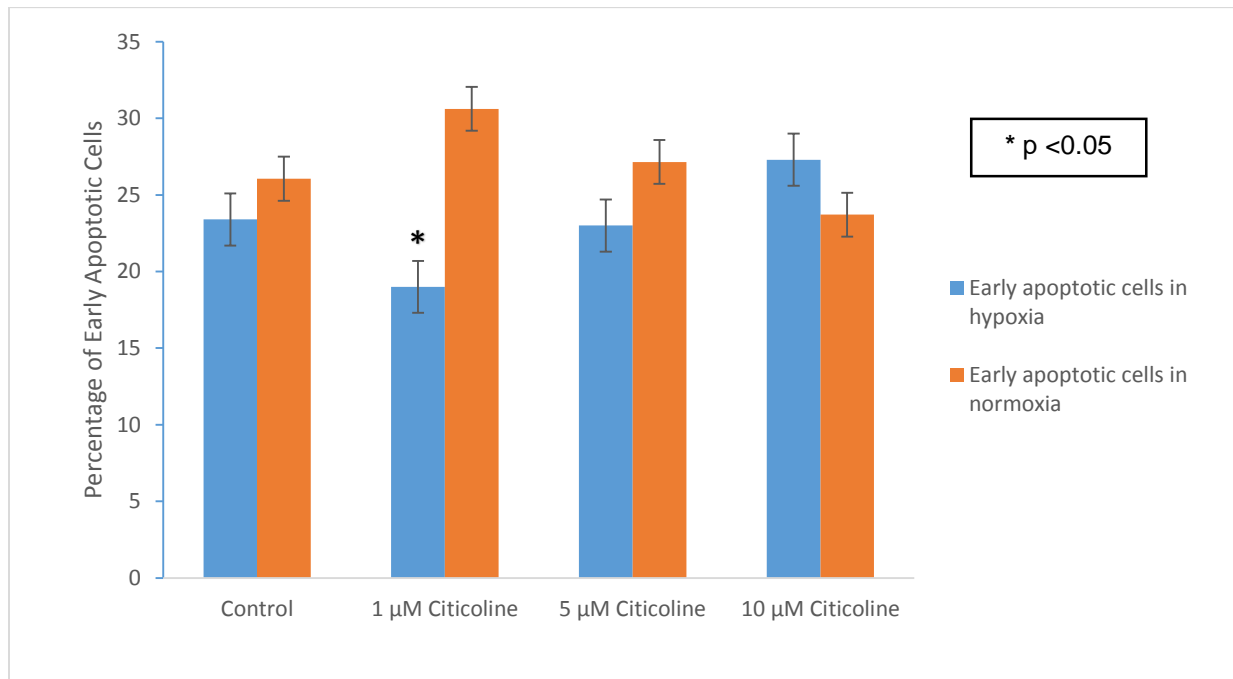


Figure 48. Percentage of early apoptotic cells treated with different concentrations of citicoline (1 $\mu\text{M}$ , 5  $\mu\text{M}$  and 10  $\mu\text{M}$ ) in hypoxia and normoxia conditions. In hypoxia, there was a 19% decrease in the percentage of early apoptotic cells in 1  $\mu\text{M}$  citicoline treated cells ( $p < 0.05$ ) compared to untreated cells. In 5  $\mu\text{M}$  citicoline treated cells, the percentage of early apoptotic cells decreased by 2% ( $p > 0.05$ ), but increased by 16% ( $p > 0.05$ ) in 10  $\mu\text{M}$  citicoline treated cells compared to control cells. In normoxia, there was a 17% increase in the percentage of early apoptotic cells in 1  $\mu\text{M}$  citicoline treated cells ( $p < 0.05$ ) compared to untreated cells. In 5  $\mu\text{M}$  citicoline treated cells, the percentage of early apoptotic cells increased by 4% ( $p > 0.05$ ), but decreased by 9% ( $p > 0.05$ ) in 10  $\mu\text{M}$  citicoline treated cells compared to control cells. The bars

represent the standard deviations. Experiments were performed in triplicate wells and repeated at least three times.

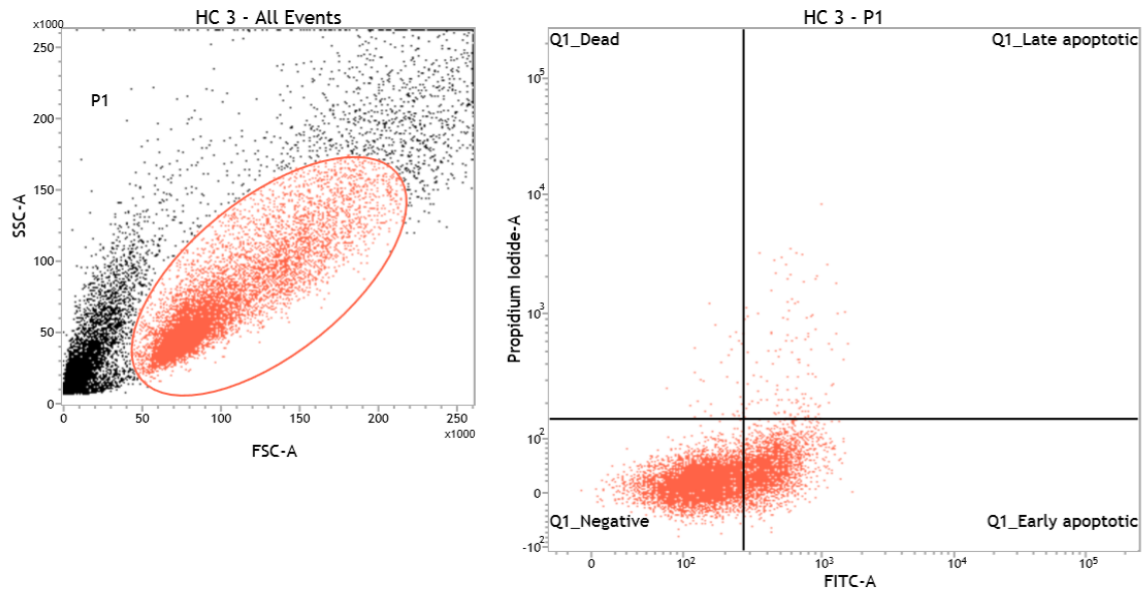


Figure 49. Flow charts of control cells in hypoxia conditions. Lower right quadrant, annexin V positive and PI negative cells indicate early apoptotic cells; upper right quadrant, annexin V and PI-positive cells represent necrotic or late apoptotic cells. Lower left quadrant annexin V negative and PI negative cells indicate live cells; upper left quadrant annexin V negative and PI positive cells indicate dead cells.

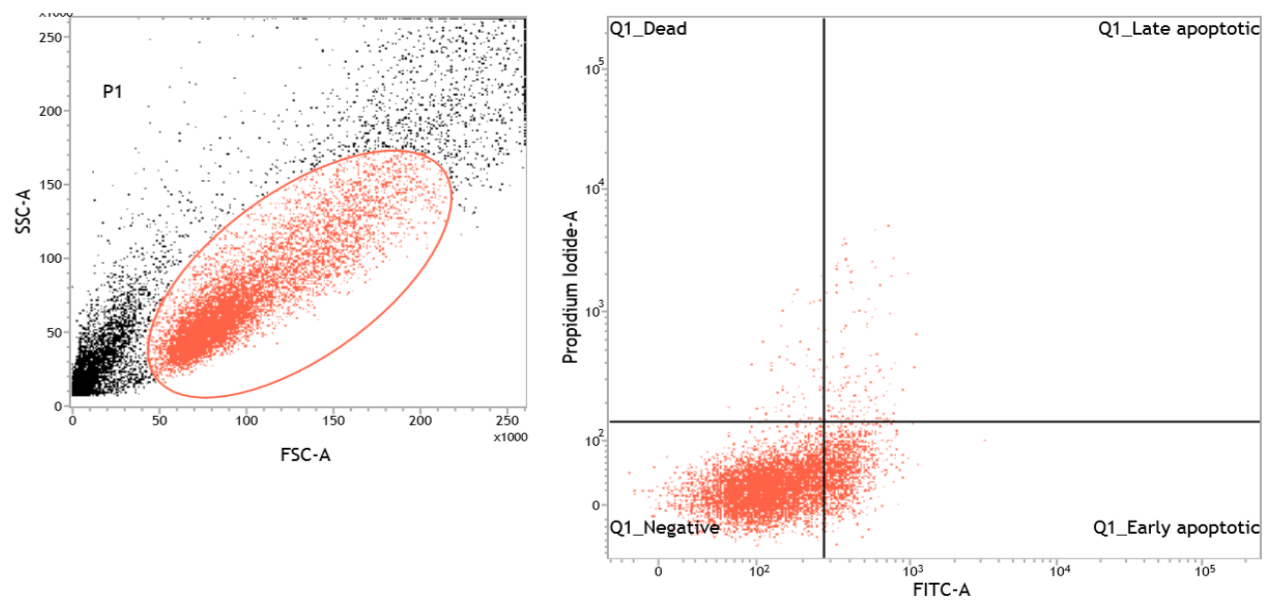


Figure 50. 1  $\mu$ M citicoline treated cells in hypoxia conditions.

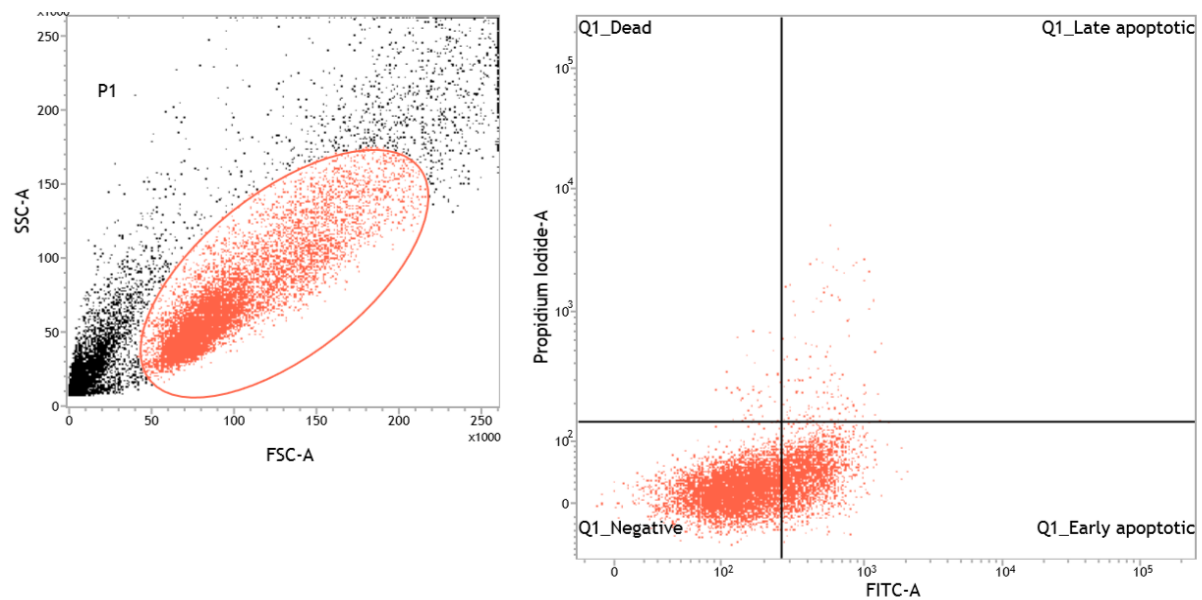


Figure 51. 5  $\mu$ M citicoline treated cells in hypoxia conditions.

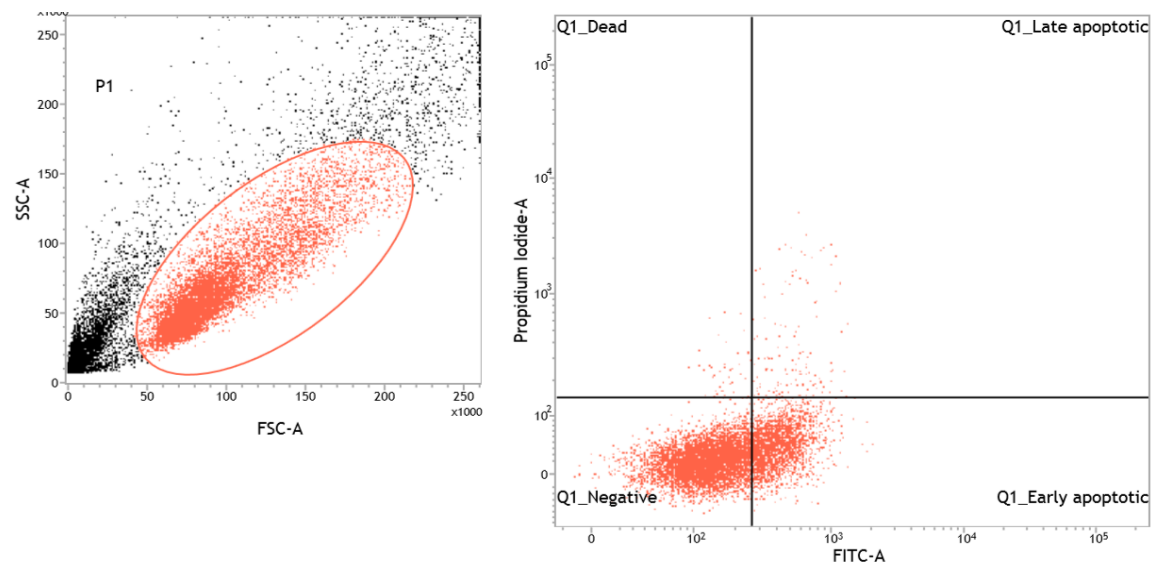


Figure 52. 10  $\mu$ M citicoline treated cells in hypoxia conditions.

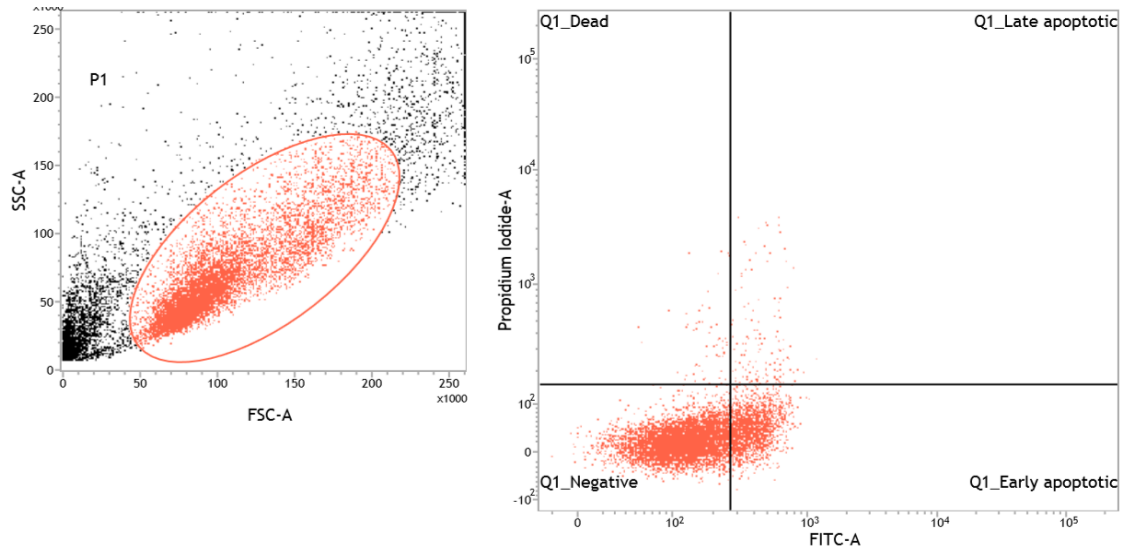


Figure 53. Control cells in normoxia conditions.



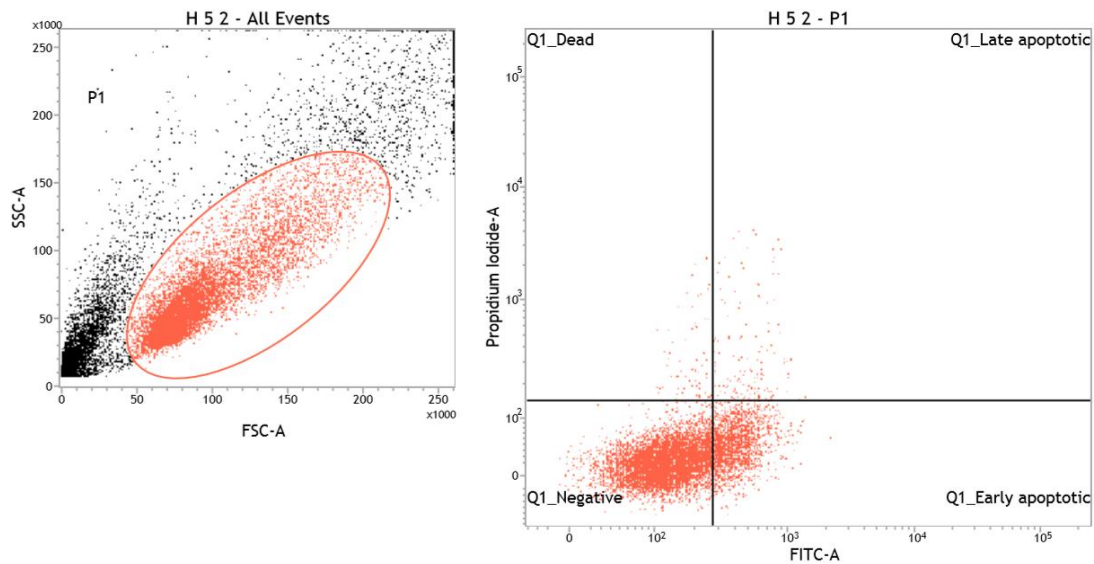


Figure 54. 1  $\mu$ M citicoline treated cells in normoxia conditions.

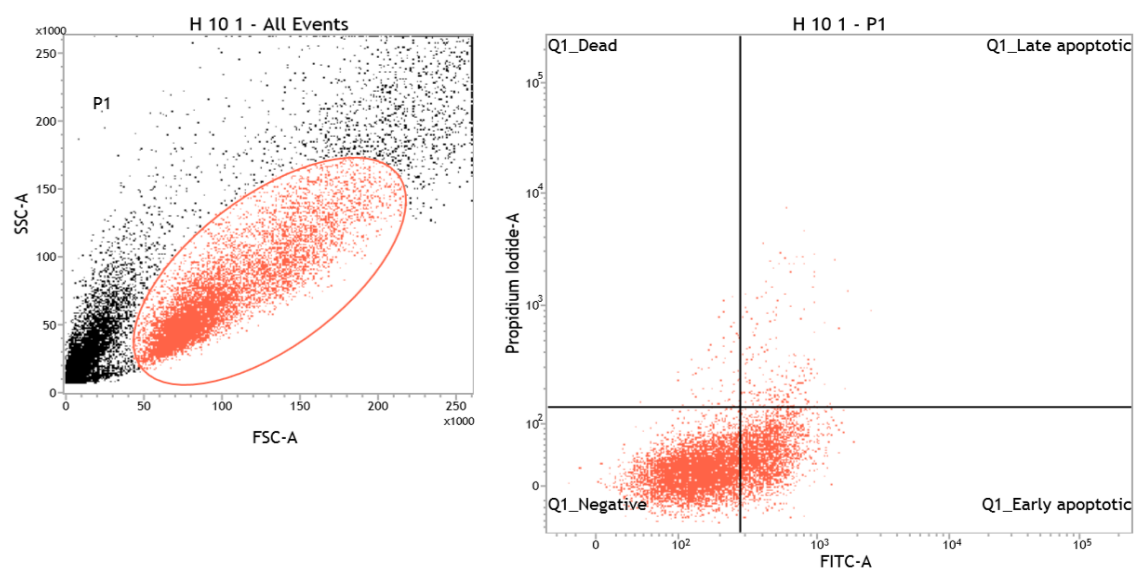


Figure 55. 5  $\mu$ M citicoline treated cells in normoxia conditions.

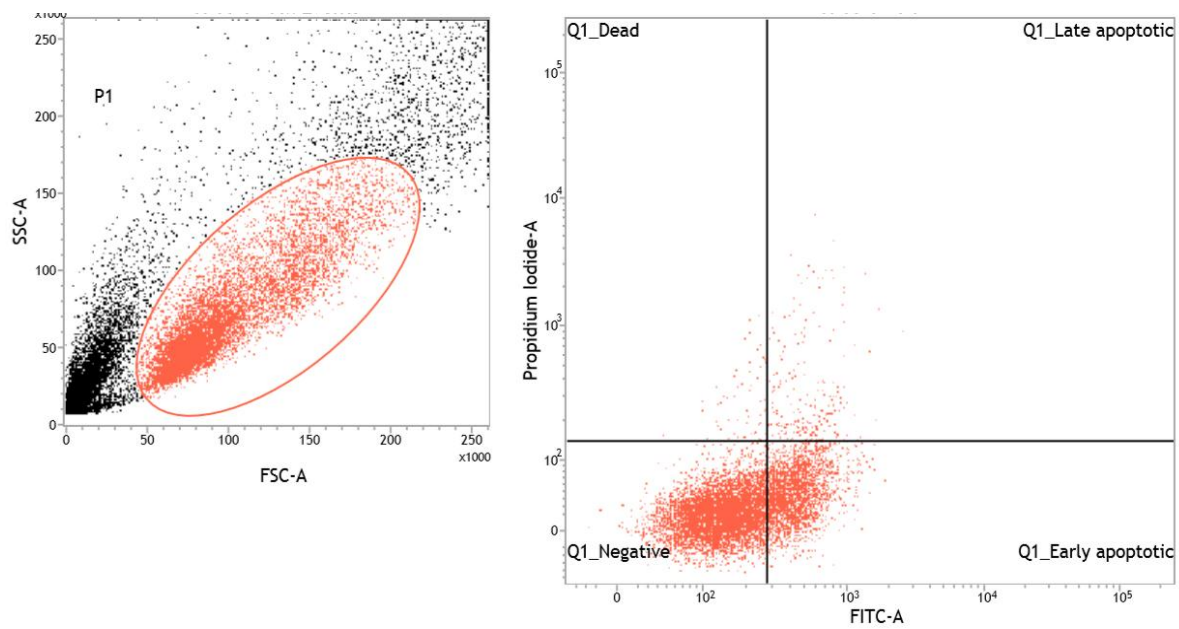


Figure 56. 10  $\mu$ M citicoline treated cells in normoxia conditions.

## Real Time PCR.

Real-time RT-PCR is a very sensitive and reliable technique to analyse gene expression. It allows the detection of the expression of a wide range of genes in the same sample simultaneously, due to the combination of real-time PCR and microarrays. The RT<sup>2</sup> Profiler PCR Array used in this study was designed to analyse a panel of genes related to the apoptotic pathway.

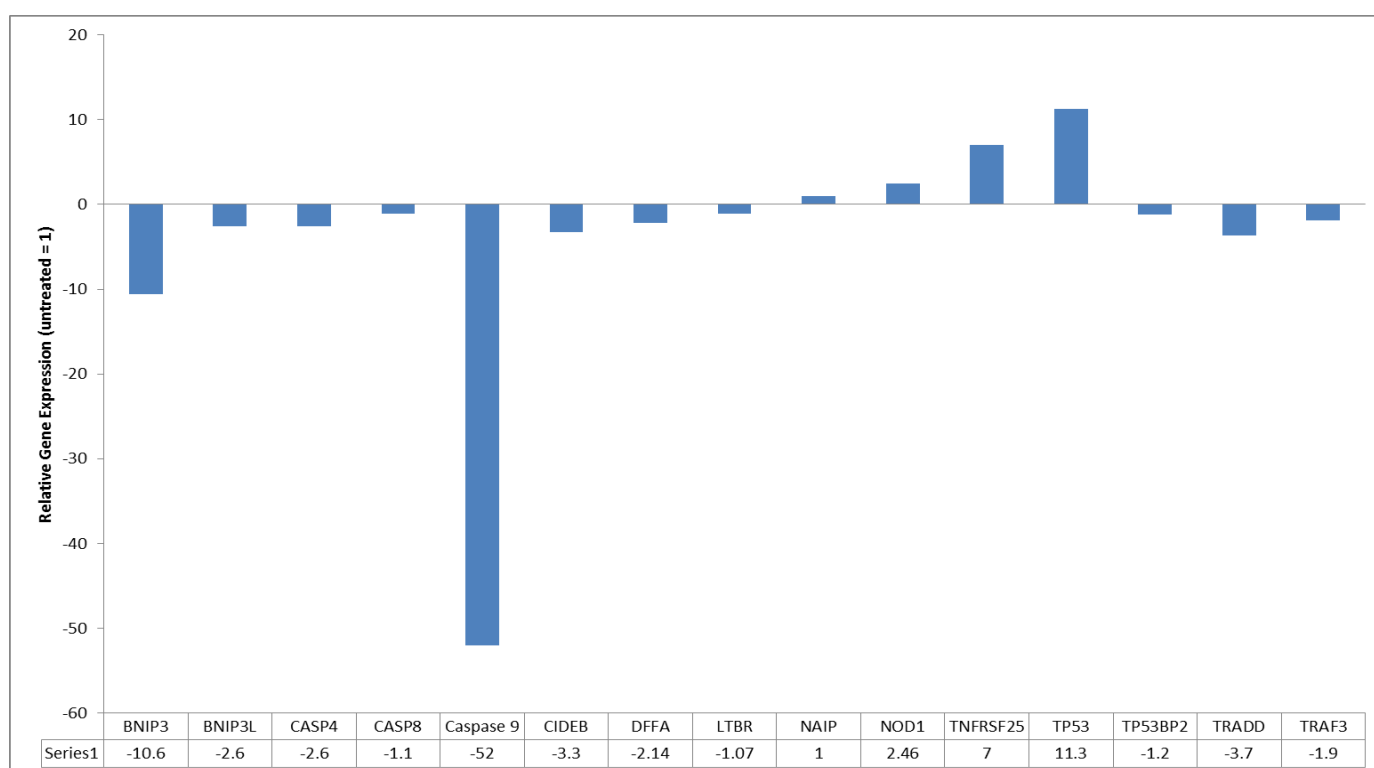


Figure 57. Relative gene expression between control cells and cells treated with 10  $\mu$ M citicoline was calculated using qRT-PCR (GAPDH, HPRT1 and RPLPO were taken as endogenous control). The results show a significant decrease in caspase 9 expression with 10  $\mu$ M citicoline treatment. Expression of neuronal apoptosis inhibitory protein (NAIP), Nucleotide-binding oligomerization domain-containing protein 1(NOD1), tumour necrosis factor receptor superfamily member 25 (TNFRSF25) and tumour protein p53 (TP53) was induced by 10  $\mu$ M

choline treatment. There was also a reduction in the expression of BCL2/adenovirus E1B 19 kDa protein-interacting protein 3(BNIP3), BCL2/adenovirus E1B 19 kDa protein-interacting protein 3-like (BNIP3L), caspase 4, caspase 8, protein cell death-inducing DFFA-like effector B (CIDEB), Lymphotoxin-beta receptor (LTBR), pentapeptide thymopentin Binding Protein 2 (TP5BP2), tumor necrosis factor receptor type 1-associated DEATH domain protein (TRADD), and TNF receptor-associated factor 3 (TRAF3).

# Chapter 4 Discussion

## **Discussion.**

Despite the significant scientific approaches on the clinical as well as on the experimental level, ischemic stroke treatment is still based on general intensive care procedures and on reperfusion therapy with recombinant tissue plasminogen activator (rtPA). RtPA improved functional outcome in patients treated soon after acute ischemic stroke in randomized trials. However, reperfusion has definite risks. It brought devastating results for some patients in the form of fatal edema or intracranial hemorrhage following thrombolysis. Reperfusion after a long period of ischemia can cause a larger infarct than that linked to permanent vessel occlusion in some animal stroke models. Therefore, while reperfusion may reduce infarct size and enhance clinical outcome in some patients, in others it may aggravate the brain injury and produce cerebral reperfusion injury. Moreover, rtPA treatment does not suit a wide spectrum of stroke patients and it must be administered within a 4.5 h window after the onset of symptoms due to an increasing risk of hemorrhage. Therefore, novel therapeutic options for ischemic stroke are urgently needed (Kleinschnitz et al., 2012, Pan et al., 2007).

In combination with thrombolytic agents such as rtPA, citicoline shows a significant reduction of infarct size in a rat model of focal Ischemia. It reduces cell damage after transient forebrain ischemia, prolongs the duration of ischemia required to produce a given behavioural deficit or infarct size and improves neurological recovery. Moreover, citicoline has potential in reducing neurological deficits resulting from ischemic stroke in humans. In clinical trials citicoline improves cognitive and behavioural parameters and

function on neurological levels in ischemic stroke patients (Krupinski et al., 2002, Overgaard, 2014).

Moreover, in one study, citicoline treatment demonstrated a reduction in Cerebral WM (white matter) lesions and apoptosis compared to control group. The study was conducted by experimentally inducing white matter lesions (which can be caused by chronic cerebral ischemia) in the rat brain by permanent occlusion of both common carotid arteries, which can affect cognitive function, and this model is similar to that of vascular dementia. This technique induces certain learning disorders by restricting the blood flow in the cerebral cortex and hippocampus by up to 40-82% for several months. Therefore, it can be used to study vascular dementia and cerebral WM lesions (Lee et al., 2009).

In a similar study, the effect of CDP-choline on brain plasticity markers expression in the acute phase of cerebral infarct was examined in an experimental animal model. It was conducted by using Male Sprague-Dawley rats that were subjected to permanent middle cerebral artery occlusion (pMCAO) and treated or not with CDP-choline (500 mg/kg) daily for 14 days starting 30 min after pMCAO. Subsequently, functional status, lesion volume, apoptosis, and cellular proliferation were measured. Citicoline significantly improved functional recovery and decreased lesion volume at 14 days compared to the control group. According to the data from the study, citicoline improved functional recovery after permanent middle cerebral artery occlusion in association with reductions in lesion volume and apoptosis. It increased cell proliferation, vasculogenesis and synaptophysin levels in the peri-infarct area of the ischemic stroke (Gutiérrez-Fernández et al., 2012). A meta-analysis was conducted to assess the neuroprotective

actions of citicoline and the results showed that the weighted mean difference meta-analysis showed a reduction in infarct volume by 27.8%, citicoline effect on reducing infarct volume was higher in proximal occlusive models of middle cerebral artery (MCA) compared with distal occlusion in the stratified analysis, and the efficacy was superior using multiple doses than single dose and when a co-treatment was administered compared with citicoline monotherapy (Bustamante et al., 2012).

However, a randomised, placebo-controlled, sequential trial in patients with moderate-to-severe acute ischaemic stroke admitted at university hospitals in Germany, Portugal, and Spain was performed in 2012. This study showed that citicoline is not efficacious in the treatment of moderate-to-severe acute ischaemic stroke (Dávalos et al., 2012).

The bioavailability of citicoline after oral administration is 100% and it has shown different pharmacological actions, with beneficial effects in some models of cerebral ischemia and collaborative effects with other drugs tested in the treatment of stroke.

The clinical development of citicoline as a therapy for acute ischemic stroke was initiated in the United States in the 1990s. The first US phase II to III trial was performed to assess the effect of 3 doses (500, 1000, and 2000 mg/d) of citicoline against placebo. The results demonstrated significant improvement of neurological, functional, and global outcomes with citicoline treatment at 500 and 2000 mg/d compared with placebo 12 weeks after stroke onset (Dávalos et al., 2002). Although citicoline was used as a form of ischemic stroke treatment in a number of trials since then, there are no other studies so far that have investigated the effect of citicoline modulation of angiogenesis related to stroke recovery. Understanding the mechanisms through which citicoline stimulates angiogenesis, has the potential of exploring its benefit in stimulating tissue remodelling



after ischemic stroke. Therefore, this study was designed to investigate the role of citicoline in modulation of angiogenesis. In case of stroke, treatment normally start after the incident, however, the laboratory restriction in this study was that the treatment with citicoline was prior to the placing of the cells in the hypoxia chamber which could not be opened once it was filled with hypoxia gas.

Angiogenesis is a highly regulated process that is dependent on homogenous balance between pro-angiogenic and anti-angiogenic microenvironmental signals. Several studies have highlighted the important role of ERK activation in regulation of endothelial cell process during angiogenesis (Rizzo, 2007). In conjunction with this, Western blotting results demonstrated that citicoline induced pERK1/2 expression, a key mitogenic signalling protein known to be involved in angiogenesis and generally stimulated by growth factors through interaction with their receptors (Slevin et al., 2006). ERK2/ERK1 (also known as p42/p44MAPK, respectively, and officially named MAPK 1 and 3) are two isoforms of extracellular signal-regulated kinase (ERK) that belong to the family of mitogen-activated protein kinases (MAPKs). The activation of ERK2/ERK1 by phosphorylation regulates several cytoplasmic and nuclear targets that are responsible for a number of important biological mechanisms such as proliferation, migration, differentiation and cell survival. In some cases, depending on the longitude and magnitude of activation, ERK activity has been involved in neurodegenerative diseases and brain injury following ischemia in animal models (Cagnol et al., 2010).

Although this study established the effect of citicoline on ERK1/2 phosphorylation from Western blot analysis, citicoline was found to have no mitogenic effect using Human Cerebrovascular Microvessel endothelial cell (HCMEC/D3). Cells in cell proliferation

assay were treated in normoxia only because of the extended period of 72 hours which would be excessive in case of hypoxia. Moreover, from the data collected in this study, citicoline (10  $\mu$ M) did not show a significant increase the proliferation of HCMEC/D3 after 72 h incubation comparing to the untreated cells. These results are in agreement with published data demonstrating that citicoline had no effect on cell proliferation using a similar dose (Krupinski et al., 2012).

It is hypothesized that citicoline modulates tube like structure formation and this study is the first to demonstrate that citicoline is highly angiogenic and therefore may contribute to the revascularization process aiding tissue recovery. It also demonstrated that citicoline (10  $\mu$ M) was more effective in promoting the formation of tube-like structures in HCMEC/ than FGF-2 which is a well-known potent angiogenic factor. Since maintenance of angiogenesis is one of the keys to both short-term and chronic revascularization after stroke, these findings could be very valuable for analysing the potential mechanisms through which citicoline treatment results in patient recovery. From Western blotting results, citicoline was also found to increase Her-2 expression. Therefore, GW2974, which is a Her-2 inhibitor, was used to inhibit Her-2 expression in order to determine the molecular pathway in which citicoline promoter tube formation. The results from Western blotting showed that citicoline treatment alone induced ERK1/2 expression but in combination with Her-2 inhibitor, ERK1/2 expression was blocked. However, when cells were treated with FGF-2 in combination with Her-2 inhibitor, there was no effect on FGF-2 induced ERK1/2 expression demonstrating specificity of the inhibitor.

Moreover, one of the angiogenesis assays that can be conducted in vitro is the short-term culture of endothelial cells in Matrigel™, which is a gelatinous protein mixture, obtained from Engelbreth-Holm-Swarm mouse sarcoma cells. It is a fast and simple assay to perform and also provides in vitro demonstration of endothelial cell mechanisms including survival, apoptosis, and tube formation. It is also important for studying the effects of drugs on angiogenesis in vitro before these are developed into clinical treatments (Khoo et al, 2011). In a pilot study, citicoline was established to increase tube formation in HCMEC/D3. Therefore, in this study a tube formation assay was performed to confirm findings from Western blot results. The results showed an inhibitory effect of Her-2 inhibitor on tube formation by blocking the stimulatory effect of citicoline. In combination with FGF-2, Her-2 inhibitor did not show inhibitory effect on FGF-2 activity. Therefore, one of the novel findings that emerged from this study is the action of citicoline in promoting tube formation and Erk1/2 activation through Her-2 receptor.

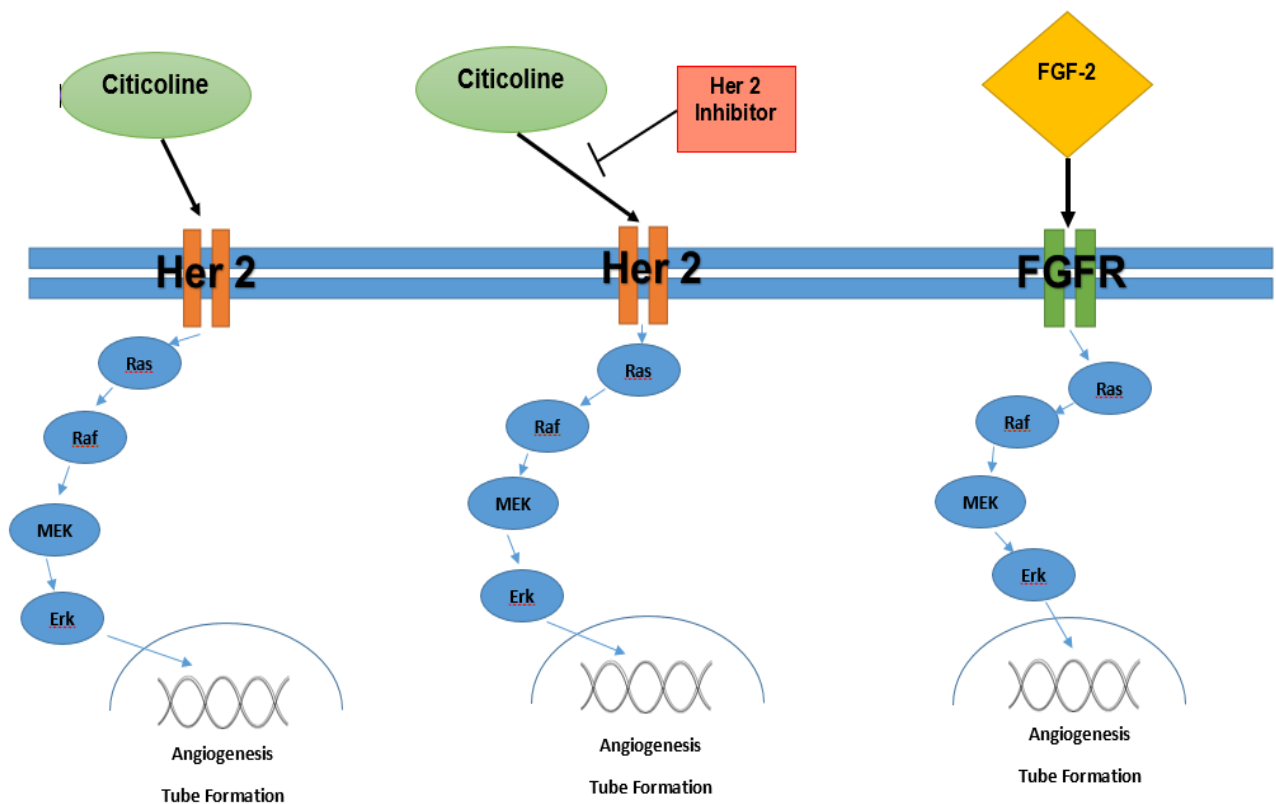


Figure 58. Proposed pathway of citicoline induced ERK1/2 expression. Binding of citicoline to HER-2 initiates a series of intracellular signals, including activation of Ras-Raf-MEK-ERK pathway, which leads to induction of tube formation. Her-2 inhibition does not affect FGF-2 induced ERK1/2 expression since FGF-2 acts of FGFR receptor.

Moreover, the results from the Kinexus antibody microarray screen showed a notable increase (> 100%) of the phosphorylation of HER-2. HER-2 is from a family of receptors that are expressed in various tissues of epithelial, mesenchymal and neuronal origin, and they are involved in regulating various cellular pathways such as proliferation, differentiation, migration and apoptosis (Olayioye, 2001). This protein, initially discovered as an activated oncogenic

variant, is overexpressed in many epithelial tumours including breast and ovarian cancers (Bourguignon, 2007). In breast cancer cells, overexpression of ErbB2 (HER-2) leads to constitutive activation of the ERK and PI3K/Akt pathways (Chen, 2008). In addition, HER-2-overexpressing breast cancers tend to be more angiogenic than other breast cancers (Klos, 2000). High levels of Her-2 expression is established to be associated with increase in angiogenesis (Kumar et al, 2001). Moreover, Her-2 is involved in the regulation of vascular endothelial growth factor (VEGF), which is one of the most potent inducers of angiogenesis that induces endothelial cell proliferation and migration. In human breast cancer, overexpression of Her-2 is associated with increased VEGF expression. Moreover, VEGF expression in human mammary tumours is associated with increased microvessel density and reduced survival rate (Klos et al., 2000). The ability of citicoline to activate intra-cellular signal transduction pathways and induce phosphorylation of down-stream angiogenic molecules was investigated using Kinexus-phospho-protein screen. Histone phosphorylation was studied in several mammalian cells undergoing apoptosis. After treating cells with a number of apoptotic inducers, H2B was found to be phosphorylated in cells undergoing apoptosis comparing to normal or growing cells (Ajiro, 2000). In this study; Kinexus results showed that H2B decreased ten times in the HCMEC/D3 stimulated with citicoline comparing to control untreated cells. Recently, phosphorylation of histone H2B at serine 14 (S14), a posttranslational modification required for nuclear condensation, has been established to be associated with apoptosis (Zhuang et al., 2007, Ajiro et al., 2010). Similarly, one

of the studies showed that apoptosis-specific histone H2B phosphorylation was highly elevated and DNA fragmentation activity in the cytoplasm was detected in cells that were undergoing apoptosis (Ajiro et al., 2004).

Conversely, in this study, there was a notable increase (> 100%) of the phosphorylation of IRS-1 after treating cells with citicoline. Insulin receptor substrate 1 (IRS-1) is a member of adaptor proteins that link signalling from upstream activators to multiple downstream effectors to modulate normal growth, metabolism, survival, and differentiation (Dearth, 2007). Although IRS proteins signal through many pathways, their main function is regulation of the phospholipid kinase phosphatidylinositol 3-kinase (PI3-K) and extracellular signal regulated kinase (ERK) pathways (Houghton, 2011). PI3-K is known to link IGF-IR signalling with the Akt/PKB activation pathway/s associated with cell protection from apoptosis. Activation of PI3-K regulates Akt, which is a serine-threonine kinase that plays an important role in cell survival. Akt protection against apoptosis involves direct inhibition (phosphorylation) of pro-apoptotic signals such as Bad and FOXO3A (Pan et al., 2007).

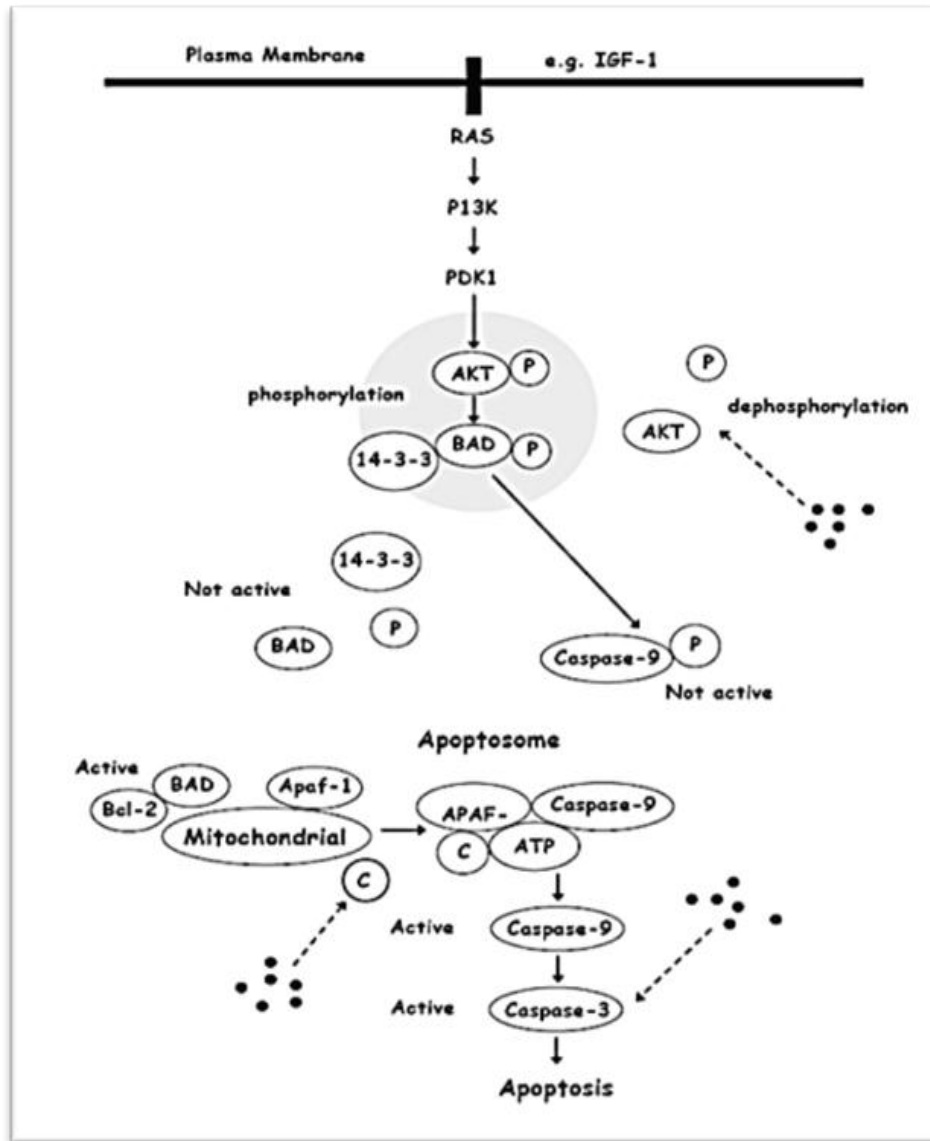


Figure 59. The PI3K/Akt signalling pathway. Phosphorylation of Akt phosphorylates BAD and a non-active form of caspase-9. Phosphorylation of caspase-9 by phosphorylated Akt prevents formation of the apoptosome complex, and thus the downstream event of apoptosis is inhibited. (\*) depicts chrysin (Khoo et al., 2010).

Caspases, which is a family of acting proteases, have been demonstrated to be overexpressed during focal and global ischaemia. After an ischaemic attack, neurones and glial cells in the infarcted core and in the penumbra zone surrounding it, tissue with obstructed glucose and oxygen supply, die progressively as the ischaemic injury initiate apoptosis. Although cerebral impairment resulting from ischaemia is only partly dependent on caspase initiation, caspase inhibition has been shown to be beneficial for tissue survival in several experimental models of cerebral ischaemia (Krupinski et al., 2002).

Along with several growth factors, VEGF activates PI3k by binding to its receptor, which is known to induce angiogenesis. Angiogenesis is crucial for the progression of normal physiological events, such as embryonic growth, as well as for pathogenic processes such as cancer. Angiogenesis can be induced by constitutively active PI3k and Akt, and therefore, inhibition of PI3k pathway restricts angiogenesis. Akt regulates several cellular mechanisms including cell survival, glycogen metabolism, cellular transformation, and myogenic differentiation. It is activated by PI3K through binding of its pleckstrin homology domain to the lipid products of PI3K and by phosphorylation at Thr-308 and Ser-473 residues by two phosphoinositide dependent protein kinases, PDK1 and PDK2 (Jiang et al., 2000). In acute ischemic lesions, inflammatory responses and injury to the endothelia of blood vessels have been detected simultaneously. Consequently, it is important to restore blood flow and protect neurons in order to reduce brain damage following an ischemic attack. Besides, extending the therapeutic window would be beneficial to treat a wider range of patients with acute brain ischemia (Nakase et al., 2011).



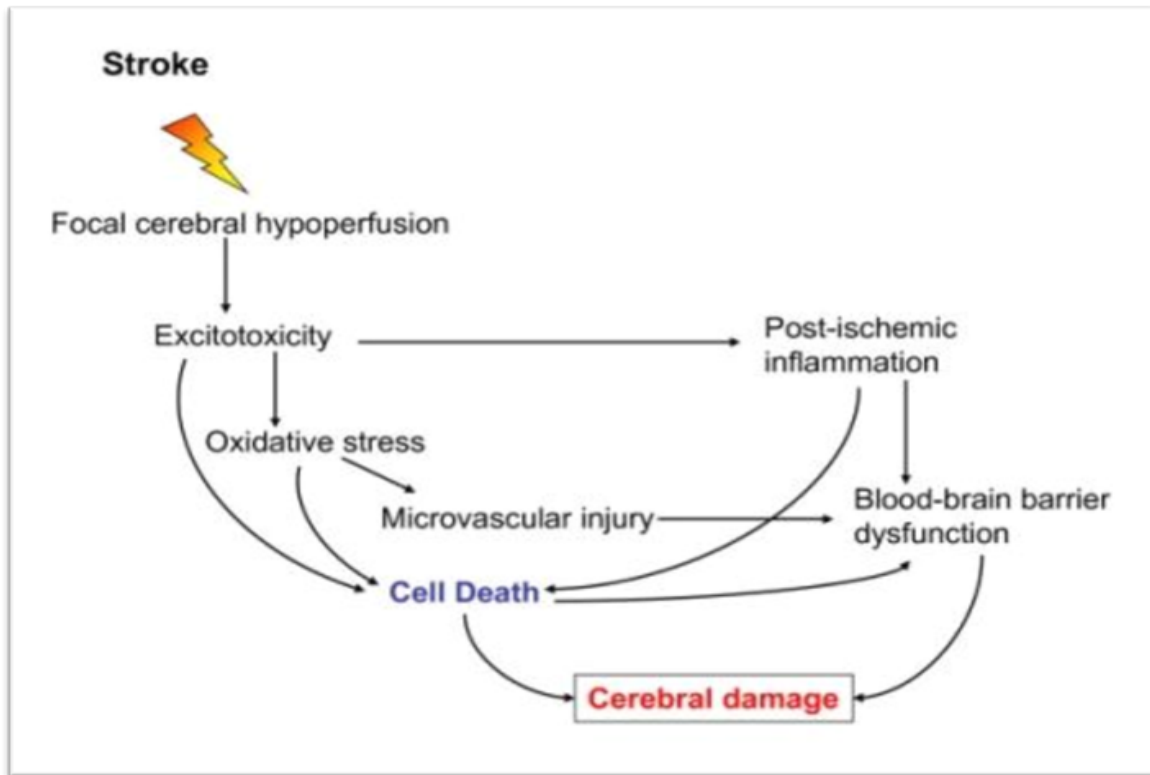


Figure 60. Ischemic cascade leading to cerebral damage. Ischemic stroke leads to hypoperfusion of a brain area that initiates a complex biochemical reactions. Excitotoxicity, oxidative stress, microvascular injury, blood-brain barrier dysfunction and postischemic inflammation lead to apoptosis in neurons, glia and endothelial cells. The extent and longitude of ischemia determines the volume of cerebral damage (Lakhan, 2009).

In this study, results show an increase (> 100%) of the phosphorylation Apoptosis signal-regulating kinase 1 (ASK1) also known as mitogen-activated protein kinase kinase kinase 5 (MAP3K5). ASK1 is one of the main elements regulating reactive oxygen species (ROS) - induced JNK and p38 activation leading to differentially regulated apoptosis (Pressinotti et al., 2009). ROS, such as superoxide anion ( $O_2^{\bullet-}$ ), hydrogen peroxide ( $H_2O_2$ ), and the hydroxyl radical ( $HO^{\bullet}$ ), have several effects on major cellular mechanisms (Pan et al., 2010). Moreover, it has been reported that

during the cellular response to oxidant injury initiated by ROS, Akt is activated (Wang et al., 2000). ROS are produced as part of normal cellular metabolism and defence mechanisms and at low levels, they take part in regulation of cellular growth, differentiation, proliferation and apoptosis. Several biochemical and cellular reactions such as inflammatory response, increased ROS synthesis, damage of blood brain barrier and calcium overload are triggered by cerebral ischemia resulting from vascular diseases. With cerebral reperfusion, ROS synthesis is further activated leading to cytotoxicity through lipid peroxidation, oxidation of proteins and DNA fragmentation. It was demonstrated that ROS are synthesised upon ischemia onset in an animal model. Moreover, correlated cellular damage is parallel to the level of ROS. In addition, increased cerebrovascular permeability was established to be associated with the initial phase of reperfusion that can be reduced by inhibition of ROS production (Olmez et al., 2012). These results highlight a possible signalling pathways through which citicoline modulates angiogenesis and apoptosis. Therefore, they portray citicoline as a possible therapeutic target for improving tissue recovery, revascularisation and neuro-protection in ischemic stroke.

Propidium iodide (PI) has been used as DNA binding fluorescent dye to detect DNA damage. P.I binds to cell nuclei with fluorescence intensity that is correlated with the extent of DNA degradation. This is important because gradual degradation of inter-nucleosomal DNA is a hallmark of apoptosis (Crompton et al., 1992). Uptake of the fluorescent exclusion dye P.I relies upon propidium iodide being impermeable to cells with an intact plasma membrane, however when cell integrity becomes compromised it becomes able to access the nucleus where it complexes with DNA rendering the

nucleus highly fluorescent (Brana et al., 2002). In his study, P.I staining was used to detect hypoxia induced DNA damage in HCMEC/D3 cells. A combination of DNA-binding dye DAPI and PI were used to detect apoptotic cells under the fluorescence microscope. In this study, cells were considered apoptotic when displayed signs of apoptosis such as nuclear condensation, fragmentation, uptake of PI stain (red colour) into the nucleus, disruption of cell cytoplasm and distortion of the cells. The normal cells appeared swollen with round clear blue nuclei. For induction of in vitro ischemia, cells were incubated in hypoxia with oxygen concentration of <1.0%. The cells were treated with different concentrations of citicoline and incubated for 24 hours in hypoxia along with untreated cells. Dead cells were quantified by use of propidium iodide, and the results showed up to 34% reduction ( $P<0.001$ ) in hypoxia induced DNA damage in cells treated with citicoline. Therefore, citicoline demonstrated a significant protective effect against hypoxia induced apoptosis.

Although the experiment was repeated three times, the results from the flow cytometry did not show statistical significance and therefore considered to be inconclusive. In a study, Annexin V/PI staining has been found to lead to a significant number of false positive events (up to 40%), which are associated with PI staining of RNA within the cytoplasmic compartment (Rieger et al., 2010). Therefore, Annexin V/PI staining protocol could be modified to minimize error and to achieve more accurate results. The nucleosome is a basic unit of chromatin consisting of a segment of DNA wound around an octamer containing two copies of each H2A, H2B, H3, and H4 core histone. Posttranslational modifications of histone tails regulate numerous biological processes including transcription, DNA repair, and apoptosis. As a response to DNA damage,

serine 14 residue in the NH<sub>2</sub>-terminal tail of histone H2B is rapidly phosphorylated at sites of DNA double-strand breaks (Fernandez-Capetillo et al., 2004).

In this study, phosphorylation of H2B at serine 14 residue in the NH<sub>2</sub>-terminal was examined in HCMEC/D3 undergoing hypoxia induced apoptosis to test the protective effect of citicoline against cell death. The results showed up to 78% inhibition of H2B Ser14 expression in cells treated with citicoline. H2B phosphorylation at serine 14 (Ser14) is catalyzed by Mst1 kinase and has been linked to chromatin condensation during apoptosis. The activation of MAPKs (ERK1/2, JNK1/2 and p38) is regulated by caspase-3, which phosphorylates H2B at Ser14 leading to chromatin condensation during apoptosis (Lu et al., 2010). Therefore, in this study, the effect of citicoline on caspase-3 expression was examined and the results show an inhibition of up to 86% compared to untreated cells in hypoxia conditions. Activation of caspase 3 was induced by hypoxia which led to the activation of H2B phosphorylation at Ser14. For the first time, this study demonstrates that citicoline downregulates of H2B phosphorylation at Ser14 through caspase 3 pathway. In a previous study, caspase-3 activation has been linked to triggered necrosis and apoptosis, and exacerbated cerebral edema and neuronal death after intracerebral haemorrhage (Wang et al., 2013). In middle cerebral artery occlusion (MCAO) rats, treatment with citicoline 500 mg/kg intraperitoneally was found to decrease the expression of all procaspases, as well as the expression of cleaved caspase-3. This was accompanied by a reduction in the number of cells bearing nuclear DNA fragments. The expression of caspase-cleaved products of PARP (PARP 89 kDa) was reduced in citicoline-treated ischaemic rats (Krupinski et al., 2002).

PARP-1 catalyzes poly-ADP ribosylation which is a posttranslational modification and is one of the initial cellular responses to DNA damage. It binds to the damage sites and is activated auto-modification which causes chromatin de-condensation around damage sites, recruitment of repair machineries such as DNA ligase III–XRCC-1 base excision repair complexes, and enhance rapid DNA damage repair, especially in the case of single-strand breaks (SSBs) (Sugimura et al., 2008).

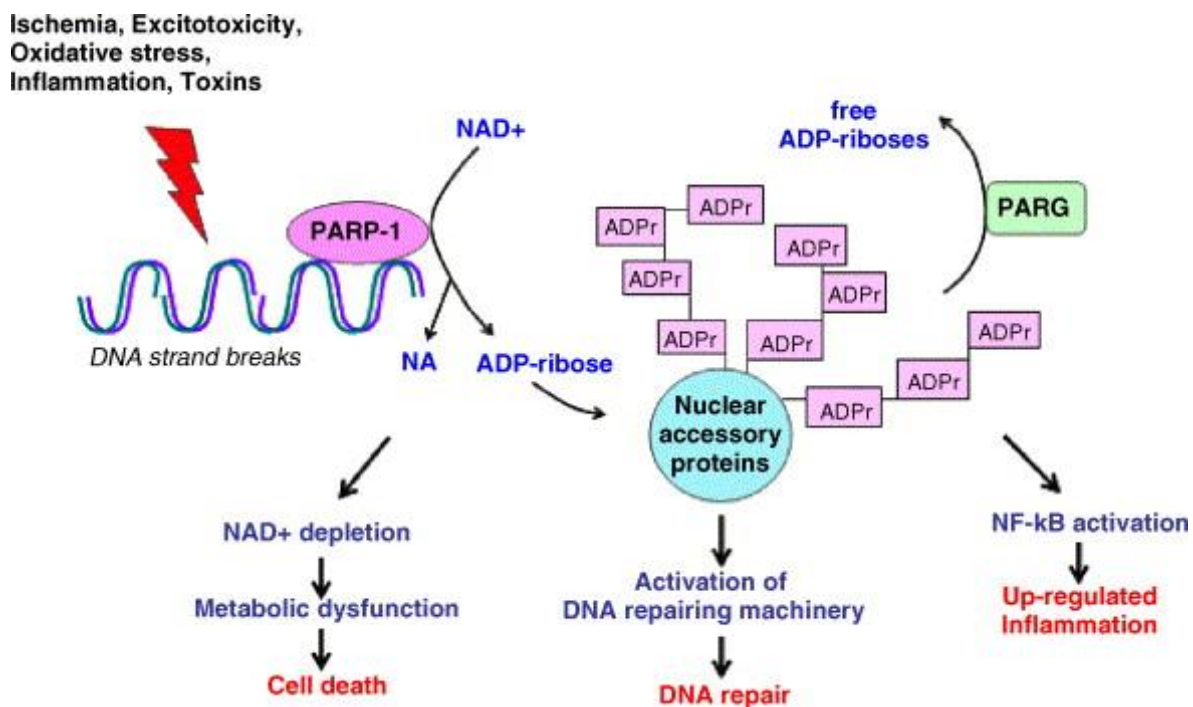


Figure 61. A representation of PARP roles in cell physiology. DNA damage caused by ischemia, excitotoxicity, oxidative stress, inflammation or toxins leads to PARP-1 activation. Nicotinamide adenine dinucleotide (NAD<sup>+</sup>) is required during PARP-1 activation and as a result, ADP-riboses is generated around accessory proteins including histone and PARP-1. Simultaneously, poly (ADP-ribose) glycohydrolase (PARG) degrades poly (ADP-riboses). DNA repair mechanism and enabling DNA accessibility are activated by moderate DNA damage to facilitate DNA repair. However, severe DNA damage stimulates the over-activation of PARP which may deplete the

stores of cellular energy leading to cell death. PARP can also enhance inflammatory responses by acting as a co-activator of nuclear factor kappa B (NF- $\kappa$ B), which is a central transcription factor for pro-inflammatory genes (TM., 2007).

Due to its role in NF- $\kappa$ B driven expression of inflammatory mediators by glia during the neuroimmune response, PARP-1 is involved in the pathogenesis of neurodegenerative disorders, where is excessive release of pro-inflammatory products by activated glia causes neurotoxicity. Such neurodegenerative disorders include Parkinson's disease (PD) where there is an abundance of PARP-containing nuclei in the dopaminergic neurons of the substantia nigra (Infante et al., 2007, Chiarugi et al., 2003). PARP-1 is also involved in another neurodegenerative disease, which is Alzheimers disease (AD). Increased levels of peripheral blood mononuclear cells (PBMCs) expressing proinflammatory proapoptotic PARP-1 where found in AD patients (Kassner et al., 2008). PARP-1 plays a role in autoimmune CNS injury such as multiple sclerosis, which is an inflammatory disorder of the brain and spinal cord in which focal lymphocytic infiltration leads to damage of myelin and axons (Compston et al., 2008). In a mouse model of multiple sclerosis, PARP-1 knockout showed a decrease in the severity of the disease outcome (Krishnakumar et al, 2010). It also has been reported that cells lacking PARP-1 are more susceptible to apoptosis induced by DNA-damaging agents that activate the base excision repair pathway compared to normal cells (Oliver et al., 1999). It is evident that PARP-1 is an important element in neuronal death pathways initiated by experimental stroke and in N-methyl-D-aspartate (NMDA), nitric oxide, and 1-methyl-4-phenyl-1,2,3,6-tetrahydropyridine (MPTP) toxicity (Goto et al, 2002). MPTP is a neurotoxin that causes Parkinsonism, and it has benefited in revealing greater

information about the pathogenesis of Parkinson's disease. In a study, mice lacking the gene for PARP showed higher reduction in MPTP neurotoxicity compared to wild type mice. The study concluded that PARP activation plays a critical role in MPTP-induced Parkinsonism and suggested that inhibitors of PARP may have protective benefit in the treatment of Parkinson's disease (Mandir et al., 1999). Moreover, Nitric oxide (NO) and peroxynitrite, generated from NO and superoxide anion, have been implicated as mediators of neuronal damage following focal ischemia. In a study PARP-1 knockout showed a significant increase in protection against glutamate-NO-mediated ischemic insults in vitro and major decreases in infarct volume after reversible middle cerebral artery occlusion (Eliasson et al., 1997).

In addition, caspase-3 was also essential for apoptosis-associated proteolysis of 14 caspase substrates as well as nuclear collapse, chromatin margination, and DNA fragmentation (Slee et al., 2001). During drug-induced apoptosis in a variety of cells, PARP is cleaved into 89-kDa fragment that contain the active site and 24-kDa fragments that contain the DNA-binding domain of the enzyme. Such cleavage essentially inactivates the enzyme by destroying its ability to respond to DNA strand breaks (Boulares et al., 1999). Moreover, by using poly (ADP-ribosyl)ation, PARP-1 has the ability to modify a variety of chromatin proteins, including histones, and thereby dramatically alter chromatin structure (Kraus et al., 2003). In this study, cells expressed caspase 3 and cleaved 89-kDa PARP when exposed to hypoxia which is demonstrated in Western blotting results. Treatment with 10  $\mu$ M citicoline showed 88% reduction of cleaved PARP expression and 86% inhibition of active caspase-3 expression. These results shows for the first time that citicoline is protective against cell death in stroke

mimicking conditions by inhibiting caspase 3 cleavage of PARP. To confirm results from Western blotting, indirect immunofluorescence was used to investigate the effect of citicoline on caspase 3 and H2B Ser14 activity in hypoxia treated cells. The cells were incubated for 24 hours in hypoxia conditions with or without different citicoline concentrations. After fixation, the cells were stained using anti-active caspase 3 or H2B Ser14 with the nuclei counterstained with DAPI. The results were consistent with Western blotting results by showing citicoline at 10  $\mu$ M concentration as the optimum concentration for caspase 3 and H2B Ser14 inhibition. Citicoline at 10  $\mu$ M concentration showed an inhibition of 70% in H2B Ser14 expression and an inhibition of 72% in active caspase 3 expression. Cells incubated in normoxia conditions showed no activation of caspase 3 and H2B Ser14.

In this study human apoptosis RT<sup>2</sup> profiler PCR array, which profiles the expression of 84 key genes involved in programmed cell death, was used to determine the effect of citicoline on the expression of these genes in hypoxia. This array includes TNF ligands and their receptors, members of the bcl-2, caspase, IAP, TRAF, CARD, death domain, death effector domain, and CIDE families, as well as genes involved in the p53 and DNA damage pathways. Cells were seeded into 2xT75 flasks to obtain sufficient RNA concentration for this experiment. The optimum citicoline concentration was determined to be 10  $\mu$ M, and therefore cells in one T75 flask were treated with 10  $\mu$ M citicoline and the second flask was used for control (untreated) cells. Both flasks were incubated for 24 hours in hypoxia before performing RNA extraction and real time PCR.

The results showed a significant decrease in caspase 8 expression in cells treated with 10  $\mu$ M citicoline compared to control cells. **Caspase-9** is synthesized as 46 kDa



precursor protein that is implicated in apoptosis. **Caspase-8** is a member of the cysteine proteases, which are associated in apoptosis and cytokine modulation. Caspase-8 is produced as an inactive single polypeptide chain zymogen procaspase and is activated by proteolytic cleavage. Caspase-8 is known to propagate the apoptotic signal either through the intrinsic or the extrinsic apoptotic pathway. In the extrinsic pathway, caspase 8 cleaves the BH3 Bcl2-interacting protein, which leads to the release of cytochrome c from mitochondria. Cytochrome c then binds with Apaf-1, the mammalian Ced-4 homologue, together with dATP. The resultant complex recruits Caspase-9 leading to its activation. Activated Caspase-9 cleaves downstream caspases such as Caspase-3, -6 and -7 initiating the caspase cascade. In the extrinsic apoptotic pathway, activation of death receptors through bindings of ligands leads to FADD and caspase 8 recruitment, which activates caspase 8. Activation of caspase 8 directly activates caspase 3 leading to apoptosis (Kruidering et al., 2000, Oberst et al., 2010, Kuida et al., 2000). In this study, and for the first time, citicoline is shown to be protective against hypoxia induced cell death by inhibiting the expression of caspase 9 and caspase 8.

The results from PCR array displayed a significant decrease in BNIP3 expression in cells treated with 10  $\mu$ M citicoline. **BNIP3 (Bcl-2/adenovirus E1B 19-kDa interacting protein 3)** is a proapoptotic protein that contains a single Bcl-2 homology 3 (BH3) domain and is classified in the BH3-only subfamily of Bcl-2 proteins (Zhang et al., 2009). BNIP3 plays a role in hypoxia-mediated cell death by causing mitochondrial dysfunction via activation of Bax or Bak, which leads to mitochondrial fragmentation and release of cytochrome c (Kubli et al., 2007). **Bnip3L** is a proapoptotic member of the Bcl-2 family that induces cell death, and plays an essential role in cardiac cell death

during hypoxia. Bnip3L is activated by hypoxia-inducible factor 1 (HIF-1) in response to hypoxia (Fei et al., 2004). In a study, inhibiting of HIF-1 $\alpha$  or Bnip-3L with small interfering RNA (siRNA) completely blocked the hypoxia-induced apoptosis and Bnip3L expression (Krick et al., 2005). **Caspase 4** belongs to inflammatory caspases, which contain a long prodomain with a caspase recruitment domain (CARD). It can be activated by danger or stress signals, such as UV irradiation, or molecules released from injured cells, such as uric acid crystals, which are collectively called danger-associated molecular patterns, induce an inflammatory response mediated by inflammasomes (Sollberger et al., 2012). The results from this study shows an inhibitory effect of citicoline on caspase 4 expression.

Caspase-4 is localized to the ER membrane and is primarily activated in ER stress-induced apoptosis. Ischemia can cause neuronal damage, which is related to stress acting on the ER, leading to intraluminal accumulation of unfolded proteins. ER stress induces three major cellular responses: unfolded protein response (UPR), ER-associated degradation, and apoptosis. Excessive or long-termed ER stress results in apoptotic cell death, involving nuclear fragmentation, condensation of chromatin, and shrinkage of the cell body. Reduction of caspase-4 expression decreases ER stress-induced apoptosis (Hitomi et al., 2004).

In this study, citicoline was found to reduce the expression of **protein cell death-inducing DFFA-like effector B (CIDEB)**. CIDEB mediates lipid droplet (LD) fusion, as well as very-low-density lipoprotein (VLDL) maturation (Singaravelu et al., 2013). It contains an N-terminal CIDE-N domain that shares sequence similarity to the N-terminal CAD domain (NCD) of DNA fragmentation factors Dffa/Dff45/ICAD and Dffb/Dff40/CAD

(Wu et al., 2008). CIDE-B protein is localized in mitochondria and forms homodimers and heterodimers with other family members. By localizing to mitochondria, CIDE-B may interact directly with Bcl-2 family proteins such as Bcl-2 and Bcl-XL to chelate anti-apoptotic proteins, thereby inducing apoptosis. CIDE-B could also directly cause mitochondria alteration such as disruption of mitochondria membrane potential, induction of the production of reactive oxygen species, and the release of apoptosis-inducing factors (Chen, 2000). DNA fragmentation factor subunit alpha (DFFA) is a caspase-3 substrate that must be cleaved before apoptotic internucleosomal DNA fragmentation can proceed. DFFA (45 kDa) exists as complex with DFFB (40 kDa) to form DFF. DFF is a cytosolic factor, which is required for the initiation of endonuclease-mediated DNA fragmentation and can be directly activated by caspase-3 in vitro. Therefore, DFF serves as a component in the executioner phase of apoptosis (Granville et al., 1998, Wolf et al., 1999).

**Lymphotoxin- $\beta$  receptor (LTBR)**1 is a member of the tumour necrosis factor receptor (TNFR) superfamily and is ubiquitously expressed on the surface of most cell types, except T and B lymphocytes. Membrane anchored lymphotoxin (LT)  $\alpha 1\beta 2$  and LIGHT (homologous to LT, inducible expression, competes with herpes simplex virus (HSV) glycoprotein D for HSV entry mediator (HVEM), a receptor expressed on T lymphocytes), both members of the TNF superfamily, are functional ligands for the LT $\beta$  receptor (LTBR). LIGHT is able to induce cell death via the non-death domain containing receptor LTBR to activate both caspase-dependent and caspase-independent pathway (Chen et al., 2003, Wimmer et al., 2012). From the microarray results, it was found to be reduced by citicoline treatment. Ligand-induced activation of

LTBR triggers the formation of receptor-associated cytoplasmic signalling complexes containing TNFR-associated factors (TRAFs) that regulate interactions of the receptor with downstream kinases. TRAF3 has been shown to mediate activation of JNK and induction of cell death by LTBR (Bista et al., 2010).

In this study, the expression of **tumor necrosis factor receptor type 1-associated DEATH domain protein (TRADD)** was found to be reduced by citicoline. TRADD is an adapter molecule that contains an N-terminal TRAF binding domain and a C-terminal death domain along with nuclear import and export sequences that function as a transport system between the cytoplasm and nucleus. It links the interaction between tumor necrosis factor receptor-1 (TNFR-1) and receptor-interacting serine/threonine-protein kinase 1 (RIP1). The death domain of TRADD contains the nuclear import sequence and expression of the core death domain (nuclear TRADD) causes a special nuclear localization and activation of a distinct apoptotic pathway. Activation of TNFR-1 by binding of ligand leads to TRADD recruitment, which then recruit and activate the initiator caspase, caspase-8, and ultimately result in effector caspase activation, and apoptosis (Bender et al., 2005, Park et al, 2014).

**Tumour protein p53 binding protein 2 (TP53BP2)** is a gene that encodes two proteins apoptosis-stimulating of p53 protein 2 (ASPP2) and tumour suppressor p53-binding protein 2 (p53BP2) (Takahashi et al., 2004). ASPP2 changes the promoter specificity of p53 by increasing the DNA binding and transactivation of p53 on the pro-apoptotic genes such BAX which induces apoptosis (Sun et al., 2008). Blocking endogenous ASPP expression inhibits the apoptotic function of endogenous p53 in response to apoptotic stimuli (Samuels-Lev et al., 2001). 53BP2 interaction with p53,

mediates some of p53 functions such as apoptosis induction and cell cycle arrest and overexpression of 53BP2 was found to induce apoptosis (Mori et al., 2000, Yang et al., 1999). TNF receptor superfamily 25 (TNFRSF25) is a member of the TNF-receptor family with a typical death domain. TNFRSF25 induces NF- $\kappa$ B and promotes cell survival signals via TRADD and TRAF2 (Fang et al., 2008). TRAF2 activation induces NF- $\kappa$ B expression, which in turn inhibits apoptosis by suppressing caspase 8 (Wang et al., 1998). Nucleotide-binding oligomerization domain-containing protein 1 (NOD1) is one of the most prominent members of the NLR (NOD-LRR) family -proteins. Upon activation, NOD1 initiates signal transduction mechanisms that include stimulation of NF- $\kappa$ B through receptor-interacting serine/threonine-protein kinase 2 (RIP2) binding to IAPs (Correa et al., 2012). The neuronal apoptosis inhibitory protein (NAIP) is a member of human inhibitors of apoptosis IAP family that is characterized by highly conserved N-terminal motifs called baculovirus inhibitor of apoptosis repeats (BIR). The BIR domains of NAIP are potent inhibitors of caspase 3 (Maier et al., 2002). Over-expression of NAIP has demonstrated protective properties against apoptosis induced by a variety of signals in vitro (Perrelet et al., 2000).

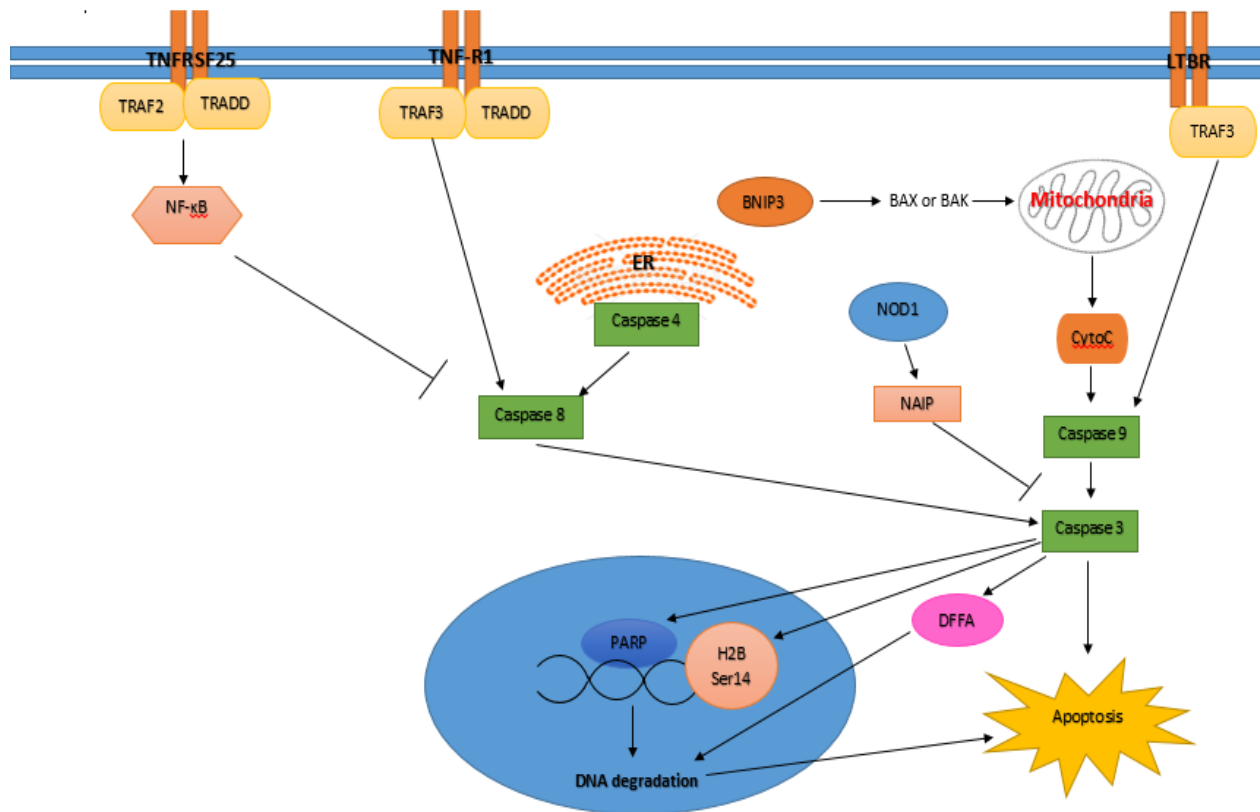
## **Conclusion.**

Stroke is caused by focal cerebral ischemia resulting from occlusion of a cerebral blood vessel, usually an artery. Regardless of ischemia severity, collateral circulation may develop by enlargement of pre-existing anastomotic channels or angiogenesis (DA et al., 1998). Angiogenesis induction stimulates endogenous recovery mechanisms such as neurogenesis, synaptogenesis, and neuronal and synaptic plasticity. These mechanisms are all associated with long-term repair and restoration process of the brain after an ischemic event (Ergul et al., 2012). Citicoline is a neuroprotectant and neurorestorative agent that is used as a trial treatment of acute ischemic stroke (Dávalos et al., 2011). It increases the neuronal plasticity within non-injured and functionally connected brain regions as well as to promote functional recovery (Hurtado et al., 2007). However, the exact the molecular mechanisms in which citicoline acts is not fully understood. Therefore, this project investigates the roles and mechanisms through which citicoline induce in vitro angiogenesis (EC proliferation, migration, and tube formation) which lead to several important and novel findings. The proliferation assay showed that citicoline presented no mitogenic or chemotactic on hCMEC/D3 proliferation. However, citicoline significantly increased cell migration and tube formation in Matrigel™. The results from Kinexus analysis showed an up-regulation of Her-2 expression by citicoline. This finding was supported by Western blotting results. Citicoline was found to increase Her-2 expression in hCMEC/D3, and therefore, citicoline stimulation of angiogenesis through Her-2 phosphorylation was further examined using Her-2 inhibitor. Inhibition of Her-2 blocked the angiogenic effect of

citicoline by inhibiting Erk1/2 expression and tube formation in Matrigel™ , which suggests that citicoline induce hCMEC/D3 angiogenesis through Her-2 pathway.

Citicoline has also shown protective effects against apoptotic processes after stroke (Sahin et al., 2010). The Kinexus results revealed that citicoline significantly down-regulated the expression of Histone H2B Ser14 in HCMEC/D3. H2B phosphorylation at serine 14 (Ser14) has been linked to chromatin condensation during apoptosis (Lu et al., 2010). Citicoline suppression of H2B Ser14 expression was supported by Western blotting, and immunofluorescence results confirming the protective effect of citicoline against apoptosis through H2B Ser 14 inhibition. Another marker of apoptosis (caspase-3) was examined using Western blotting and immunofluorescence. Caspase-3 is required neuromas typical hallmarks of apoptosis, and is essential for apoptotic chromatin condensation and DNA fragmentation in numbers of cell types (Porter et al., 1999). Western blotting and immunofluorescence results demonstrated a significant inhibition of caspase-3 activity by citicoline, which further provides accumulative evidences of the protective effects of citicoline against apoptosis. Cleaved caspase-3 and cleaved PARP expression parallels apoptosis (Puig et al., 2001). Results from Western blotting showed inhibitory effect of citicoline against PARP expression, which revealed more information about the pathway in which citicoline acts as an antiapoptotic agent. However, results from detecting apoptosis using flow cytometry showed a level of inconsistency which could be improved using an alternative protocol. In this study P.I staining was used to detect apoptotic cells under the fluorescence microscope. Cells were considered apoptotic when displayed signs of apoptosis such as nuclear condensation, fragmentation, uptake of PI stain (red colour) into the nucleus, disruption

of cell cytoplasm and shrinkage of the cells. The normal cells appeared swollen with round clear blue nuclei. The results displayed a protective effect of citicoline on



hCMEC/D3 against apoptosis induced by hypoxia. The Human Apoptosis RT<sup>2</sup> Profiler PCR Array was used to detect the effect of citicoline on the expression of 84 key genes involved in programmed cell death. The results showed a significant inhibition of citicoline against several pro-apoptotic genes including BNIP3, BNIP3L, caspase 4, caspase 8, caspase 9, CIDEB, DFFA, LTBR, TP53BP2, TRADD, and TRAF3. They also show a significant stimulatory effect of citicoline on the expression a number of anti-apoptotic genes including NAIP, NOD1, TNFRSF25, and TP53.

Figure 62. Proposed apoptotic pathway in which citicoline acts.



## **Further Work.**

This study demonstrated the role of citicoline in modulation of angiogenesis using in vitro angiogenesis assays. However, there is a need for a confirmation of these results to establish windows of opportunity to greatly increase the potential of citicoline in stroke therapy. Therefore, it is worthwhile to use vivo assays such as middle cerebral artery occlusion (MCAO) rat model to demonstrate citicoline effect as a pro-angiogenic agent. It would also be useful to investigate the same apoptotic and angiogenic pathways explored in this study in *vivo*, and use immunohistochemical staining to detect the expression of the key proteins involved.

Although the present study demonstrated citicoline up-regulation and down-regulation of the genes involved in the apoptotic pathway, there is a need for confirmation of these genes by Western blotting, for a better understanding of the underlying molecular mechanisms by which citicoline is responsible for the modulation of cell survival.

The results from flow cytometry showed a level of inconsistency across all conditions, which could be due to false positive events associated with PI staining of RNA within the cytoplasmic compartment. Therefore, it would be advisable to modify the conventional Annexin V-FITC Apoptosis protocol by adding RNase for cytoplasmic RNA removal.

In the therapeutic process of acute ischemic stroke, the effectiveness of drug delivery is very important. Therefore, it would be interesting to investigate different in vivo drug delivery systems to find the optimum method of delivering citicoline to the target tissue.

# Chapter 5 References

## References.

- A.Hamid Boulares, A. G. (1999). Role of Poly(ADP-ribose) Polymerase (PARP) Cleavage in Apoptosis CASPASE 3-RESISTANT PARP MUTANT INCREASES RATES OF APOPTOSIS IN TRANSFECTED CELLS. *Journal of Biological Chemistry*, 22932-22940.
- Afonso PV, O. S. (2007). Human blood-brain barrier disruption by retroviral-infected lymphocytes: role of myosin light chain kinase in endothelial tight-junction disorganization. *The Journal of Immunology*, 2576-2583.
- Ajiro K, S. A. (2010). Reciprocal Epigenetic Modification of Histone H2B occurs in Chromatin during Apoptosis in vitro and in vivo. *Cell Death Differ*, 984-993.
- Ajiro K, T. J. (2004). Isolation and characterization of mammalian cells that are undergoing apoptosis by a bovine serum albumin density gradient. *Anal Biochem*, 226-233.
- Ajiro, K. (2000). Histone H2B phosphorylation in mammalian apoptotic cells. An association with DNA fragmentation. *J Biol Chem*, 439-443.
- Alan G. Porter, P. N. (1997). Death substrates come alive. *BioEssays*, 501–507.
- Alnemri ES, L. D. (1996). Human ICE/CED-3 protease nomenclature. *Cell*, 171.
- Altat M, S. N. (2007). Histone modifications in response to DNA damage. *Mutation Research/Fundamental and Molecular Mechanisms of Mutagenesis*, 81–90.
- American Diabetes Association. (2008). Diagnosis and Classification of Diabetes Mellitus. *Diabetes Care January*, S55-S60.
- Ann Hoeben, B. L. (2004). Vascular Endothelial Growth Factor and Angiogenesis. *Pharmacological Reviews*, 549-580.
- Annette L. Henneberry, T. A. (2001). Phosphatidylcholine Synthesis Influences the Diacylglycerol Homeostasis Required for Sec14p-dependent Golgi Function and Cell Growth. *Mol. Biol. Cell*, 511-520.
- Anny-Claude Luissint, C. A.-O. (2012). Tight junctions at the blood brain barrier: physiological architecture and disease-associated dysregulation. *Fluids and Barriers of the CNS*, 9-23.
- Antoni Dávalos, J. S. (2011). Citicoline Preclinical and Clinical Update 2009–2010. *Stroke*, S36-S39.

- Antoni Dávalos, M. P., José Castillo, M. P., José Álvarez-Sabín, M. P., Julio J. Secades, M. P., Joan Mercadal, B., Sonia López, B., . . . Rafael Lozano, M. (2002). Oral Citicoline in Acute Ischemic Stroke An Individual Patient Data Pooling Analysis of Clinical Trials. *Stroke*, 2850-2857.
- Arumugam Muruganandam, L. M. (1997). Development of immortalized human cerebrovascular endothelial cell line as an in vitro model of the human blood-brain barrier. *The FASEB Journal*, 1187-1197.
- B. B. Weksler, E. A.-L. (2005). Blood-brain barrier-specific properties of a human adult brain endothelial cell line. *The FASEB Journal*, 1872-1874.
- Babette Weksler, I. A.-O. (2013). The hCMEC/D3 cell line as a model of the human blood brain barrier. *FLUIDS AND BARRIERS OF THE CNS*.
- Bauer KR, B. M. (2007). Descriptive analysis of estrogen receptor (ER)-negative, progesterone receptor (PR)-negative, and HER2-negative invasive breast cancer, the so-called triple-negative phenotype: a population-based study from the California cancer Registry. *Cancer*, 1721-1728.
- Bender LM, M. M. (2005). The adaptor protein TRADD activates distinct mechanisms of apoptosis from the nucleus and the cytoplasm. *Cell Death Differ*, 473-481.
- Beni B. Wolf, J. C.-M. (1999). Calpain Functions in a Caspase-Independent Manner to Promote Apoptosis-Like Events During Platelet Activation. *Blood*, 1683-1692.
- Bicker J, A. G. (2014). Blood-brain barrier models and their relevance for a successful development of CNS drug delivery systems: A review. *European Journal of Pharmaceutics and Biopharmaceutics*, 409–432.
- Bing-Hua Jiang, J. Z. (2000). Phosphatidylinositol 3-kinase signaling mediates angiogenesis and expression of vascular endothelial growth factor in endothelial cells. *PNAS*, 1749–1753.
- Birk Poller, H. G.-O. (2008). The human brain endothelial cell line hCMEC/D3 as a human blood-brain barrier model for drug transport studies. *Journal of Neurochemistry*, 1358–1368.
- Bista P, Z. W. (2010). TRAF3 controls activation of the canonical and alternative NFkappaB by the lymphotoxin beta receptor. *J Biol Chem*, 12971-12978.
- Bleackley, M. B. (2002). CYTOTOXIC T LYMPHOCYTES: ALL ROADS LEAD TO DEATH. *NATURE REVIEWS* , 401- 409.

- Boon Yin Khoo, S. L. (2010). Apoptotic Effects of Chrysin in Human Cancer Cell Lines. *Int J Mol Sci*, 2188–2199.
- Boone JJ, B. J. (2009). Involvement of the HER2 pathway in repair of DNA damage produced by chemotherapeutic agents. *Molecular Cancer Therapeutics*. , 3015-3023.
- Bornstein, N. M. (2009). *Stroke: Practical Guide for Clinicians*. Tel Aviv: Karger Medical and Scientific Publishers.
- Brian S. Cummings, J. M. (2000). Phospholipase A2s in Cell Injury and Death. *Perspectives in Pharmacology*, 793–799.
- Bruce Alberts, A. J. (2002). *Molecular Biology of the Cell*. New York: garland science.
- Bustamante A, G. D.-B. (2012). Citicoline in pre-clinical animal models of stroke: a meta-analysis shows the optimal neuroprotective profile and the missing steps for jumping into a stroke clinical trial. *J Neurochem*. , 217-225.
- Cagnol S, C. J. (2010). ERK and cell death: mechanisms of ERK-induced cell death—apoptosis, autophagy and senescence. *FEBS J*, 2-21.
- Cai Huang, K. J. (2004). MAP kinases and cell migration. *Journal of Cell Science*, 4619-4628.
- Caplan, L. R. (2009). *Caplan's Stroke: A Clinical Approach*. Philadelphia: Elsevier Health Sciences.
- Caplan, L. R. (2010). *Stroke*. ReadHowYouWant.com.
- Carlo R. Bartoli, S. D. (2012). Direct Measurement of Blood Flow in Microvessels Grown in Matrigel™ In Vivo. *Journal of Surgical Research*, e55–e60.
- Carmeliet, P. (2000). Mechanisms of angiogenesis and arteriogenesis. *nature MEDICINE*, 389-95.
- Castri P, L. Y. (2014). Poly(ADP-ribose) polymerase-1 and its cleavage products differentially modulate cellular protection through NF-kappaB-dependent signaling. *Biochimica et Biophysica Acta (BBA) - Molecular Cell Research*, 640–651.
- Chang Hwan Park, Y. S. (2005). Neuroprotective effect of citicoline against KA-induced neurotoxicity in the rat retina. *Experimental Eye Research*, 350–358.
- Chen Z, G. K. (2000). Mitochondria localization and dimerization are required for CIDE-B to induce apoptosis. *J Biol Chem*, 22619-22622.

- Cheung WL, A. K. (2003). Apoptotic phosphorylation of histone H2B is mediated by mammalian sterile twenty kinase. *Cell*, 507-517.
- Chiarugi A, M. M. (2003). Poly(ADP-ribose) polymerase-1 activity promotes NF-kappaB-driven transcription and microglial activation: implication for neurodegenerative disorders. *Journal of Neurochemistry*, 306–317.
- Chieko Aoyama, H. L. (2004). Structure and function of choline kinase isoforms in mammalian cells. *Progress in Lipid Research*, 266–281.
- Chi-Hang Wong, H. C.-Y.-K.-S.-G.-Y. (2009). Apoptotic histone modification inhibits nuclear transport by regulating RCC1. *Nature Cell Biology*, 36 - 45.
- Christos Platarasa, S. T. (2000). Effect of CDP-choline on brain acetylcholinesterase and Na<sup>+</sup>,K<sup>+</sup>-ATPase in adult rats. *Clinical Biochemistry*, 351–357.
- Chun-Chi Liang, A. Y.-L. (2007). In vitro scratch assay: a convenient and inexpensive method for analysis of cell migration in vitro. *Nature Protocols*, 329 - 333.
- Cohen-Kashi Malina K, C. I. (2009). Closing the gap between the in-vivo and in-vitro blood-brain barrier tightness. *Brain Research*, 12–21.
- Compston A, C. A. (2008). Multiple sclerosis. *Lancet*, 1502-1517.
- Cooper, G. M. (2000). Microtubules. In G. M. Cooper, *The Cell, 2nd edition A Molecular Approach*. Sunderland: Sinauer Associates.
- Cornelia Noack, C. S. (2014). Cardiovascular effects of levodopa in Parkinson's disease. *Parkinsonism & Related Disorders*.
- Corinne Brana, C. B. (2002). A method for characterising cell death in vitro by combining propidium iodide staining with immunohistochemistry. *Brain Research Protocols*, 109–114.
- Correa RG, M. S. (2012). Roles of NOD1 (NLRC1) and NOD2 (NLRC2) in innate immunity and inflammatory diseases. *Biosci Rep*, 597-608.
- Crompton T, P. M. (1992). Propidium iodide staining correlates with the extent of DNA degradation in isolated nuclei. *Biochem Biophys Res Commun.* , 532-537.
- Cun-Yu Wang, M. W. (1998). NF-κB Antiapoptosis: Induction of TRAF1 and TRAF2 and c-IAP1 and c-IAP2 to Suppress Caspase-8 Activation. *Science*, 1680-1683.

- D.W. Nicholson, G. M. (2013). Caspases and Cell Death. In *Encyclopedia of Biological Chemistry (Second Edition)* (pp. 388–396). London: Elsevier Inc.
- DA., G. (1998 ). Angiogenesis and stroke. *Drug News Perspect*, 265-270.
- Damaso Crespo, R. V.-V. (1995). Structural changes induced by cytidine-5'-diphosphate choline (CDP-choline) chronic treatment in neurosecretory neurons of the supraoptic nucleus of aged CFW-mice. *Mechanisms of Ageing and Development*, 183-193.
- Dauchy S, M. F. (2009). Expression and transcriptional regulation of ABC transporters and cytochromes P450 in hCMEC/D3 human cerebral microvascular endothelial cells. *Biochemical Pharmacology*, 897–909.
- David Alway, J. W. (2009). *Stroke Essentials for Primary Care: A Practical Guide*. Alexandria: Springer Science & Business Media.
- David J Granville, H. J. (1998). Overexpression of Bcl-XL prevents caspase-3-mediated activation of DNA fragmentation factor (DFF) produced by treatment with the photochemotherapeutic agent BPD-MA. *FEBS Letters*, 51–154.
- David M Stern, M. C. (1991). Endothelium and Regulation of Coagulation. *Diabetes Care*, 160-166.
- Dávalos A, A.-S. J.-T.-V., & investigators., I. C. (2012). Citicoline in the treatment of acute ischaemic stroke: an international, randomised, multicentre, placebo-controlled study (ICTUS trial). *Lancet.*, 349-357.
- Deepti Navaratna, S. G. (2009). Special Focus: Angiogenesis in the Central Nervous System Mechanisms and targets for angiogenic therapy after stroke. *Cell Adhesion & Migration* , 216-223.
- Dieter A. Kubli, J. E. (2007). Bnip3 mediates mitochondrial dysfunction and cell death through Bax and Bak. *Biochem J*, 407–415.
- Douglas W. Losordo, S. D. (2004). Therapeutic Angiogenesis and Vasculogenesis for Ischemic Disease. *Circulation*, 2487-2491.
- Edward M. Conway, D. C. (2001). Molecular mechanisms of blood vessel growth. *Cardiovascular Research*, 507–521.
- Eliasson MJ, S. K. (1997). Poly(ADP-ribose) polymerase gene disruption renders mice resistant to cerebral ischemia. *Nature Medicine*, 1089 - 1095.
- Elmore, S. (2007). Apoptosis: A Review of Programmed Cell Death. *Toxicol Pathol*, 495–516.

- Ergul A, A. A. (2012). Angiogenesis: A Harmonized Target for Recovery after Stroke. *Stroke*, 2270-2274.
- Eveline E. Schneeberger, R. D. (2004). The tight junction: a multifunctional complex. *American Journal of Physiology*, C1213-C1228.
- Evgeni G. Ponimaskin, M. H.-Y. (2007). Chapter 2 Monitoring Receptor-Mediated Changes of Intracellular cAMP Level by Using Ion Channels and Fluorescent Proteins as Biosensors. In A. Chattopadhyay, *Serotonin Receptors in Neurobiology*. CRC Press.
- F J Oliver, J. M.-d. (1999). Resistance to endotoxic shock as a consequence of defective NF-kappaB activation in poly (ADP-ribose) polymerase-1 deficient mice. *The EMBO Journal*, 4446–4454.
- Fei Hua, M. G. (2005). Effects of Bcl-2 Levels on Fas Signaling-Induced Caspase-3 Activation: Molecular Genetic Tests of Computational Model Predictions. *The Journal of Immunology*, 985-995.
- Fei P, W. W.-D. (2004). Bnip3L is induced by p53 under hypoxia, and its knockdown promotes tumor growth. *Cancer Cell*, 597-609.
- Fernandez-Capetillo O, A. C. (2004). Phosphorylation of histone H2B at DNA double-strand breaks. *J Exp Med.* , 1671-1677.
- Fioravanti M, Y. M. (2000). Cytidinediphosphocholine (CDP choline) for cognitive and behavioural disturbances associated with chronic cerebral disorders in the elderly. *Cochrane Database Syst Rev*.
- Fisher, M. (2009). *Stroke: Investigation and management*. Amsterdam: Elsevier Health Sciences.
- Françoise Roux, P.-O. C. (2005). Rat Brain Endothelial Cell Lines for the Study of Blood–Brain Barrier Permeability and Transport Functions. *Cellular and Molecular Neurobiology*, 41-57.
- Frank Schuettauf, R. R. (2006). Citicoline and lithium rescue retinal ganglion cells following partial optic nerve crush in the rat. *Experimental Eye Research*, 1128–1134.
- Frederick K. Goodwin, K. R. (2007). *Manic-Depressive Illness: Bipolar Disorders and Recurrent Depression*. New York: Oxford University Press Inc.



- Gabriele Multhoff, J. R. (2014). Critical Role of Aberrant Angiogenesis in the Development of Tumor Hypoxia and Associated Radioresistance. *Cancers*, 813-828.
- Goldstein, L. B. (2011). *A Primer on Stroke Prevention and Treatment: An overview based on AHA/ASA Guidelines*. North Carolina: John Wiley & Sons.
- Gomez-Martín C, L.-R. F.-C.-S. (2014). A critical review of HER2-positive gastric cancer evaluation and treatment: from trastuzumab, and beyond. *Cancer Letters*, 30–40.
- Goto S, X. R. (2002). Poly(ADP-ribose) polymerase impairs early and long-term experimental stroke recovery. *Stroke*, 1101-1106.
- Gumbleton M, A. K. (2001). Progress and limitations in the use of in vitro cell cultures to serve as a permeability screen for the blood-brain barrier. *JOURNAL OF PHARMACEUTICAL SCIENCES*, 1681-98.
- Guoyao Wu, Y.-Z. F. (2004). Glutathione Metabolism and Its Implications for Health. *The American Society for Nutritional Sciences*, 489-492.
- Gutiérrez-Fernández M, R.-F. B.-C.-G.-A.-T. (2012). CDP-choline treatment induces brain plasticity markers expression in experimental animal stroke. *Neurochem Int*, 310-7.
- Hall, C. D. (1999). Rho GTPases Control Polarity, Protrusion, and Adhesion during Cell Movement. *J Cell Biol.*, 1235–1244.
- Han BH, X. D. (2002). Selective, Reversible Caspase-3 Inhibitor Is Neuroprotective and Reveals Distinct Pathways of Cell Death after Neonatal Hypoxic-ischemic Brain Injury. *J Biol Chem.*, 128-136.
- Heart and Stroke Foundation. (2014, July). Retrieved from [http://www.heartandstroke.com/site/c.iklQLcMWJtE/b.3484151/k.7916/Stroke\\_\\_\\_Ischemic\\_stroke.htm](http://www.heartandstroke.com/site/c.iklQLcMWJtE/b.3484151/k.7916/Stroke___Ischemic_stroke.htm)
- Heath, J. R. (2008). *Principles of Cell Proliferation*. Oxford: John Wiley & Sons.
- Helga E. de Vries, J. K. (1997). The Blood-Brain Barrier in Neuroinflammatory Diseases. *Pharmacological Reviews*, 143-156.
- Hitomi J, K. T. (2004). Involvement of caspase-4 in endoplasmic reticulum stress-induced apoptosis and Abeta-induced cell death. *J Cell Biol*, 347-356.
- Houghton, H. E. (2011). Insulin receptor substrate regulation of phosphoinositide 3-kinase. *Clin Cancer Res*, 206-211.

- Hurtado O, C. A. (2007). A chronic treatment with CDP-choline improves functional recovery and increases neuronal plasticity after experimental stroke. *Neurobiol Dis*, 105-111.
- Hynda K. Kleinman, G. R. (2005). Matrigel™ : Basement membrane matrix with biological activity. *Seminars in Cancer Biology*, 378–386.
- Hyun Joon Lee, J. S. (2009). Citicoline Protects Against Cognitive Impairment in a Rat Model of Chronic Cerebral Hypoperfusion. *J Clin Neurol*, 33–38.
- Itallie, J. M. (2009). Physiology and Function of the Tight Junction. *Cold Spring Harb Perspect Biology*.
- Ito Y, P. P. (2000). The novel triterpenoid 2-cyano-3,12-dioxoolean-1,9-dien-28-oic acid induces apoptosis of human myeloid leukemia cells by a caspase-8-dependent mechanism. *Cell Growth Differentiation*, 261-267.
- JAIN, R. K. (2001). Normalizing tumor vasculature with anti-angiogenic therapy: A new paradigm for combination the. *Nature* , 987 - 989.
- Janardhan S, S. P. (2006). Choline kinase: an important target for cancer. *Curr Med Chem*. 1169-86.
- Jane Williams, L. P. (2010). *Acute Stroke Nursing*. Chichester: John Wiley & Sons.
- Bustamante A, G. D. G.-B. L. C. M. R. A. M. J., 2012. Citicoline in pre-clinical animal models of stroke: a meta-analysis shows the optimal neuroprotective profile and the missing steps for jumping into a stroke clinical trial.. *J Neurochem.* , pp. 217-225.
- Dávalos A, A.-S. J. C. J. D.-T. E. F. J. M.-V. E. S. J. S. T. C. V. M. J. C. E. S. J. & investigators., I. C. T. o. a. S. (. t., 2012. Citicoline in the treatment of acute ischaemic stroke: an international, randomised, multicentre, placebo-controlled study (ICTUS trial). *Lancet.*, pp. 349-357.
- Jawahar Mehta, N. S. D., 2013. *Biochemical Basis and Therapeutic Implications of Angiogenesis*. New York: Springer-Verlag.
- Jerzy Krupinski, M. A. S. M.-N. R. A.-B. E. B. P. C. J. A. P. D. L. N. R. M. G.-S. J. S. a. M. S., 2012. Citicoline induces angiogenesis improving survival of vascular/human brain microvessel endothelial cells through pathways involving ERK1/2 and insulin receptor substrate-1. *Vasc Cell.*, p. 4:20.
- Jerome KR, S. D. (2003). Measurement of CTL-induced cytotoxicity: the caspase 3 assay. *Apoptosis*, 563-571.

- Jerzy Krupinski, M. A.-N.-B.-S. (2012). Citicoline induces angiogenesis improving survival of vascular/human brain microvessel endothelial cells through pathways involving ERK1/2 and insulin receptor substrate-1. *Vasc Cell.*, 4:20.
- Jessica Gorgui, M. G. (2014). Hypertension as a Risk Factor for Ischemic Stroke in Women. *Canadian Journal of Cardiology*, 774–782.
- Johannes Binder, K. S. (2012). *Stroke*. Oxford: Oxford University Press.
- Jonathan Pratt, B. A. (2014). Induction of autophagy biomarker BNIP3 requires a JAK2/STAT3 and MT1-MMP signaling interplay in Concanavalin-A-activated U87 glioblastoma cells. *Cellular Signalling*, 917–924.
- Jon Infante, P. S.-J.-R.-Q. (2007). Poly (ADP-ribose) polymerase-1 (PARP-1) genetic variants are protective against Parkinson's disease. *Journal of the Neurological Sciences*, 68–70.
- Jr., R. R. (2012). ERK1/2 MAP kinases: Structure, function, and regulation. *Pharmacological Research*, 105–143.
- Justin C Yarrow, Z. E. (2004). A high-throughput cell migration assay using scratch wound healing, a comparison of image-based readout methods. *BMC Biotechnology*.
- Justin C Yarrow, Z. E. (2004). A high-throughput cell migration assay using scratch wound healing, a comparison of image-based readout methods. *BMC Biotechnology*, 2004.
- Kamlesh Sodani, A. K.-J.-J.-L.-S. (2012). GW583340 and GW2974, human EGFR and HER-2 inhibitors, reverse ABCG2- and ABCB1-mediated drug resistance. *Biochemical Pharmacology*, 1613–1622.
- Karina J. Price, A. T. (2012). Matrigel™ Basement Membrane Matrix influences expression of microRNAs in cancer cell lines. *Biochemical and Biophysical Research Communications*, 343–348.
- Karsten Overgaard. (2014). The Effects of Citicoline on Acute Ischemic Stroke: A Review. *Journal of Stroke and Cerebrovascular Diseases*.
- Khoo CP, M. K. (2011). A comparison of methods for quantifying angiogenesis in the Matrigel assay in vitro. *Tissue Eng Part C Methods*, 895-906.
- Kiem Vu, B. W.-O. (2009). Immortalized Human Brain Endothelial Cell Line HCMEC/D3 as a Model of the Blood-Brain Barrier Facilitates In Vitro Studies of Central

- Nervous System Infection by *Cryptococcus neoformans*. *Eukaryot Cell*, 1803–1807.
- Kim BS, P. J. (2014). Fucoidan/FGF-2 induces angiogenesis through JNK- and p38-mediated activation of AKT/MMP-2 signalling. *Biochemical and Biophysical Research Communications*, 1333–1338.
- Kleinschnitz C, P. N. (2012). Experimental therapy approaches for ischemic stroke. *Nervenarzt*, 1275-1281.
- K., K. (2000). Caspase-9. *Int J Biochem Cell Biol.* , 121-124.
- K. Kiguchi, L. R. (2005). Chemopreventive and therapeutic efficacy of orally active tyrosine kinase inhibitors in a transgenic mouse model of gallbladder carcinoma. *Clinical Cancer Research* , 5572–5580.
- Konstantin Gaengel, G. G. (2009). Endothelial-Mural Cell Signaling in Vascular Development and Angiogenesis. *Arteriosclerosis, Thrombosis, and Vascular Biology*, 630-638.
- Kraus WL, L. J. (2003). PARP Goes Transcription. *Cell*, 677-683.
- Kroon ME, K. P. (2000). Hypoxia in combination with FGF-2 induces tube formation by human microvascular endothelial cells in a fibrin matrix: involvement of at least two signal transduction pathways. *Journal of Cell Science* , 825-833.
- Kruidering M, E. G. (2000). Caspase-8 in apoptosis: the beginning of "the end"? *UBMB Life*, 85-90.
- Krupinski J, F. I. (2002). CDP-choline reduces pro-caspase and cleaved caspase-3 expression, nuclear DNA fragmentation, and specific PARP-cleaved products of caspase activation following middle cerebral artery occlusion in the rat. *Neuropharmacology*, 846-854.
- Kubota, Y. (2012). Tumor Angiogenesis and Anti-angiogenic Therapy. *The Keio Journal of Medicine*, 47-56.
- Kuida, K. (2000). Caspase-9. *The International Journal of Biochemistry & Cell Biology*, 121–124.
- Kusch-Poddar M, D. J. (2005). Evaluation of the immortalized human brain capillary endothelial cell line BB19 as a human cell culture model for the blood-brain barrier. *Brain Research*, 21–31.

- L Lazzaroni, F. F. (1999). The use of Matrigel™ \* at low concentration enhances in vitro blastocyst formation and hatching in a mouse embryo model. *Fertility and Sterility*, 1133–1137.
- L. L. Rubin, D. E. (1991). A Cell Culture Model of the Blood-Brain Barrier. *J Cell Biol*, 1725–1735.
- Lei Fang, B. A. (2008). Essential role of TNF receptor superfamily 25 (TNFRSF25) in the development of allergic lung inflammation. *J Exp Med*, 1037–1048.
- Liam Portt, G. N. (2011). Anti-apoptosis and cell survival: A review. *Biochimica et Biophysica Acta (BBA) - Molecular Cell Research*, 238–259.
- Lindley, R. I. (2008). *Stroke The Facts*. New York: Oxford University Press.
- Liu X, Z. H. (1997). DFF, a heterodimeric protein that functions downstream of caspase-3 to trigger DNA fragmentation during apoptosis. *Cell*, 175-184.
- Lu C, S. Y. (2010). MAPKs and Mst1/Caspase-3 pathways contribute to H2B phosphorylation during UVB-induced apoptosis. *Science China Life Sciences*. , 663-668.
- Lu Zhang, L. L. (2009). BNIP3 mediates cell death by different pathways following localization to endoplasmic reticulum and mitochondrion. *FASEB J*, 3405–3414.
- M Chiong, Z. V. (2011). Cardiomyocyte death: mechanisms and translational implications. *Cell Death and Disease*.
- M Sobrado, M. L. (2003). Combined nimodipine and citicoline reduce infarct size, attenuate apoptosis and increase bcl-2 expression after focal cerebral ischemia. *Neuroscience*, 107–113.
- Mads Hald Andersen, J. C. (2005). Regulators of apoptosis: suitable targets for immune therapy of cancer. *Nature Reviews Drug Discovery*, 399-409.
- Mandir AS, P. S.-L.-R. (1999). Poly(ADP-ribose) polymerase activation mediates 1-methyl-4-phenyl-1, 2,3,6-tetrahydropyridine (MPTP)-induced parkinsonism. *The National Academy of Sciences*, 5774-5779.
- María Alonso de Leciñana, M. G.-T. (2006). Effect of combined therapy with thrombolysis and citicoline in a rat model of embolic stroke. *Journal of the Neurological Sciences*, 121–129.

- Mark M. Moasser, A. B. (2001). The Tyrosine Kinase Inhibitor ZD1839 (“Iressa”) Inhibits HER2-driven Signaling and Suppresses the Growth of HER2-overexpressing Tumor Cells. *Cancer Research*, 7184-7188.
- Marta Barrachina, I. D. (2003). Neuroprotective effect of citicoline in 6-hydroxydopamine-lesioned rats and in 6-hydroxydopamine-treated SH-SY5Y human neuroblastoma cells. *Journal of the Neurological Sciences*, 105–110.
- Marta Barrachina, J. S.-S. (2002). Citicoline increases glutathione redox ratio and reduces caspase-3 activation and cell death in staurosporine-treated SH-SY5Y human neuroblastoma cells. *Brain Research*, 84–90.
- Martin R. Sprick, H. W. (2004). The interplay between the Bcl-2 family and death receptor-mediated apoptosis. *Biochimica et Biophysica Acta*, 125 – 132.
- Mathias Ndhlovu, B. E. (2011). Identification of  $\alpha$ -tubulin as an autoantigen recognized by sera from patients with neuropsychiatric systemic lupus erythematosus. *Brain, Behavior, and Immunity*, 279–285.
- Maxime Lévesque, M. A. (2013). The kainic acid model of temporal lobe epilepsy. *Neuroscience & Biobehavioral Reviews*, 2887–2899.
- Melanie H. Cobb, a. E. (1995). How MAP Kinases Are Regulated. *The Journal of Biological Chemistry*, 14843-14846.
- Mensch J, L. L. (2010). Application of PAMPA-models to predict BBB permeability including efflux ratio, plasma protein binding and physicochemical parameters. *International Journal of Pharmaceutics*, 182–197.
- Michael E. Duffey, B. H. (1981). Regulation of epithelial tight junction permeability by cyclic AMP. *Nature*, 451 - 453.
- Michel V, B. M. (2012). The ubiquitous choline transporter SLC44A1. *Cent Nerv Syst Agents Med Chem.*, 70-81.
- Michel V, Y. Z. (2006). Choline transport for phospholipid synthesis. *Exp Biol Med (Maywood)*., 490-504.
- Mori T, O. H. (2000). Aberrant overexpression of 53BP2 mRNA in lung cancer cell lines. *FEBS Letters*, 124-128.
- Myoung-Gwi Ryou, G. R.-H. (2013). Pyruvate minimizes rtPA toxicity from in vitro oxygen-glucose deprivation and reoxygenation. *Brain Research*, 66–75.
- N. Joan Abbott, L. R. (2006). Astrocyte–endothelial interactions at the blood–brain barrier. *Nature Reviews Neuroscience*, 41-53.

- Naoyo Nishida, H. Y. (2006). Angiogenesis in Cancer. *Vasc Health Risk Management*, 213–219.
- Nelson, A. H. (2008). Adherens and Tight Junctions: Structure, Function and Connections to the Actin Cytoskeleton. *Biochim Biophys Acta*, 660–669.
- Oberst A, P. C. (2010). Inducible dimerization and inducible cleavage reveal a requirement for both processes in caspase-8 activation. *J Biol Chem*, 16632-16642.
- Olmez I, O. H. (2012). Reactive oxygen species and ischemic cerebrovascular disease. *Neurochem Int.* , 208-212.
- Osamu Sawadaa, L. P. (2014). All-trans-retinal induces Bax activation via DNA damage to mediate retinal cell apoptosis. *Experimental Eye Research*, 27–36.
- Overgaard, K. (2014). The Effects of Citicoline on Acute Ischemic Stroke: A Review. *Journal of Stroke and Cerebrovascular Diseases*.
- Ozhan Eyigora, C. C. (2012). Intravenous CDP-choline activates neurons in supraoptic and paraventricular nuclei and induces hormone secretion. *Brain Research Bulletin*, 286–294.
- Pan J, C. Q. (2010). Reactive oxygen species-activated Akt/ASK1/p38 signaling pathway in nickel compound-induced apoptosis in BEAS 2B cells. *Chem Res Toxicol*, 568-577.
- Pan J, K. A.-S. (2007). Reperfusion injury following cerebral ischemia: pathophysiology, MR imaging, and potential therapies. *Neuroradiology.* , 93-102.
- Paolo Fagone, S. J. (2013). Phosphatidylcholine and the CDP–choline cycle. *Biochimica et Biophysica Acta (BBA) - Molecular and Cell Biology of Lipids*, 523–532.
- Park YH, J. M. (2014). Death domain complex of the TNFR-1, TRADD, and RIP1 proteins for death-inducing signaling. *Biochem Biophys Res Commun*, 1155-1161.
- Pedro Ramos-Cabrera, J. A.-M. (2011). Serial MRI study of the enhanced therapeutic effects of liposome-encapsulated. *Pharmaceutical Nanotechnology*, 228–233.
- Peiwen Fei, W. W.-h.-D. (2004). Bnip3L is induced by p53 under hypoxia, and its knockdown promotes tumor growth. *Cancer Cell*, 597–609.
- Perrelet D, F. A. (2000). IAP family proteins delay motoneuron cell death in vivo. *Eur J Neurosci*, 2059-2067.

- Phillip W. Dickson, G. D. (2013). Chapter Two – Tyrosine Hydroxylase: Regulation by Feedback Inhibition and Phosphorylation. *Advances in Pharmacology*, 13–21.
- Popp, A. J. (2011). *Guide to the Primary Care of Neurological Disorders*. New York : Thieme.
- Porter AG, J. R. (1999). Emerging roles of caspase-3 in apoptosis. *Cell Death Differ*, 99-104.
- Pressinotti NC, K. H. (2009). Differential expression of apoptotic genes PDIA3 and MAP3K5 distinguishes between low- and high-risk prostate cancer. *Mol Cancer*, 8:130.
- Puig B, T. A. (2001). Cleaved caspase-3, caspase-7 and poly (ADP-ribose) polymerase are complementarily but differentially expressed in human medulloblastomas. *Neurosci Lett*, 85-88.
- Raga Krishnakumar, W. L. (2010). The PARP Side of the Nucleus: Molecular Actions, Physiological Outcomes, and Clinical Targets. *Molecular Cell*, 8–24.
- Rajesh P. Rastogi, R. a. (2009). APOPTOSIS: MOLECULAR MECHANISMS AND PATHOGENICITY. *EXCLI Journal*, 155-181.
- Rao Muralikrishna Adibhatla, J. H. (2001). Effects of Citicoline on Phospholipid and Glutathione Levels in Transient Cerebral Ischemia. *Stroke*, 2376-2381.
- Rao Muralikrishna Adibhatla, R. D. (2008). Integration of cytokine biology and lipid metabolism in stroke. *Frontiers in Bioscience*, 1250-1270.
- Ricardo G. Correa, S. M. (2012). Roles of NOD1 (NLRC1) and NOD2 (NLRC2) in innate immunity and inflammatory diseases. *Biosci Rep*, 597–608.
- Richard A. Hawkins, R. L. (2006). Structure of the Blood–Brain Barrier and Its Role in the Transport of Amino Acids. *The Journal of Nutrition* , 218S-226S.
- Richard J. Wurtman, M. R. (2000). Effect of Oral CDP-Choline on Plasma Choline and Uridine Levels in Humans. *Biochemical Pharmacology*, 989–992.
- Rieger AM, H. B. (2010). Conventional apoptosis assays using propidium iodide generate a significant number of false positives that prevent accurate assessment of cell death. *Journal of Immunological Methods*, 81–92.
- Robert Auerbach, R. L. (2003). Angiogenesis Assays: A Critical Overview. *Clinical Chemistry*, 32-40.
- Robert J. Wityk, R. H. (2007). *Stroke*. ACP Press.



- Roberta Giuliani, M. B. (1999). Role of endothelial cell extracellular signal-regulated kinase1/2 in urokinase-type plasminogen activator upregulation and in vitro angiogenesis by. *Journal of Cell Science*, 2597-2606 .
- Rocío García-Cobos, A. F.-G.-F.-T. (2009). Citicoline, use in cognitive decline: Vascular and degenerative. *Journal of the Neurological Sciences*, 188–192.
- Roisean E. Ferguson, H. P. (2005). Housekeeping proteins: A preliminary study illustrating some limitations as useful references in protein expression studies. In H. P. Roisean E. Ferguson, *Proteomics* (pp. 566–571). Weinheim: WILEY-VCH Verlag GmbH & Co.
- Román, J. Á.-S. (2013). The Role of Citicoline in Neuroprotection and Neurorepair in Ischemic Stroke. *Brain Sci*, 1395-1414.
- Ronan Jamboua, b. F.-A. (2009). Citicoline (CDP-choline): What role in the treatment of complications of infectious diseases. *The International Journal of Biochemistry & Cell Biology*, 1467–1470.
- Ruddell RG1, K. B.-P. (2009). Lymphotoxin-beta receptor signaling regulates hepatic stellate cell function and wound healing in a murine model of chronic liver injury. *Hepatology*, 227-239.
- S. Sahina, T. A. (2010). Effects of citicoline used alone and in combination with mild hypothermia on apoptosis induced by focal cerebral ischemia in rats. *Journal of Clinical Neuroscience*, 227–231.
- Samuels-Lev Y, O. D. (2001). ASPP proteins specifically stimulate the apoptotic function of p53. *Mol Cell*, 781-794.
- Savitz, P. S. (2011). Investigational Therapies for Ischemic Stroke: Neuroprotection and Neurorecovery. *Neurotherapeutics*, 434–451.
- Schramek, H. (2002). MAP Kinases: From Intracellular Signals to Physiology and Disease. *APS Journals*, 62-67.
- Secades JJ, L. J. (2006). Citicoline: pharmacological and clinical review, 2006 update. *Methods Find Exp Clin Pharmacol.* , 1-56.
- Shinsuke Nakagawa, M. A. (2009). A new blood–brain barrier model using primary rat brain endothelial cells, pericytes and astrocytes. *Neurochemistry International*, 253–263.
- Singaravelu R, L. R. (2013). Human serum activates CIDEB-mediated lipid droplet

- enlargement in hepatoma cells. *Biochem Biophys Res Commun.*, 447-452.
- Sirin Baspınara, S. B. (2014). The relation of beclin 1 and bcl-2 expressions in high grade prostatic intraepithelial neoplasia and prostate adenocarcinoma: A tissue microarray study. *Pathology - Research and Practice*, 412–418.
- Slamon DJ, L.-J. B. (2001). Use of Chemotherapy plus a Monoclonal Antibody against HER2 for Metastatic Breast Cancer That Overexpresses HER2. *New England Journal of Medicine*, 783-792.
- Slee EA, A. C. (2001). Executioner caspase-3, -6, and -7 perform distinct, non-redundant roles during the demolition phase of apoptosis. *The Journal Biological Chemistry.*, 7320-7326.
- Slevin M, K. P. (2006). Can angiogenesis be exploited to improve stroke outcome? Mechanisms and therapeutic potential. *Clin Sci (Lond)*, 171-83.
- Smith, F. G. (2010). The Kennedy pathway—De novo synthesis of phosphatidylethanolamine and phosphatidylcholine. *IUBMB Life*, 414–428.
- Sollberger G, S. G. (2012). Caspase-4 is required for activation of inflammasomes. *J Immunol*, 1992-2000.
- Stefan S. Kassner, G. A. (2008). Novel Systemic Markers for Patients with Alzheimer Disease? – A Pilot Study. *Current Alzheimer Research*, 358-366 .
- Stefanie Krick, B. G. (2005). Role of Hypoxia-Inducible Factor-1 $\alpha$  in Hypoxia-Induced Apoptosis of Primary Alveolar Epithelial Type II Cells. *American Journal of Respiratory Cell and Molecular Biology*, 395-403.
- Sugimura K, T. S. (2008). PARP-1 ensures regulation of replication fork progression by homologous recombination on damaged DNA. *Journal of Cell Biology*, 1203-1212.
- Sumpio BE, R. J. (2002). Cells in focus: endothelial cell. *The International Journal of Biochemistry & Cell Biology*, 1508–1512.
- Sun WT, H. P. (2008). p53 target DDA3 binds ASPP2 and inhibits its stimulation on p53-mediated BAX activation. *Biochem Biophys Res Commun*, 395-398.
- Suzanne C. O'Connell Smeltzer, B. G. (2010). *Brunner & Suddarth's Textbook of Medical-surgical Nursing, Volume 1*. Lippincott Williams & Wilkins.
- Taizen Nakase, S. Y. (2011). Free radical scavenger, edaravone, reduces the lesion size of lacunar infarction in human brain ischemic stroke. *BMC Neurology* , 11-39 .

- T.M. Kauppinen, R. S. (2007). The role of poly(ADP-ribose) polymerase-1 in CNS disease. *Neuroscience*, 1267–1272.
- Temitope R. Sodunke, K. K. (2007). Micropatterns of Matrigel™ for three-dimensional epithelial cultures. *Biomaterials*, 4006–4016.
- Tesfaigzi, Y. M. (2009). How ERK1/2 Activation Controls Cell Proliferation and Cell Death Is Subcellular Localization the Answer? *Cell Cycle.*, 1168-1175.
- TM., K. (2007). Multiple roles for poly(ADP-ribose)polymerase-1 in neurological disease. *Neurochemistry International*, 954-958.
- Toulmond S, T. K. (2004). Neuroprotective effects of M826, a reversible caspase-3 inhibitor, in the rat malonate model of Huntington's disease. *Br J Pharmacol.*, 689-697.
- Tymen T. Keller, A. T. (2003). infections and endothelial cells. *Cardiovascular Research*, 40–48.
- V. Rema, K. B. (2008). Cytidine-5-diphosphocholine supplement in early life induces stable increase in dendritic complexity of neurons in the somatosensory cortex of adult rats. *Neuroscience*, 556–564.
- Vance, Z. L. (2008). Thematic Review Series: Glycerolipids. Phosphatidylcholine and choline homeostasis. *The Journal of Lipid Research*, 1187-1194.
- Vasudevan, D. (2013). *Textbook of Biochemistry for Medical Students*. London: JP Medical Ltd.
- Vu K, W. B. (2009). Immortalized human brain endothelial cell line HCMEC/D3 as a model of the blood-brain barrier facilitates in vitro studies of central nervous system infection by *Cryptococcus neoformans*. *Eukaryot Cell.*, 1803–1807.
- Wang T, H. Y. (2013). [Gly14]-Humanin offers neuroprotection through glycogen synthase kinase-3 $\beta$  inhibition in a mouse model of intracerebral hemorrhage. *Behavioural Brain Research*, 132–139.
- Wang X, M. K. (2000). Epidermal growth factor receptor-dependent Akt activation by oxidative stress enhances cell survival. *J Biol Chem*, 14624-14631.
- Wardlaw JM, M. V. (2012). Recombinant tissue plasminogen activator for acute ischaemic stroke: an updated systematic review and meta-analysis. *Lancet*, 2364-2372.

- Weiss, G. B. (1995). Metabolism and actions of cdpcholine as an endogenous compound and administered exogenously as citicoline. *Life Sciences*, 637–660.
- Wei-Yuan Houa, b. D.-X.-P.-J. (2008). The homeostasis of phosphatidylcholine and lysophosphatidylcholine was not disrupted during tri-o-cresyl phosphate-induced delayed neurotoxicity in hens. *Toxicology*, 56–63.
- Weksler B, R. I. (2013). The hCMEC/D3 cell line as a model of the human blood brain barrier. *Fluids Barriers CNS*, 10-16.
- Wimmer N, H. B. (2012). Lymphotoxin  $\beta$  receptor activation on macrophages induces cross-tolerance to TLR4 and TLR9 ligands. *J Immunol*, 3426-3433.
- Wu X, L. E. (2014). Cell death-inducing DFFA-like effector b is required for hepatitis C virus entry into hepatocytes. *J Virol*, 8433-8444.
- Yang JP, H. M. (1999). NF-kappaB subunit p65 binds to 53BP2 and inhibits cell death induced by 53BP2. *Oncogene*, 5177-5186.
- Zhi Huang, D.-P. Y.-X. (2008). JNK regulates cell migration through promotion of tyrosine phosphorylation of paxillin. *Cellular Signalling*, 2002–2012.
- Zhuang S, Y. Y. (2007). ERK promotes hydrogen peroxide-induced apoptosis through caspase-3 activation and inhibition of Akt in renal epithelial cells. *Am J Physiol Renal Physiol*, F440-F447.

## **Appendices.**

### **Appendix 1.**

#### **Reagents.**

Acrylamide/Bis solution (Bio-Rad Laboratories).

Alexa Fluor® Goat Anti-Rabbit (Life Technologies, UK).

Ammonium persulphate (Sigma, UK).

Annexin V-FITC Apoptosis Detection Kit (Sigma, UK).

Anti-Caspase 3, Active antibody produced in rabbit polyclonal (Sigma, UK).

Anti-Caspase 3 antibody produced in rabbit (Sigma, UK).

Anti-Cleaved PARP antibody rabbit polyclonal (abcam).

Anti-ErbB2/Her-2, clone EP1045Y, Rabbit Monoclonal Antibody (Abcam, UK).

Anti-ERK1/2 (K-23) rabbit monoclonal IgG antibody (Santa Cruz Biotechnology).

Anti-Histone H2B rabbit polyclonal antibody (Millipore, USA).

Anti-PARP rabbit polyclonal antibody (abcam).

Anti-phospho-erbB2 (Y1221), clone 7F8 rabbit monoclonal (Abcam, UK).

Anti-Phospho-Erk1/2 (E-4) mouse monoclonal antibody (Santa Cruz Biotechnology).

Anti-phospho-Histone H2B (Ser14) Polyclonal Antibody (Millipore, USA).

BD Matrigel™™ Basement Membrane Matrix (BD Biosciences, UK)

Bio-Rad protein assay kit (Bio-Rad Laboratories, Germany).

Bis (N,N"-methylenebisacrylamide), (Sigma, UK).

BLUeye Prestained Protein Ladder (Geneflow, UK).

Bovine serum albumin, BSA (Sigma, UK).

Bromophenol blue (Serva).

Citicoline (Ferrer, Spain).

Coomassie brilliant blue (BDH, UK).

DMSO, Dimethyl sulfoxide (Sigma, UK).

Endothelial Basal Medium-2, EBM-2 (Lonza, USA).

ErbB-2 inhibitor GW2974 (Sigma, UK).

Ethanol (Fisher Scientific International, UK).

EZ-ECL chemiluminescence detection kit for HRP (Biological industries, Israel)

Fibroblast growth factor-2 (R&D System, UK).

Foetal Bovine Serum, FBS (Lonza, USA).

Giemsa stain (Sigma, UK).

Glycerol (BDH,UK).

Glycine (BDH,UK).

Hoescht stain solution (H6024) (Sigma, UK).

Hydrochloric acid (BDH, UK).

Hypoxia gas (Boc Gases, UK)

Isopropanol (Sigma, UK).

Methanol (Fisher Scientific International)

Milk (Local store, UK)

N,N,N',N'- tetramethylethylenediamine (TEMED)( Sigma, UK).

Normal Goat Serum (10%) (Life Technologies, UK).

Paraformaldehyde, PFA (General Purpose Reagent, UK).

Phosphate Buffer Saline, PBS (Lonza, USA).

Polyclonal Goat Anti-rabbit Immunoglobulin/Horseradish peroxidase, HRP (Dako, Denmark)

Polyclonal Rabbit Anti-goat Immunoglobulin /Horseradish peroxidase, HRP (Dako, Denmark).

Poly-L-lysine solution 0.1 % (w/v) in H<sub>2</sub>O (Sigma, UK).

Propidium iodide,PI (Sigma Aldrich, USA).

RNase-Free DNase Set (Qiagen, UK).

RNeasy Mini Kit (Qiagen, UK).

RT<sup>2</sup> First Strand Kit (Qiagen, UK).

RT<sup>2</sup> SYBR Green qPCR Master Mixes (Qiagen, UK).

Sodium chloride (Sigma, UK).

Sodium Dodecyl Sulphate,SDS (BDH, UK).

Sodium hydroxide (BDH, UK).

Staurosporine solution from Streptomyces sp1 mM in DMSO (Sigma Aldrich,USA).

Tris (hydroxymethyl) methylamine (BDH, UK)

Trizam® base, minimum 99.9% titration (Sigma,USA)

Trypsin10X (Sigma, UK)

Tween-20 (Sigma, UK).

VECTASHIELD Mounting Medium with DAPI (Vector Laboratories, UK).

Virkon disinfectant (Antec International).

## **Appendix 2.**

### **Preparation of the Kinexus buffer.**

1. 20 mM MOPS, pH 7.0 (any other buffer without Tris at this pH could be substituted).
2. 2 mM EGTA (to bind calcium).
3. 5 mM EDTA (to bind magnesium and manganese).
4. 30 mM sodium fluoride (to inhibit protein-serine phosphatases).
5. 60 mM glycerophosphate, pH 7.2 (to inhibit protein-serine phosphatases).
6. 20 mM sodium pyrophosphate (to inhibit protein-serine phosphatases).
7. 1 mM sodium orthovanadate (to inhibit protein-tyrosine phosphatases).
8. 1 mM phenylmethylsulfonylfluoride (to inhibit proteases).
9. 3 mM benzamidine (to inhibit proteases).
10. 5  $\mu$ M pepstatin A (to inhibit proteases).
11. 10  $\mu$ M leupeptin (to inhibit proteases).
12. 1% Triton X-100 (can be substituted with 1% Nonidet P-40).
  - Important Note: Do not add if you intend to first prepare a cytosolic fraction;
  - 13. 1 mM dithiothreitol (To disrupt disulfate bonds).
  - Important Note: Dithiothreitol must be added to lysis buffer immediately before use.



### **Appendix 3.**

#### **List of figures.**

Figure 1. Citicoline Structure.

Figure 2. The CDP-choline pathway.

Figure 3. The points where citicoline has been reported to have a pharmacologic effect in the ischemic cascade are marked in red.

Figure 4. A representation of the two major types of stroke.

Figure 5. Angioblasts in the embryo accumulate during the process of vasculogenesis, and expands and remodels in angiogenesis.

Figure 6. The scanning electron micrograph displays pericytes wrapping their processes around a small blood vessel in the mammary gland of a cat.

Figure 7. A representation of the BBB. It is formed by capillary endothelial cells, embedded in basal lamina and surrounded by astrocytic perivascular endfeet.

Figure 8. A representation of different in vitro cell-based blood–brain barrier (BBB) models.

Figure 9. Signalling pathways for cell migration regulated Erk.

Figure 10. A representation of the two major apoptotic pathways; the extrinsic and the intrinsic pathway.

Figure 11. Standard curve for protein amount estimation in  $\mu\text{g}$ .

Figure 12. The Kinexus antibody microarray screen performed by Kinexus on BAEC

Figure 13. Chemical structure of GW2974 (Kamlesh Sodani, 2012).

Figure 14. Representative western blot showing HER2 expression in cells untreated and treated with different concentrations of citicoline (1  $\mu$ M, 5  $\mu$ M and 10  $\mu$ M).

Figure 15. . Representative western blot showing pilot experiment to determine optimal HER2 inhibitor concentration.

Figure 16. Representative western blot showing 25 ng FGF-2 and 10  $\mu$ M citicoline effect on pErk expression with and without 5  $\mu$ M HER2 inhibitor.

Figure 17. Citicoline (10  $\mu$ M) significantly increased the formation of tube-like structures of HCMEC/D3 with a stronger effect than fibroblast growth factor-2 (FGF-2).

Figure 18. Representative examples of the effect of citicoline on tube formation with or without Her-2 inhibitor in comparison to FGF-2, FGF-2 + Her-2 inhibitor, and control cells.

Figure 19. Pro-angiogenic effects of citicoline and FGF-2 on hCMEC/D3 tube formation.

Figure 20. A) Control (untreated) cells in hypoxia. B) 1  $\mu$ M citicoline treated cells in hypoxia. C) 5  $\mu$ M citicoline treated cells in hypoxia. D) 10  $\mu$ M citicoline treated cells in hypoxia.

Figure 21. Pro-angiogenic effects of citicoline on hCMEC/D3 cell migration.

Figure 22. A) Control untreated cells in hypoxia. B) 1 $\mu$ M citicoline treated cells in hypoxia. C) 5 $\mu$ M citicoline treated cells in hypoxia. D) 10  $\mu$ M citicoline treated cells in hypoxia.

Figure 23. Quantitative analysis of the apoptotic cells in percentage. Cells treated with different concentrations of citicoline (1  $\mu$ M, 5  $\mu$ Mm, 10  $\mu$ M) in hypoxia conditions.

Figure 24. A) Control untreated cells in normoxia. B) 1  $\mu$ M citicoline treated cells in normoxia. C) 5  $\mu$ M citicoline treated cells in normoxia. D) 10  $\mu$ M citicoline treated cells in normoxia.

Figure 25. Representative Western blot showing the effect of citicoline on PARP expression in normoxia and hypoxia.

Figure 26. Representative Western blot showing showing the effect of citicoline on caspase 3 expression in normoxia and hypoxia.

Figure 27. Apoptotic stimulation activates caspases which in turn activates Mst1. Mst1 is activated by caspases upon exposure to apoptotic stimuli.

Figure 28. Representative Western blot showing the effect of citicoline on H2B expression in normoxia and hypoxia.

Figure 29. Active caspase-3 expression in cells treated with different concentrations of citicoline (1  $\mu$ M, 5  $\mu$ M, 10  $\mu$ M) in hypoxia conditions.

Figure 30. Control (untreated) cells in hypoxia.

Figure 31. 1  $\mu$ M citicoline treated cells in hypoxia conditions.

Figure 32. 5  $\mu$ M citicoline treated cells in hypoxia conditions.

Figure 33. 10  $\mu$ M citicoline treated cells in hypoxia conditions.

Figure 34. Control cells in normoxia conditions.

Figure 35. 1  $\mu$ M citicoline treated cells in normoxia conditions.

Figure 36. 5  $\mu$ M citicoline treated cells in normoxia conditions.

Figure 37. 10  $\mu$ M citicoline treated cells in normoxia conditions.

Figure 38. H2B Ser14 expression in cells treated with different concentrations of citicoline (1  $\mu$ M, 5  $\mu$ M, 10  $\mu$ M) in hypoxia conditions.

Figure 39. Control cells in hypoxia conditions.

Figure 40. 1  $\mu$ M citicoline treated cells in hypoxia conditions.

Figure 41. 5  $\mu$ M citicoline treated cells in hypoxia conditions.

Figure 42. 10  $\mu$ M citicoline treated cells in hypoxia conditions.

Figure 43. Control cells in normoxia.

Figure 44. 1  $\mu$ M citicoline treated cells in normoxia conditions.

Figure 45. 5  $\mu$ M citicoline treated cells in normoxia conditions.

Figure 46. 10  $\mu$ M citicoline treated cells in normoxia conditions

Figure 47. Percentage of late apoptotic cells treated with different concentrations of citicoline (1 $\mu$ M, 5  $\mu$ M and 10  $\mu$ M) in hypoxia and normoxia conditions.

Figure 48. Percentage of early apoptotic cells treated with different concentrations of citicoline (1 $\mu$ M, 5  $\mu$ M and 10  $\mu$ M) in hypoxia and normoxia conditions.

Figure 49. Flow charts of control cells in hypoxia conditions.

Figure 50. 1  $\mu$ M citicoline treated cells in hypoxia conditions.

Figure 51. 5  $\mu$ M citicoline treated cells in hypoxia conditions.

Figure 52. 10  $\mu$ M citicoline treated cells in hypoxia conditions.

Figure 53. Control cells in normoxia conditions.

Figure 54. 1  $\mu$ M citicoline treated cells in normoxia conditions.

Figure 55. 5  $\mu$ M citicoline treated cells in normoxia conditions.

Figure 56. 10  $\mu$ M citicoline treated cells in normoxia conditions.

Figure 57. Relative gene expression between control cells and cells treated with 10  $\mu$ M citicoline was calculated using qRT-PCR (GAPDH, HPRT1 and RPLPO were taken as endogenous control).

Figure 58. Proposed pathway of citicoline induced ERK1/2 expression.

Figure 59. The PI3K/Akt signalling pathway. Phosphorylation of Akt phosphorylates BAD and a non-active form of caspase-9.

Figure 60. Ischemic cascade leading to cerebral damage.

Figure 61. A representation of PARP roles in cell physiology. DNA damage caused by ischemia, excitotoxicity, oxidative stress, inflammation or toxins leads to PARP-1 activation.

Figure 62. Proposed apoptotic pathway in which citicoline acts.

## **Appendix 4.**

### **List of tables.**

Table 1. Examples of how Matrigel™ promotes differentiation in different cell types.

Table 2. The volume of BSA, dH<sub>2</sub>O and Bio-Rad required to establish the standard curve.

Table 3. Preparation of separating gel.

Table 4. Preparation of stacking gel.

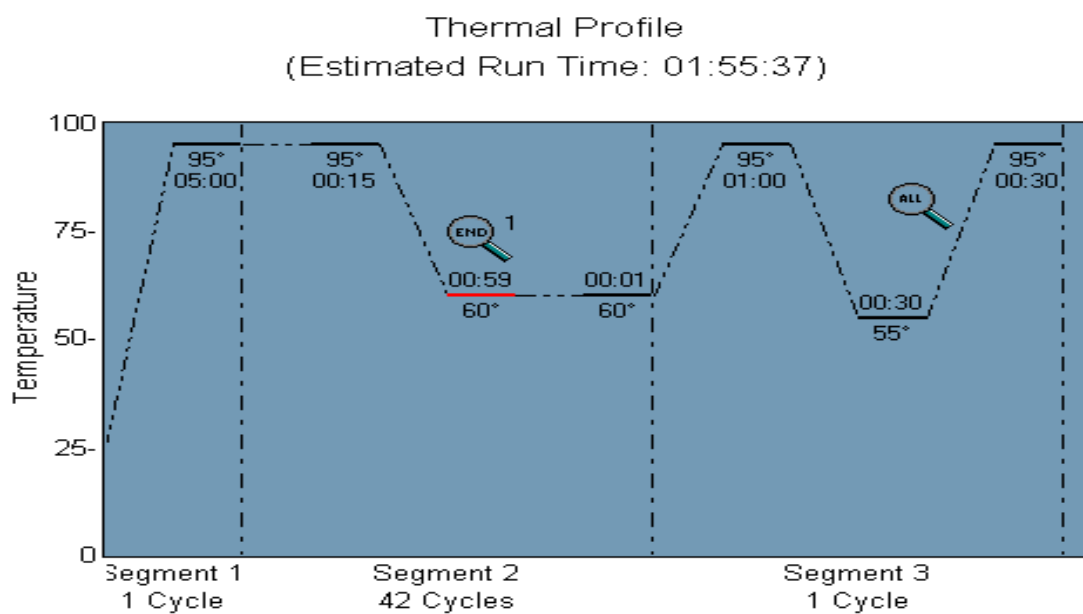
Table 5. The real-time cyclers settings.

Table 6. The effects of citicoline on hCMEC/D3 cells proliferation.

## Appendix 5.

### PCR data.

#### Untreated Sample.



#### Amplification Plots

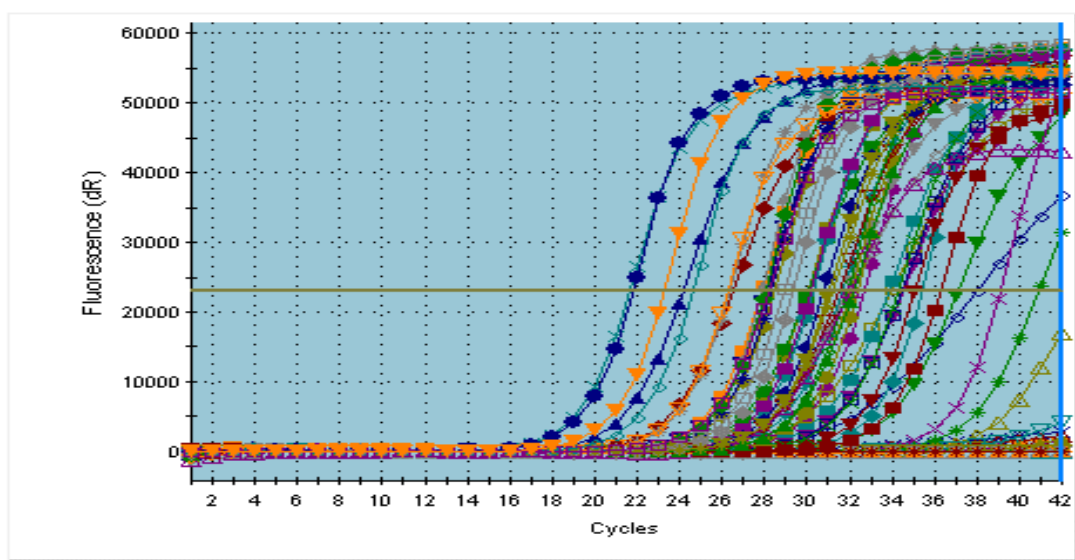


## Plate Setup

	1	2	3	4	6	6	7	8	9	10	11	12
A	Unknown	Unknown	Unknown	Unknown	Unknown	Unknown	Unknown	Unknown	Unknown	Unknown	Unknown	Unknown
B	Unknown	Unknown	Unknown	Unknown	Unknown	Unknown	Unknown	Unknown	Unknown	Unknown	Unknown	Unknown
C	Unknown	Unknown	Unknown	Unknown	Unknown	Unknown	Unknown	Unknown	Unknown	Unknown	Unknown	Unknown
D	Unknown	Unknown	Unknown	Unknown	Unknown	Unknown	Unknown	Unknown	Unknown	Unknown	Unknown	Unknown
E	Unknown	Unknown	Unknown	Unknown	Unknown	Unknown	Unknown	Unknown	Unknown	Unknown	Unknown	Unknown
F	Unknown	Unknown	Unknown	Unknown	Unknown	Unknown	Unknown	Unknown	Unknown	Unknown	Unknown	Unknown
G	Unknown	Unknown	Unknown	Unknown	Unknown	Unknown	Unknown	Unknown	Unknown	Unknown	Unknown	Unknown
H	Unknown	Unknown	Unknown	Unknown	Unknown	Unknown	Unknown	Unknown	Unknown	Unknown	Unknown	Unknown

## Analysis Sel./Setup-Term Settings View

Amplification-based threshold using search range of 5 to 60 percent.

Moving average points for amplification = 3, dissociation = 3.

Dissociation graphical temperature separation = 0.50.

Baseline Settings Plate: \* indicates manual baseline cycle range settings.

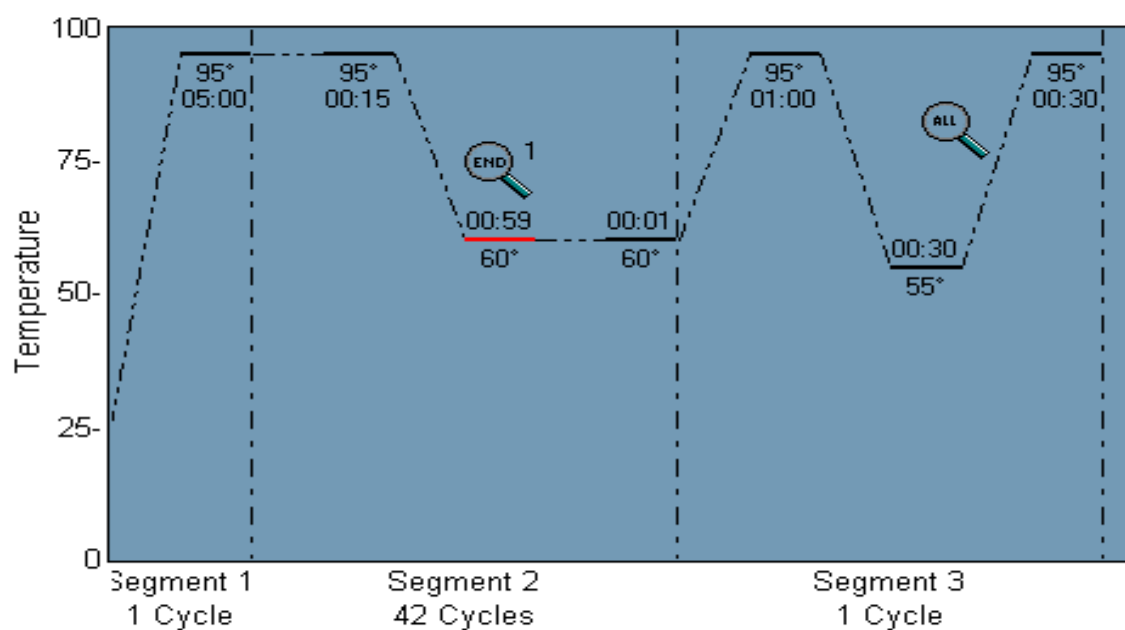
	1	2	3	4	6	6	7	8	9	10	11	12
A	Unknown	Unknown	Unknown	Unknown	Unknown	Unknown	Unknown	Unknown	Unknown	Unknown	Unknown	Unknown
B	Unknown	Unknown	Unknown	Unknown	Unknown	Unknown	Unknown	Unknown	Unknown	Unknown	Unknown	Unknown
C	Unknown	Unknown	Unknown	Unknown	Unknown	Unknown	Unknown	Unknown	Unknown	Unknown	Unknown	Unknown
D	Unknown	Unknown	Unknown	Unknown	Unknown	Unknown	Unknown	Unknown	Unknown	Unknown	Unknown	Unknown
E	Unknown	Unknown	Unknown	Unknown	Unknown	Unknown	Unknown	Unknown	Unknown	Unknown	Unknown	Unknown
F	Unknown	Unknown	Unknown	Unknown	Unknown	Unknown	Unknown	Unknown	Unknown	Unknown	Unknown	Unknown
G	Unknown	Unknown	Unknown	Unknown	Unknown	Unknown	Unknown	Unknown	Unknown	Unknown	Unknown	Unknown
H	Unknown	Unknown	Unknown	Unknown	Unknown	Unknown	Unknown	Unknown	Unknown	Unknown	Unknown	Unknown



Well	Well Type	Threshold (dR)	Ct (dR)
A1	Unknown	22988.050	No Ct
A2	Unknown	22988.050	No Ct
A3	Unknown	22988.050	No Ct
A4	Unknown	22988.050	No Ct
A5	Unknown	22988.050	No Ct
A6	Unknown	22988.050	No Ct
A7	Unknown	22988.050	No Ct
A8	Unknown	22988.050	No Ct
A9	Unknown	22988.050	No Ct
A10	Unknown	22988.050	No Ct
A11	Unknown	22988.050	No Ct
A12	Unknown	22988.050	No Ct
B1	Unknown	22988.050	30.11
B2	Unknown	22988.050	No Ct
B3	Unknown	22988.050	No Ct
B4	Unknown	22988.050	No Ct
B5	Unknown	22988.050	37.97
B6	Unknown	22988.050	No Ct
B7	Unknown	22988.050	37.12
B8	Unknown	22988.050	No Ct
B9	Unknown	22988.050	No Ct
B10	Unknown	22988.050	No Ct
B11	Unknown	22988.050	32.70
B12	Unknown	22988.050	27.93
C1	Unknown	22988.050	24.22
C2	Unknown	22988.050	26.60
C3	Unknown	22988.050	40.91
C4	Unknown	22988.050	32.07
C5	Unknown	22988.050	33.96
C6	Unknown	22988.050	No Ct
C7	Unknown	22988.050	39.12
C8	Unknown	22988.050	No Ct
C9	Unknown	22988.050	28.19
C10	Unknown	22988.050	No Ct
C11	Unknown	22988.050	30.11
C12	Unknown	22988.050	27.95
D1	Unknown	22988.050	28.54
D2	Unknown	22988.050	31.70
D3	Unknown	22988.050	No Ct
D4	Unknown	22988.050	No Ct
D5	Unknown	22988.050	No Ct
D6	Unknown	22988.050	No Ct
D7	Unknown	22988.050	No Ct
D8	Unknown	22988.050	No Ct
D9	Unknown	22988.050	32.39
D10	Unknown	22988.050	33.85
D11	Unknown	22988.050	No Ct
D12	Unknown	22988.050	No Ct
E1	Unknown	22988.050	28.39
E2	Unknown	22988.050	No Ct
E3	Unknown	22988.050	No Ct
E4	Unknown	22988.050	31.85
E5	Unknown	22988.050	No Ct
E6	Unknown	22988.050	No Ct
E7	Unknown	22988.050	No Ct
E8	Unknown	22988.050	No Ct
E9	Unknown	22988.050	No Ct

## Treated Sample.

Thermal Profile  
(Estimated Run Time: 01:55:37)



Amplification Plots

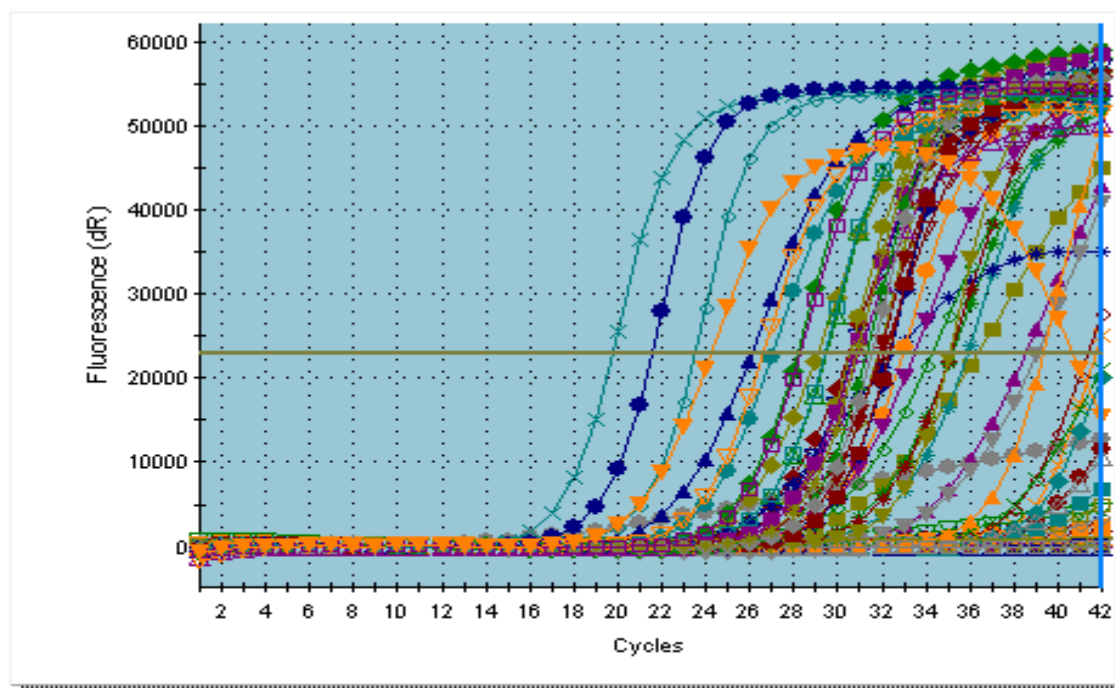


## Plate Setup

	1	2	3	4	5	6	7	8	9	10	11	12
A	Unknown	Unknown	Unknown	Unknown	Unknown	Unknown	Unknown	Unknown	Unknown	Unknown	Unknown	Unknown
B	Unknown	Unknown	Unknown	Unknown	Unknown	Unknown	Unknown	Unknown	Unknown	Unknown	Unknown	Unknown
C	Unknown	Unknown	Unknown	Unknown	Unknown	Unknown	Unknown	Unknown	Unknown	Unknown	Unknown	Unknown
D	Unknown	Unknown	Unknown	Unknown	Unknown	Unknown	Unknown	Unknown	Unknown	Unknown	Unknown	Unknown
E	Unknown	Unknown	Unknown	Unknown	Unknown	Unknown	Unknown	Unknown	Unknown	Unknown	Unknown	Unknown
F	Unknown	Unknown	Unknown	Unknown	Unknown	Unknown	Unknown	Unknown	Unknown	Unknown	Unknown	Unknown
G	Unknown	Unknown	Unknown	Unknown	Unknown	Unknown	Unknown	Unknown	Unknown	Unknown	Unknown	Unknown
H	Unknown	Unknown	Unknown	Unknown	Unknown	Unknown	Unknown	Unknown	Unknown	Unknown	Unknown	Unknown

## Analysis Sel./Setup-Term Settings View

Amplification-based threshold using search range of 5 to 60 percent.

Moving average points for amplification = 3, dissociation = 3.

Dissociation graphical temperature separation = 0.50.

Baseline Settings Plate: \* indicates manual baseline cycle range settings.

	1	2	3	4	5	6	7	8	9	10	11	12
A	Unknown	Unknown	Unknown	Unknown	Unknown	Unknown	Unknown	Unknown	Unknown	Unknown	Unknown	Unknown
B	Unknown	Unknown	Unknown	Unknown	Unknown	Unknown	Unknown	Unknown	Unknown	Unknown	Unknown	Unknown
C	Unknown	Unknown	Unknown	Unknown	Unknown	Unknown	Unknown	Unknown	Unknown	Unknown	Unknown	Unknown
D	Unknown	Unknown	Unknown	Unknown	Unknown	Unknown	Unknown	Unknown	Unknown	Unknown	Unknown	Unknown
E	Unknown	Unknown	Unknown	Unknown	Unknown	Unknown	Unknown	Unknown	Unknown	Unknown	Unknown	Unknown
F	Unknown	Unknown	Unknown	Unknown	Unknown	Unknown	Unknown	Unknown	Unknown	Unknown	Unknown	Unknown
G	Unknown	Unknown	Unknown	Unknown	Unknown	Unknown	Unknown	Unknown	Unknown	Unknown	Unknown	Unknown
H	Unknown	Unknown	Unknown	Unknown	Unknown	Unknown	Unknown	Unknown	Unknown	Unknown	Unknown	Unknown

Well	Well Type	Threshold (dR)	Ct (dR)
A1	Unknown	22988.057	No Ct
A2	Unknown	22988.057	No Ct
A3	Unknown	22988.057	No Ct
A4	Unknown	22988.057	No Ct
A5	Unknown	22988.057	No Ct
A6	Unknown	22988.057	No Ct
A7	Unknown	22988.057	No Ct
A8	Unknown	22988.057	No Ct
A9	Unknown	22988.057	No Ct
A10	Unknown	22988.057	No Ct
A11	Unknown	22988.057	No Ct
A12	Unknown	22988.057	No Ct
B1	Unknown	22988.057	36.37
B2	Unknown	22988.057	No Ct
B3	Unknown	22988.057	No Ct
B4	Unknown	22988.057	No Ct
B5	Unknown	22988.057	No Ct
B6	Unknown	22988.057	No Ct
B7	Unknown	22988.057	No Ct
B8	Unknown	22988.057	No Ct
B9	Unknown	22988.057	No Ct
B10	Unknown	22988.057	No Ct
B11	Unknown	22988.057	No Ct
B12	Unknown	22988.057	No Ct
C1	Unknown	22988.057	26.14
C2	Unknown	22988.057	30.60
C3	Unknown	22988.057	35.21
C4	Unknown	22988.057	No Ct
C5	Unknown	22988.057	No Ct
C6	Unknown	22988.057	No Ct
C7	Unknown	22988.057	No Ct
C8	Unknown	22988.057	No Ct
C9	Unknown	22988.057	30.82
C10	Unknown	22988.057	No Ct
C11	Unknown	22988.057	No Ct
C12	Unknown	22988.057	No Ct
D1	Unknown	22988.057	29.15
D2	Unknown	22988.057	35.89
D3	Unknown	22988.057	No Ct
D4	Unknown	22988.057	No Ct
D5	Unknown	22988.057	No Ct
D6	Unknown	22988.057	No Ct
D7	Unknown	22988.057	29.59
D8	Unknown	22988.057	No Ct
D9	Unknown	22988.057	30.66
D10	Unknown	22988.057	No Ct
D11	Unknown	22988.057	38.57
D12	Unknown	22988.057	No Ct
E1	Unknown	22988.057	32.58
E2	Unknown	22988.057	41.40
E3	Unknown	22988.057	No Ct
E4	Unknown	22988.057	39.08
E5	Unknown	22988.057	No Ct
E6	Unknown	22988.057	No Ct
E7	Unknown	22988.057	No Ct
E8	Unknown	22988.057	32.93
E9	Unknown	22988.057	No Ct
E10	Unknown	22988.057	No Ct
E11	Unknown	22988.057	28.25
E12	Unknown	22988.057	No Ct
F1	Unknown	22988.057	31.86
F2	Unknown	22988.057	29.51
F3	Unknown	22988.057	33.46
F4	Unknown	22988.057	41.78
F5	Unknown	22988.057	No Ct
F6	Unknown	22988.057	32.04
F7	Unknown	22988.057	No Ct
F8	Unknown	22988.057	No Ct
F9	Unknown	22988.057	No Ct

Gene	Treated	Untreated	Both		
BRAF V-raf murine sarcoma viral oncogene homolog B1	x			BNIP3	-10.6
CFLAR CASP8 and FADD-like apoptosis regulator	x			BNIP3L	-2.6
CYCS Cytochrome c, somatic	x			CASP4	-2.6
FADD Fas (TNFRSF6)-associated via death domain	x			CASP8	-1.1
IGF1R Insulin-like growth factor 1 receptor	x			Caspase 9	-52
Nuclear factor of kappa light polypeptide gene enhancer in B-cells 1	x			CIDEB	-3.3
PYCARD PYD and CARD domain containing	x			DFFA	-2.14
TRAF2 TNF receptor-associated factor 2	x			LTBR	-1.07
BIRC6 Baculoviral IAP repeat containing 6		x		NAIP	1
BNIP2 BCL2/adenovirus E1B 19kDa interacting protein 2		x		NOD1	2.46
CASP10 Caspase 10, apoptosis-related cysteine peptidase		x		TNFRSF25	7
CASP6 Caspase 6, apoptosis-related cysteine peptidase		x		TP53	11.3
CASP7 Caspase 7, apoptosis-related cysteine peptidase		x		TP53BP2	-1.2
CRADD CASP2 and RIPK1 domain containing adaptor with death domain		x		TRADD	-3.7
FAS Fas (TNF receptor superfamily, member 6)		x		TRAF3	-1.9
MCL1 Myeloid cell leukemia sequence 1 (BCL2-related)		x			
RIPK2 Receptor-interacting serine-threonine kinase 2		x			
TNFRSF11B Tumor necrosis factor receptor superfamily, member 11b		x			
TNFRSF9 Tumor necrosis factor receptor superfamily, member 9		x			
XIAP X-linked inhibitor of apoptosis		x			
BCL2L1 BCL2-like 1			x		
BNIP3 BCL2/adenovirus E1B 19kDa interacting protein 3			x		
BNIP3L BCL2/adenovirus E1B 19kDa interacting protein 3-like			x		
CASP4 Caspase 4, apoptosis-related cysteine peptidase			x		
CASP8 Caspase 8, apoptosis-related cysteine peptidase			x		
Caspase 9, apoptosis-related cysteine peptidase			x		
CIDEB Cell death-inducing DFFA-like effector b			x		
DFFA DNA fragmentation factor, 45kDa, alpha polypeptide			x		
LTBR Lymphotoxin beta receptor (TNFR superfamily, member 3)			x		
NAIP NLR family, apoptosis inhibitory protein			x		
NOD1 Nucleotide-binding oligomerization domain containing 1			x		
TNFRSF25 Tumor necrosis factor receptor superfamily, member 25			x		
TP53 Tumor protein p53			x		
TP53BP2 Tumor protein p53 binding protein, 2			x		
TRADD TNFRSF1A-associated via death domain			x		
TRAF3 TNF receptor-associated factor 3			x		

## Appendix 6.

### Protein Estimation.

#### Caspase 3 + H2B

0.05	0.1	0.2	0.3	0.4	0.5
0.44	0.613	0.77	0.93	1	1.18
0.46	0.53	0.79	0.85	1	1.1
0.01	0.1	0.2	0.3	0.4	0.5
0.45	0.5715	0.78	0.89	1	1.14

#### Normoxia

C	10	5	1
0.847	0.88	0.911	0.79
0.69	0.788	0.88	0.73
0.7685	0.834	0.8955	0.76

#### Hypoxia

C	10	5	1
0.816	0.77	0.799	0.873
0.74	0.78	1.71	1.295
0.778	0.775	1.2545	1.084

#### Amount of Protein in (µg in 2µl) Normoxia Samples

C	10	5	1
0.204011	0.249308	0.29184	0.198133

#### Amount of Protein in (µg in 2µl) Hypoxia Samples

C	10	5	1
0.210581	0.208506	0.540111	0.422199

#### Amount of Protein in Normoxia Samples µg/µl

C	10	5	1
1.020055	1.246542	1.459198	0.990664

#### Amount of Protein in Hypoxia µg/µl Samples

C	10	5	1
1.052905	1.042531	2.700553	2.110996

#### Amount of Protein in 20 µl Normoxia

C	10	5	1
20.40111	24.93084	29.18396	19.81328

Amount of Protein in 20 µl Hypoxia

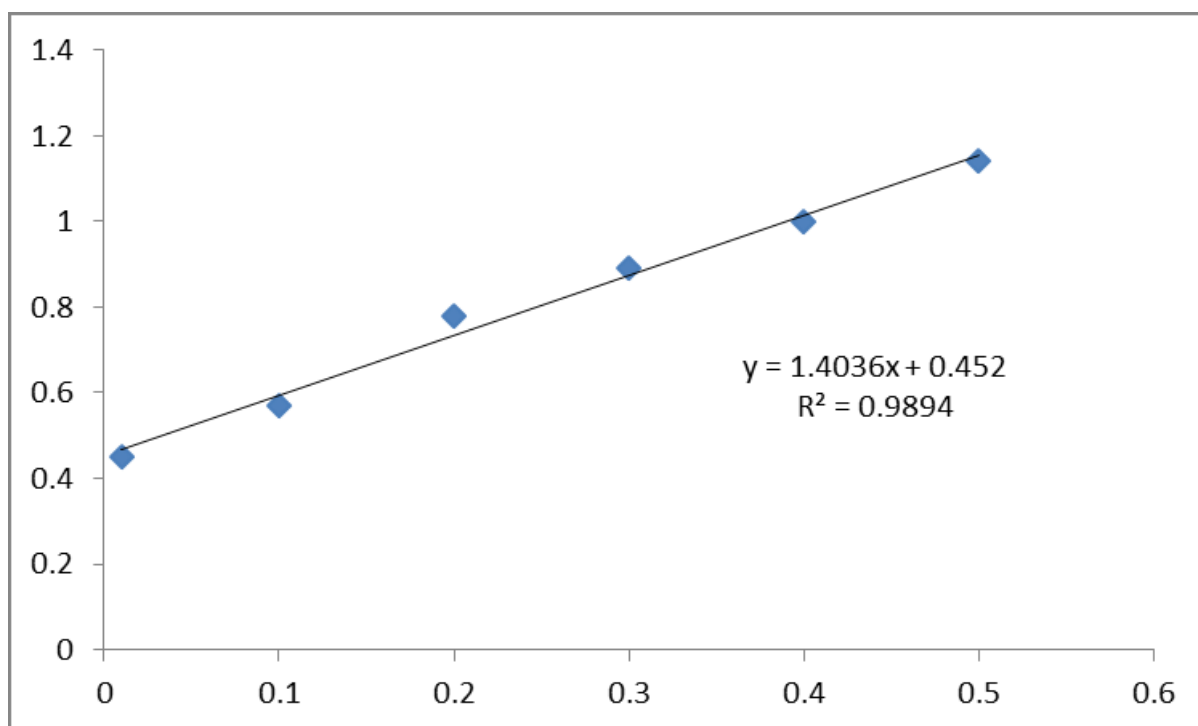
C	10	5	1
21.05809	20.85062	54.01107	42.21992

Loading Volume Normoxia

C	10	5	1
19.60678	16.04438	13.70616	20.18848

Loading Volume Hypoxia

C	10	5	1
18.99507	19.18408	7.40589	9.474201



#### PARP + Active PARP

0.01	0.1	0.2	0.3	0.4	0.5
0.5	0.613	0.783	0.95	1.054	1.152
0.468	0.603	0.774	0.913	0.978	1.261
0.01	0.1	0.2	0.3	0.4	0.5
0.484	0.608	0.7785	0.9315	1.016	1.2065

#### Normoxia

C	10	5	1
1.9	1.5	1.892	1.7
1.027	1.7	0.974	1.51
1.4635	1.6	1.433	1.605

#### Hypoxia

C	10	5	1
1.45	1.098	1.61	1.35
1.5	1.7	1.55	1.7
1.475	1.399	1.58	1.525

#### Amount of Protein in (µg in 2µl) Normoxia Samples

C	10	5	1
0.684647	0.779046	0.663555	0.782503

#### Amount of Protein in (µg in 2µl) Hypoxia Samples

C	10	5	1
0.6926	0.640041	0.765214	0.727178

#### Amount of Protein in Normoxia Samples µg/µl

C	10	5	1
3.423237	3.895228	3.317773	3.912517

#### Amount of Protein in Hypoxia µg/µl Samples

C	10	5	1
3.463001	3.200207	3.826072	3.635892



#### Amount of Protein in 20 µl Normoxia

C	10	5	1
68.46473	77.90456	66.35546	78.25035

#### Amount of Protein in 20 µl Hypoxia

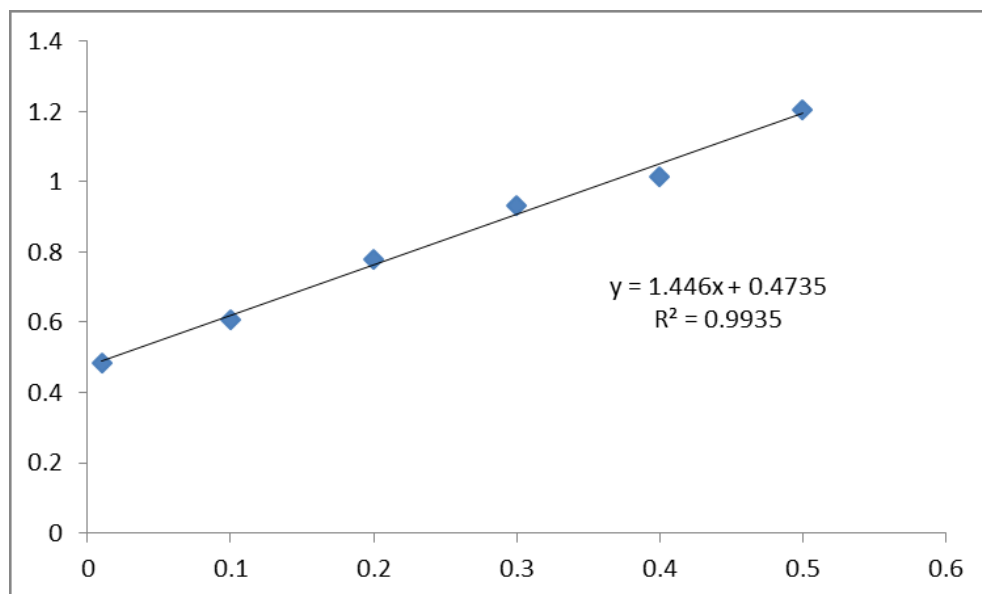
C	10	5	1
69.26003	64.00415	76.52144	72.71784

#### Loading Volume Normoxia

C	10	5	1
11.68485	10.26897	12.05628	10.2236

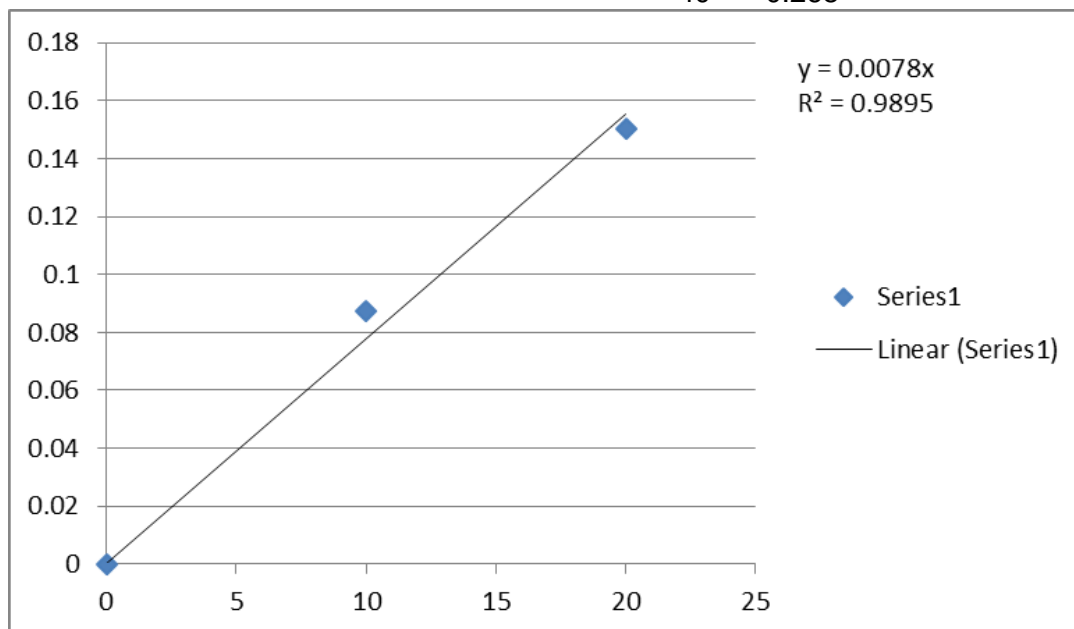
#### Loading Volume Hypoxia

C	10	5	1
11.55067	12.49919	10.45459	11.00143



BSA (mg)	O.D. 570 nm	Mean
0	0	0
10	0.160	0.1
20	0.118	0.027
40	0.197	0.152

BSA (mg)	Mean
0	0
10	0.0875
20	0.1505
40	0.268



control	10 $\mu$ M Citicoline	10 $\mu$ M Citicoline + 5 $\mu$ M Her-2 inhibitor	FGF-2	FGF-2 + 5 $\mu$ M Her-2 inhibitor
0.218	0.242	0.23	0.24	0.291
0.212	0.241	0.225	0.236	0.284
0.215	0.2415	0.2275	0.238	0.288
Amount of proteins (mg in 10 ml) (ug in 10 ul)				
27.5641	30.96154	29.166667	30.51282	36.8589744
Amount of proteins ( $\mu$ g in 20 $\mu$ l)				
55.12821	61.92308	58.333333	61.02564	73.7179487
Volume of loading ( $\mu$ l)				
control	10 $\mu$ M Citicoline	10 $\mu$ M Citicoline + 5 $\mu$ M Her-2 inhibitor	FGF-2	FGF-2 + 5 $\mu$ M Her-2 inhibitor
<b>14.51163</b>	<b>12.91925</b>	<b>13.714286</b>	<b>13.10924</b>	<b>10.8521739</b>

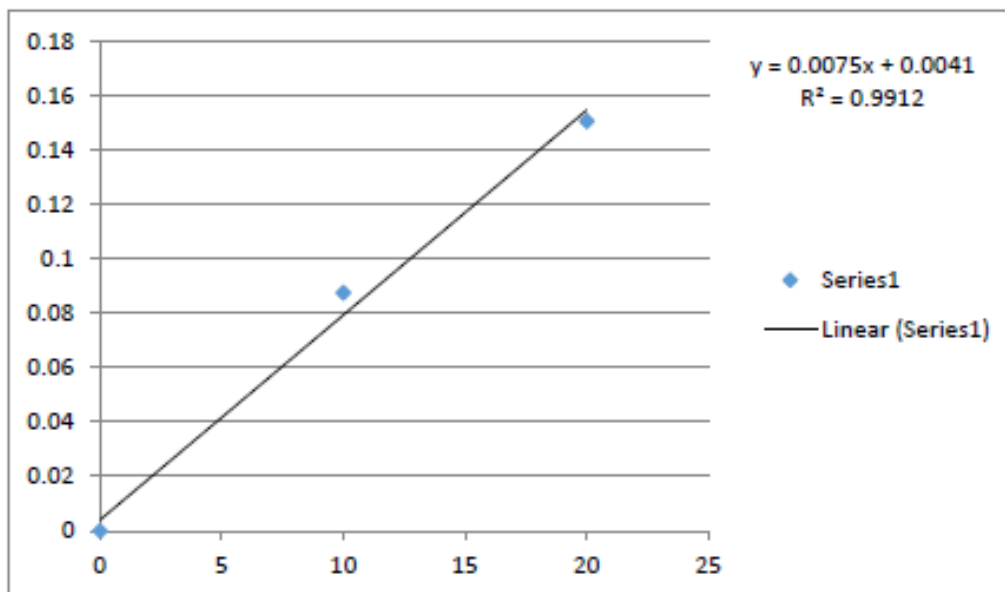
# Protein Estimation from hCMEC/D3 cell lysate for pHer-2

Bovine Serum Albumin (BSA)

O.D. 590 nm (standard curve)

BSA at 1mg/ml

BSA (mg)	O.D. 590 nm	BSA (mg)	O.D. 590 nm	Mean BSA (µg)	Mean
0	0	0	0.0845	0	0
10	0.140	0.029	0.218	10	0.0875
20	0.165	0.271	0.5	20	0.1505
40	0.518	0.482	0.268		
40					



control	10 µM Citicoline	10 µM Citicoline + 1µM Her-2 inhibitor	10 µM Citicoline + 5µM Her-2 inhibitor
0.23	0.228	0.179	0.183
0.194	0.199	0.152	0.150
0.212	0.2135	0.1655	0.167
Amount of proteins (mg in 10 ml)		(ug in 10ul)	
27.17949	27.37179	21.217949	21.34615
Amount of proteins (µg in 20 µl)			
54.35897	54.74359	42.435897	42.69231
Volume of loading (µl)			
control	10 µM Citicoline	10 µM Citicoline + 1 µM Her-2 inhibitor	10 µM Citicoline + 5 µM Her-2 inhibitor
<b>14.71698</b>	<b>14.61358</b>	<b>18.851964</b>	<b>18.73874</b>